Experimental simulations of the weathering of volcanic ash – a case study to better understand short - and long-term impacts of ash-leachable elements on the environment

A thesis presented in the partial fulfilment of the requirements for a degree of

Master of Science

In

Earth Science

At Massey University, Palmerston North

New Zealand

Alexander Robert Greig

2017

Abstract

The aim of this project is the development and testing of a new methodology for the investigation of the short- to long-term leaching behaviour of volcanic ash. Previous research has demonstrated that volcanic eruptions can have strong impacts on the environment, which result from elements that have been leached from volcanic ash. To date, there is relatively little understanding of the minor and trace element composition of ash-leached brines, and how this varies over time. These gaps in knowledge currently preclude an estimate of both the detrimental and the beneficial impacts of volcanic ash fall due to leaching on the environment, agriculture, as well as on human and animal health.

An adaption of a soxhlet reactor was found to be an adequate experimental technique for the constant flushing of volcanic ash samples with deionised water. This was designed to accelerate the weathering of a volcanic material in a laboratory setting. A number of shortcomings in the experimental method could be identified through the course of this research and should be considered in future investigations.

In this experiment nine volcanic ash samples from four different and highly active volcanoes have been tested. These volcanoes are Mt. Ruapehu and White Island in New Zealand, Mt. Kelut in Indonesia and Mt. Sakurajima in Japan. All volcanic ash samples were found to release elements into brine over the experimental time in a strongly non-linear fashion. Based on the current data set of nine ash samples, three main classes of time-variant element release behaviour are here suggested and defined, whose characteristics are primarily controlled by the element, rather than volcanic source or ash characteristics. A preliminary interpretation of these different element release pattern is that their temporal changes are most likely restrained by the strength of chemical and mechanical bond of elements to the surface of juvenile and non-juvenile ash material. Moreover, significant controls on the long-term leaching concentrations of elements were found to be by the style of eruption as well as the nature of the volcano plumbing system, confirming results of earlier batch leaching experiments. The 1995-96 Mt. Ruapehu eruption sequence in particular illustrated some significant variability in leaching behaviour as a result of specific eruption parameters. Volcanic ash samples that have been derived from a phreatomagmatic style eruption have been found to have a higher short-to long-term impact than those volcanic ash samples derived from dry magmatic eruptions.

A simple method was developed to estimate the real–world equivalent weathering time corresponding to the duration of a soxhlet reactor leaching experiment. The method, which is primarily based on the total volume of water percolating through an ash sample, and to relate this to local annual rain fall data, was found to estimate real-world weathering times in the natural environment fairly accurately. Based on these natural time constraints, detrimental short-term impacts (months to years) are concluded for lead and fluoride, and beneficial short-term impacts for calcium and manganese. Long-term beneficial effects (up to 20 years) are seen for zinc, copper and iron, while long-term detrimental impacts are concluded for the cases of lead and fluoride.

The strong dependence of the leaching rate on the effective ash surface area precludes that future forecasts of short- and long-term impacts should be made by considering local soil permeability and ash grain-size characteristics. In that way future modelling approaches via reactive and non-reactive porous media flow of ash-leached brines into soil and groundwater may form an interesting avenue for future developments of this pilot study. This approach may hold potential to give quantitative advice to regional councils, the agricultural industry and governmental agencies on detrimental and beneficial short- to long-term impacts of volcanic ash.

Acknowledgments

I would like to acknowledge all of the countless individuals who have assisted me throughout the completion of this study.

My chief supervisor Dr. Gert Lube as well as my co-supervisors Dr. Christopher Anderson and Dr. Paramsothy (Jeya) Jeyakumar who all contributed their knowledge, advice and who also kept me on the right track.

I acknowledge Dr. Roberto Calvelo Pereira for all of the help in the laboratory and his tireless assistance with the soxhlet reactor experiments.

I would like to acknowledge Professor Shane Cronin for helping to obtain the volcanic ash samples as well as his indispensable advice, without which this thesis would not have been possible.

The technicians for all the help in the laboratory Dr. Anja Moebis, Mr. Bob Toes, Mrs. Glenys Wallace and Mr. Ian Furkert.

Also Graham Freeman who provided so much help with the soxhlet reactor experiments.

Also a special thanks to Dr. Carol Stewart her help around the laboratory, obtaining volcanic ash samples and for the sharing her extensive knowledge during our meetings.

Dr. George Mason and the L.A. Alexander College Trust Board for their financial assistance.

Most of all I would like to acknowledge by parents; Margaret and Malcolm Greig and my late grandmother Mona Scherf.

I would also like to thank Joe Holden and Greg Moore.

Table of Contents

List of Tables

List of Figures

Chapter 1 Literature review

1.0 Introduction

Volcanic eruptions produce a variety of significant natural hazards. These include pyroclastic air-fall (or ash fall), pyroclastic density currents, ballistic projectiles and lahars (Scarpa, 1996; Wilson, 2014; Wilson & Kaye, 2007), all of which can cause significant damage to life, infrastructure, agriculture and the environment (Wilson, 2014). Volcanic ash is a hazard that impacts the environment and agriculture, on a physical and a chemical level, both locally and at significant distances from the vent (Wilson et al., 2012). These physical and chemical impacts are manifested in the environment in short-term to long-term time periods on soil, vegetation and animal health. The magnitude of these different impacts is not only constrained by the magnitude of an eruption, but they are also strongly influenced by properties of the volcanic ash and the environment of deposition. These impacts are manifested in different ways depending on the climate (rainfall), composition of vegetation and the type of agricultural practices being implemented.

The primary controls of the magnitude of the impacts of an eruption on the environment are the size and style of the eruption. Each eruption is unique, exhibiting individual characteristics depending on the magma type, magma plumbing system and a variety of external parameters (Cronin, Neall, Lecointre, Hedley, & Loganathan, 2003; Dellino et al., 2012). These external perimeters include interaction with surface water bodies, vent dynamics and others (Christenson, 2000; Christenson & Wood, 1993; Wohletz, Sheridan, & Brown, 1989).

The focus of this thesis is on better understanding the composition, concentration and impacts of leaching elements and chemical compounds, which are released during and after ash-fall events. Current knowledge of the variation in leaching elements in volcanic ash suggests a fundamental control by the dynamics of the eruption plume and eruption style. Moreover, volatile gases interact with strong acids to form soluble salt coatings on ash particles. In leaching experiments, a review of results in the scientific literature by Witham, Oppenheimer, and Horwell (2005) contained over 55 different water and acid soluble compounds. In the scientific literature ionic salt compounds of major cations (sodium and calcium) as well as sulphate are the most studied (Ayris & Delmelle, 2012b), while trace metals have had less emphasis. Their distribution is strongly influenced by atmospheric processes, with ambient temperatures and atmospheric water content having key controls over dispersal dynamics. Also, during an eruption volatile gases and volcanic ash particles interact in multiple physical chemical reactions in an eruption plume (Bagnato et al., 2013; Óskarsson, 1980; Rose, 1977; Taylor & Stoiber, 1973). Currently, the study of this field of volcanology is somewhat impeded by an absence of a unified methodology. This hinders comparisons of past eruptions from the source volcano and across different volcanic vents). Finding better methodologies to study and forecast the impact on the environment can aid knowledge and hazard forecasting and mitigation.

1.01 Research objectives

The aim of the project was the development of a method to investigate the behaviour of volcanic ash over time. Previous research has demonstrated the strong environmental impact with simple batch leaching tests.

Objective 1

The first objective is to develop or adopt a suitable methodology that can simulate the weathering of volcanic ash samples in a feasible time span that allows the analysis of the leaching behaviour of volcanic ash with respect to time.

Objective 2

The second objective is to deploy this new method to try to characterise the time-variant leaching of volcanic ash from a variety of sources and eruption styles.

Objective 3

The third objective is to attempt to relate the accelerated experiential weathering time to define and interpret the short-term and the long-term beneficial and detrimental impacts of ash leaching processes on the environment.

1.1 Environmental impact and hazards

1.11 Physical impacts of volcanic ash

Table 1. Summary of the physical impacts on the three core aspects of agriculture by volcanic ash

Type of Impact	**Impacts**		**Long Term**
	Deposition	**Remobilisation**	
Soil	Radiation → soil temperature → energy flux	Evaporation Δ by volcanic ash = mulching effect – hard crust	- Formation of clay Minerals - Alteration of plant ecosystem - Contaminated pasture, remobilisation
Plants	Burial, breakage and smothering	Abrasion of vegetation can be caused by remobilised volcanic ash	
Animal health	Ash Ingestion – death of animals	Δ Economy	

1.111 Ash deposit on soil

One of the most direct physical impacts of volcanic ash that is summarised in Table 1 is related to the colour-influencing albedo and hence the energy balance of a soil profile . Studies on the eruption of Mt. St. Helen’s (MSH) in 1980 best describes in quantitative detail the impacts of albedo on the soil profile (Cook, Barron, Papendick, & Williams, 1981). Black and Mack (1986) found that fine-grained light grey dacitic volcanic ash artificially applied increased albedo by 13%-28%, diminishing net radiation by 20% and soil temperatures by 6°C-10°C (Black & Mack, 1986; Cook et al., 1981). Congruent evaporation of soil water increased in the first year after the artificial application of the MSH volcanic ash. In pot trial experiments with volcanic ash from Mt. Ruapehu (Cronin, Hedley, Neall, & Smith, 1998; Cronin, Hedley, Smith, & Neall, 1997) similar effects were observed. Cronin et al. (1998); Cronin et al. (1997) did not delve further into details of the energy fluxes and albedos or extend those pot trials into the field. However, Black and Mack (1986) also did not discuss grain size or morphology beyond the volcanic ash being of a silt loam class. In the Canary Islands on arid soils with <150 mm/year rainfall, mulching with volcanic ash has benefited local dry agriculture (Diaz, Jimenez, & Tejedor, 2005; Tejedor, Jiménez, & Dıaz, 2003). Experiments adding medium-grained basaltic volcanic ash reduced evaporation from field capacity. The reduction in evaporation was proportional to the thickness of the ash. Ash layered 10cm, 5cm and 2cm thick resulted in ↓92%, ↓83% and ↓52% reductions, respectively, in the amount of water evaporated from the underlying soil profile. Interestingly, local farmers have a preference for applying depths of volcanic ash onto the soil 7-12cm thick. This volcanic ash selectively forms an insulation layer between the sunlight and the underlying soil, thus reducing soil-water evaporation from the soil profile.

The mulching effect seems like a beneficial impact of volcanic ash deposition. After MSH an increase in wheat yields in the 1980 growth season amounted to 150 million bushels (Burket, 1980). Cook et al. (1981) speculated that this was due to the mulching effect, with the volcanic ash slowing evaporation. However, the same mulching effect also impedes further infiltration of water into the soil profile ash fall (Sneva et al., 1982). In a study by Black and Mack (1986), a 40% decrease in water infiltration was found at a 1m soil depth 2 months after the experiment began. This creates an effective barrier between the soil profile and the atmospheric processes. Porosity, and hence water infiltration, is reduced with decreasing fine and the associated permeability reducing its macro-porosity (Ayris & Delmelle, 2012b; Cook et al., 1981). The reduced infiltration of water into the underlying soil profile increases the chances for increased run-off and rill erosion to occur (Cook et al., 1981). This impact has been observed in the aftermath of MSH as well as in the 1991 Hudson eruption (Wilson, Cole, Cronin, Stewart, & Johnston, 2011). Also, after rainfall the fine-grained volcanic ash formed a hard crust, creating a physical impact on plants resulting in difficulties for plants to penetrate the hard layer (Black & Mack, 1986; Cook et al., 1981; Sneva et al., 1982).

1.112 Ash interception on vegetation

Vegetation can intercept the volcanic ash before it is deposited onto the soil surface, which is summarised in Table 1 (Antos & Zobel, 1986; Ayris & Delmelle, 2012b). The intensity of volcanic ash impacts on vegetation is predominantly controlled by the ash thickness and its particle size distribution. The common factor generally agreed in the scientific literature is that a thickness of 2m would critically damage or kill any vegetation (Antos & Zobel, 2005; Eggler, 1963). One of the first intensive and best studies on the impact of volcanic ash on vegetation was following the eruption of Paricutin, Mexico, which is a large basaltic cinder cone (Eggler, 1963). Small plants were most impacted, as mosses, lichens, grasses, herbs and small seedlings were all buried under a maximum of 500mm of volcanic ash depth (Eggler, 1963; Mack, 1981; Sheets & Grayson, 1979). The impact on trees was different in ash depths below 2m, and medium pine trees between 100mm and 300mm in diameter were most resilient (Eggler, 1963; Sheets & Grayson, 1979). These medium diameter trees had strong stems, but were also flexible so they could dump ash loads rather than break as larger trees did. However, Antos and Zobel (2005) explain that the secondary succession of vegetation after volcanic ash deposition is considerably different in forested areas that can vary in both elevation and plant cover from that in flat open plains. In summary, if erosion of an area of land that had been deposited with volcanic ash occurs within 3 years after deposition then the damage to the vegetation composition is capable of returning to pre-eruption levels in 20 years (Antos & Zobel, 2005; Collins & Dunne, 1986). However, if the deposit is not eroded or stabilised then the impacts can endure for many decades. Eggler (1963) concurs, explaining that following the Paricutin eruption where volcanic ash eroded, 'pre-volcanic' plants regrew and vegetation recovery was accelerated if there was already some remaining 'pre-volcanic' vegetation.

To survive any depth of volcanic ash, plants must either grow through the layer of ash or the ash must be eroded by wind or water (Antos & Zobel, 2005; Eggler, 1963). Mack (1981) speculates that the destruction of competing plants for resources (water, sunlight and nutrients) may allow 'pre-volcanic' vegetation to grow where it had been blocked previously. In the natural environment, plants that have the physiology of renewing shoots or were deciduous (and had lost their leaves by 18 May when the first and largest MSH eruption occurred) had minimal impact. This was the case in high altitudes, but not in lower altitudes where the temperatures were warmer and plants that had renewed their shoots or leaves were significantly impacted (Antos & Zobel, 2005; Mack, 1981). In the experiments of Black and Mack (1986), plants that grew through the artificially applied volcanic ash had little problem with growth in a volcanic ash thickness of 70mm. In pot trial experiments with volcanic ash from Mt. Ruapehu, with thicknesses of 2mm, 3mm, 5mm and 10mm, no volcanic ash as a control was tested for ryegrass (Cronin et al., 1998; Cronin et al., 1997). An interesting observation was that all depth treatments produced dry matter yields higher than the control, except for the 10mm treatment that was similar to the control. In this case, this experiment reveals a very thin margin between a critical depth of volcanic ash that is either beneficial or detrimental.

The physical damage to most vascular plants (xylem, phloem) depends on the morphology (size, leaves and age etc.) of an individual species (Mack, 1981). In the aftermath of the MSH eruption there were reports that photosynthesis almost ceased in some apple orchards where leaves received a 1mm coating of volcanic ash Cook et al. (1981). Hinkley (1987) explains that volcanic ash particles (<2 µm) caused clogging of the plants' stomata. Crops and fruit are acutely vulnerable to impacts by volcanic ash, especially if they are in their growing season. For instance, coniferous trees suffered from needle damage, with a normal temperature of 28°C and a calculated 34.8°C when a needle was ash covered (Seymour, Hinckley, Morikawa, & Franklin, 1983). Mack (1981) explains that beyond the burial and the breakage of vegetation there are impacts such as decreased plant growth, yields, as well as damage on leaves and fruiting plants. Vegetation where the leaves were covered with trichomes had significantly greater detrimental impacts than otherwise smooth glossy plants (Cook et al., 1981; Smith & Staskawicz, 1977). Black and Mack (1986) revealed that volcanic ash also has the potential to significantly alter the prevailing physical energy flux processes of the soil. This leads on to the influence of the chemistry of the soil profile through fluxes of elements in the immediate short term leading to changes in the soil properties in the long term.

Remobilisation of deposited volcanic ash is primarily the result of aeolian and fluvial processes (Ayris & Delmelle, 2012b). The aeolian remobilisation of volcanic ash occurs via wind and saltation of the fine particle component and is the more physically impacting of the two processes on vegetation (Scasso, Corbella, & Tiberi, 1994; Skidmore et al., 1994; Wilson, Cole, Stewart, Cronin, & Johnston, 2011). The remobilisation of deposited volcanic ash often continues for many years after an eruption, especially in dry semi-arid environments (Sneva et al., 1982). Problems with volcanic ash remobilisation were observed up to 17 years after the 1991 Hudson eruption (Wilson, Cole, Stewart, et al., 2011). Often, mature vegetation is more resistant to remobilisation while seedlings were either abraded or buried by moving dunes of ash. In the agricultural pastures where grass grew saltation acted to abrade plant tissue in what one farmer on the Atlantic coast described as “like sandpaper” (Wilson, Cole, Stewart, et al., 2011, p. 231). In the MSH event the remobilisation of volcanic ash did not impact agriculture due to the high rainfall climate of the cascades in Washington State in proximity to the vent and high vegetation cover where the distal ash fall impacted the Columbia River Basin (Fowler & Lopushinsky, 1986). By comparison, in the Patagonian region of Argentina, South America the rainfall gradient decreases from 4000 mm/year near the Andes Mountains to less than 200mm/year on the steppe region (Peri & Bloomberg, 2002; Stewart et al., 2016). Strong wind is a constant, with storms frequenting wind speeds of 120km/hour. Patagonia is also impacted by the Southern Volcanic Zone (SVZ) of the Andean volcanic arc and produced in 26 years three major VEI 4-5 eruptions (Craig, Wilson, Stewart, Villarosa, et al., 2016; Ruggieri et al., 2011). In Armbrust (1984), experiments on the effects of wind erosion and sandblasting on cereal crops found wind breaks were more important than the development stage of the plant to increase dry matter yields. However, the best way to mitigate the impact on vegetation by remobilisation is to actively encourage vegetation cover as well as reducing its disturbance (Fowler & Lopushinsky, 1986).

1.113 Ash ingestion by farm animals

Often, in the immediate aftermath of any major volcanic eruption there are significant agricultural impacts on animal health and these need to be considered with reference to both soil as well as vegetation, as shown in Table 1. Summary of the physical impacts on the three core aspects of agriculture by volcanic ash. Farm animals of a higher order, such as cattle and sheep, are the most at risk as they are exposed in the outdoors. The magnitude of the impacts on animal health are controlled by the characteristics of the volcanic eruption: grain size, duration and content of soluble elements in the volcanic ash (Wilson, Cole, Cronin, et al., 2011). Often, the cover of pasture with even thin thicknesses of volcanic ash makes it unpalatable for many farm animals. Grazing immediately after an eruption can lead to gastrointestinal problems. An ash 'brick' in the rumen forms, inhibiting digestion and leading to asphyxiation (Wilson, Cole, Cronin, et al., 2011). This was observed in farm animals immediately after the eruption of Mt. Hudson in 1991 where up to 1,000,000 individual animal deaths have been estimated (Wilson, Cole, Cronin, et al., 2011). Even if there is rainfall immediately after ash fall, if the volcanic ash is fine-grained it may not get washed off plant surfaces (Cook et al., 1981; Craig, Wilson, Stewart, Villarosa, et al., 2016). This was observed after the eruption of MSH (Cook et al., 1981). Often, this can lead to malnutrition and starvation for any farm animals that do not have adequate supplementary feed.

Furthermore, repeated grazing and drinking of food and water sources contaminated with volcanic ash can lead to teeth abrasion. The often reported cause of deaths of animals is starvation where pasture was either unpalatable or where animals refused to eat (Craig, Wilson, Stewart, Villarosa, et al., 2016). If an animal tries to graze ash covered pasture teeth were found to be worn down, sometimes almost to the gum line (Wilson, Cole, Cronin, et al., 2011). These problems were found aggravated in the dry semi-arid steppe with continual 'ash storms' (Wilson, Cole, Stewart, et al., 2011). The time in a yearly season with respect to agricultural practices when an eruption occurs is also a significant control. The largest eruption of Mt. Ruapehu during the 1995-1996 eruption episode occurred on 11 June 1996 in the middle of winter. This was a period of the year when the contamination of feed sources was exacerbated by high stresses and low feed quality. Cronin et al. (2003) explains that the 2000 ewes that died were pregnant and lactating. Analogous with Mt. Ruapehu, the much larger eruption of Mt. Hudson occurred at the end of winter prior to the establishment of new spring growth as well as pregnant and lactating animals (Craig, Wilson, Stewart, Villarosa, et al., 2016; Craig, 2015). External market values can also be a factor in the impact on animal health. The South American eruptions were accompanied by poor market prices due to the economic collapse in Argentina (Bank, 1993; Wilson, Cole, Cronin, et al., 2011). Also the pre-eruption climate can be a factor. The 2011 Cordón Caulle eruption coincided with a severe 6-year drought, which brought less than 160mm/year of rainfall onto an already semi-arid Patagonia (Stewart et al., 2016). This increased the livestock's vulnerability to being in a poor condition, with low availability of supplementary feed to substitute poor pasture conditions.

1.12 Chemical impacts of volcanic ash

Table 2: Summary table of the chemical impacts of volcanic ash on the three core aspects of agriculture

Type of Impact	**Impacts**		**Long term**
Soil	Δ Soil chemistry flux	Chemical weathering Δ	- Formation of clay Minerals - Alteration of plant chemistry physiology and ecosystem - Skeletal fluorosis - Feed contaminated
Plant	Δ Nutrient composition ↑ toxic elements	Chemical burns → acidity	
Animal health	↑ Risk of toxic elements Element solubility	Ruminants vulnerable Gastrointestinal	

1.121 Impact on soil chemical properties

The chemical impact of volcanic ash on the soil is primarily a result of the leaching of soluble elements, which results in a number of impacts (Table 2) on soil, plants and animal health. The past case studies of Mt. Ruapehu, MSH, Mt. Hudson and Mt. Paricutin show that the physical properties of the volcanic ash (particle size distribution, shape and depth of deposition) all serve to influence physical impacts. However, chemical impacts on the environment can be just as important and both simultaneously beneficial and detrimental.

In the Mt. Ruapehu eruption sequence the input of additional elements into the soil was demonstrated (Cronin et al., 1998; Cronin et al., 1997). The most enriched element was sulphate, the pre-eruption soil tests of the top 7.5mm found extractable sulphate 6 to 7 mg/kg versus 140-189 mg/kg, seven 7 weeks after 3mm of volcanic ash from the 14th October 1995 eruption was deposited at Ohinewairua Station (Cronin et al., 1997). After 21 weeks sulphur had decreased back to near pre-eruption levels, although total sulphate remained high (Cronin et al., 1998). On the other hand, the eruption of the Cordón Caulle-volcanic complex (CC –VC) was a much larger rhyolitic eruption than Mt. Ruapehu (Cronin et al., 1998) and a median of 20 mg/kg SO_4 was noted (Stewart et al., 2016). Inputs of trace elements were also found on volcanic ash from the Popocatépetl Volcano after the April 2012-2013 activity. Rodriguez-Espinosa et al. (2015) found enrichments of plant and animal essential copper and zinc (42.50%, 44.64% enrichment, respectively), as well as toxic arsenic and mercury. No published data has been found on the impact of the enriched soils on plant chemistry or dry matter yields. In the Mt. Ruapehu eruptions beneficial inputs of selenium were found, noted to potentially improve animal health (Cronin et al., 1997). Studies by Anda (2016); (Anda & Sarwani, 2012), on the Sinabung (2010-2013) and Merapi (2010) eruptions and their effects on rice paddy fields also recognise the short-term damage and potential benefits of volcanic ash deposition.

In the aftermath of the Ruapehu 1995-1996 eruption sequence Cronin et al. (1997) found that the fine-grained (<125 µm) sulphur originating from the hydrothermal system of Mt. Ruapehu caused a marked depression in soil pH levels. However, in pot trials low pH caused an increase in plant aluminium. In this environment Cronin et al. (1997) sampled three paddocks at Ohinewairua Station and found soil pH decreased 0.5 pH units from pH 6-6.1 before the large 11 October 1995 eruption compared to pH 5.5-5.7 in December 1995 (Cronin et al., 1998). Although not tested, the change in pH is likely to have unintended effects including the solubility of soil aluminium (Zheng, 2010). However, the input of sulphur into a soil that is naturally low in soil may result in an increase in the uptake of other soil nutrients (Cronin et al., 1997). Cronin et al. (1998) discuss that increases in potassium and phosphorous uptake were the result of relieving the sulphur deficiency. This is because both potassium, and certainly more so phosphate, had relatively low abundances in the ash leachate tests (Cronin et al., 1998; Edmeades, Thorrold, & Roberts, 2005; Nye, 1977).

1.122 Soil – long-term impact (volcanic soil formation)

The leaching of soluble elements from volcanic ash is considered a long-term impact as elements within the glass network structure start to be released as weathering takes place

(Smith, Zielinski, Taylor, & Sawyer, 1983; Witham et al., 2005). The impacts of slowly soluble elements from ash fall pose a bigger impact in the long term as these are derived from the mineral structure rather than adsorption within the eruption plume. The greatest of these impacts are the changes in the properties of the soil profile, i.e. the formation of volcanic soils (Shoji, Nanzyo, & Dahlgren, 1994). In a typical soil profile of a volcanic soil (Allophanic soil) the aluminosilicate clay minerals Allophane and Imogolite dominate. Allophane is composed of a nanostructure of hollow spheres with a diameter of 4-5nm (Parfitt, 2009). In comparison, the nanostructure of Imogolite is a hollow tube that has a diameter of 2.1nm with a wall thickness of 0.7nm (Parfitt, 2009). The availability and forms of aluminosilicates appear to be a significant factor in the synthesis of Allophane and Imogolite (Lowe, 1986). Another aluminosilicate clay mineral that is often found in soils which have been derived from volcanic ash is Halloysite. This mineral is primarily associated with Rhyolitic ash (Lowe (1986). Overall the formation of these clays relies on a complex set of parameters focused around Aluminium and Silica, the deposited ash composition and the drainage characteristics of the soil. A case in point is the Waikato region, where in some soils Allophane and Halloysite are close proximity to the same parent material, the main difference being the Halloysite is in poor-drainly drained soils while Allophane is in well-drained (Lowe, 1986; Molloy, 1988).

Anthropogenic fertiliser additions onto volcanic soils have also a marked, secondary and unintended side effect. Phosphate-based fertilisers have been applied to soils in the Waikato region. Enhanced weathering of Rhyolitic glass shards have been found by Taylor, Lowe, Hardi, Smidt, and Schnug (2016) in fertilised soils as opposed to unfertilised soils. Phosphoric acid and fluoride from the added fertiliser for at least 100 years in some cases have been attributed to have modified the soil chemistry, inducing ‘dealumination’ and ‘desilication’ (Kim, Taylor, & Drewry, 2016). This is the accelerated dissolution of aluminium and silica as evidenced by decreased glass shard sizes and a decrease in the sharpness and angularity of the edges (Taylor, Kim, Briggs, Taylor, & Guinto, 2012; Taylor et al., 2016). Therefore, the resulting release into the soil profile may accelerate the formation of secondary co-precipitated minerals including Halloysite and Allophane. This phenomena of the impacts of anthropogenic fertiliser applications has been relatively unexplored in the scientific literature (Taylor & Kim, 2010). This presents another potential hazard, the increase of fluoride concentrations in the top 10cm of surface soils from 220-440 mg/kg (Kim et al., 2016). Fluoride is a toxic element to animal health in large concentrations (Craig, Wilson, Stewart, Villarosa, et al. (2016). Soil tests by Kim et al. (2016) found 44% of soils exceeded 500mg/kg above the threshold for chronic fluorosis in animals.

1.123 Impact on plant chemical compositions

In the scientific literature particular concern has been expressed about the detrimental chemical impact of volcanic ash on vegetation. Acidity generated through the leaching of soluble elements out of ash deposited onto vegetation is the primary short-term impact of volcanic eruptions on vegetation (Ayris and Delmelle (2012b). The types of leaves of plants are critical to the magnitude of impact, with broadleaf plants and fruit being more vulnerable while needles are comparably more resilient (Antos & Zobel, 1985; Cook et al., 1981; Neufeld, Jernstedt, & Haines, 1985; Sneva et al., 1982). For instance, in the aftermath of the MSH eruption, blueberry crops suffered damage (Cook et al., 1981). In an eruption of 'La Soufiére' in Guadeloupe in 1976-1977, sulfuric acid (H_2SO_4) was thought to be responsible for the unmarketable form of that season's banana crop (Le Guern, Bernard, & Chevrier, 1980). Some native and pasture grasses were qualitatively observed to show acid damage, where yellowing and dehydration was observed after the 1991 Hudson eruption (Craig, Wilson, Stewart, Villarosa, et al., 2016; Wilson, Cole, Cronin, et al., 2011). However, volcanic ash does not have to come into direct contact with vegetation to have significant impacts. Acid rain and acid aerosols (SO_2) forming 'sulphurous fogs' have had detrimental impacts (Brayshay & Grattan, 1999). One of the most well-known case studies was the Laki basaltic fissure eruption of 1783-1784 (Thordarson & Self, 2003). This resulted in most vegetation being damaged or destroyed, and in some regions in Iceland it took up to 10 years for them to begin to return to normal (Thordarson & Self, 2003). Pasture in cultivated farmers' fields all withered and showed stunted growth (Thordarson & Self, 2003). Grattan and Pyatt (1994) described how following the Laki eruption acid impacts were recorded as far away as Scotland and Italy.

The chemical impact of volcanic ash on vegetation also far impacts what can be considered as beneficial. The input of agriculturally important nutrients into soil through volcanic ash deposition also unlocks opportunities to potentially reduce fertiliser applications (Anda & Sarwani, 2012; Rodriguez-Espinosa et al., 2015). After the MSH eruption, several reports stated there was an increase in the production of wheat in the following season in Washington State, although this has been attributed to a mulching effect rather than the added leached nutrients (Antos & Zobel, 2005; Burket, 1980; Cook et al., 1981). However, Mahler (1984); Mahler and Fosberg (1983); Mahler, Mc Dole, and Fredrickson (1984) performed experiments using 20%, 35%, 50% and 75% soil-MSH ash mixtures with eight different soils. The elemental concentrations (sulphur and magnesium) were higher than the control while enhancing calcium and phosphate. Furthermore, the dry matter yield also showed increases, although they were inconsistent across different soil types. In New Zealand, Cronin et al. (1998); Cronin et al. (1997), calculated that a thickness of 25mm of volcanic ash exceeded annual topdressing requirements for sulphate. In this country this is recommended to be between 10-12kg SO_4^{2-}/ha according to the Fertiliser Association of New Zealand. The input is especially important to plant nutrient requirements as the agricultural soils surrounding Mt. Ruapehu are naturally low in soil sulphur (Edmeades et al., 2005). Field herbage collections in the Northern Rangitikei following the 14 October 1995 eruption recorded increases of extractable sulphate contents of 140-189µg/g from 6-7µg/g pre-eruption (Cronin et al., 1998). In the much larger eruption of Chaiten in 2008, Martin et al. (2009) found changes in *B, Cd, Zn, Tl, Cu* and *Ni* in Coirón Grass 8 months after initial sampling the eruption. The copper and zinc concentrations stand out as essential minor nutrients to both vegetation and animal consumers.

1.124 Chemical impact on animal health

In the scientific literature the chemical impact of volcanic ash on animals, especially relevant to agriculture, has been a source of considerable study. The element that has received most attention due to its toxicity is fluoride (F^-) (Ayris & Delmelle, 2012b; Witham et al., 2005). The deposition of the volcanic ash onto soil and vegetation leads to the dissolution of adsorbed salts and aerosols, which then are leached and transferred into farm animals (Ayris & Delmelle, 2012b; D'Addabbo et al., 2015). Despite the reputation of fluoride there is no evidence of significant fluoride uptake by vegetation (McLaughlin et al., 1997). The Hekla eruption of 5 May 1970 sheds light on this, as grass tested where ash was 10mm thick found 4,300ppm F^- after 2 days versus <30ppm F^- after 40 days (Georgsson & Pétursson, 1972). Some F^- covered pasture concentrations exceeded 4000µg g^{-1}. Therefore, fluoride is absorbed on the ash surface instead of being taken up by the vegetation itself. Ozsvath (2009) explains that the adsorption and reaction of fluoride in an animal or human is dominated by the acidity of the stomach. Flueck (2016b) explains further the complex physiochemical environment in ruminant digestive tracts. Mastication of ingested pasture takes place in an alkaline pH (8.3) environment where volcanic ash particles are pulverised. This is manifested in the farm animals through wearing of teeth and dental fluorosis (Coote, Cutress, & Suckling, 1997; Craig, Wilson, Stewart, Villarosa, et al., 2016; Cronin et al., 2003; Georgsson & Pétursson, 1972). This increases the surface area of ash and the efficiency of the dissolution of fluoride. Neutral pH (7) occurs in the rumen with acid pH (1-2) in the final stomach (Flueck, 2016b). Such a complex environment implies that neither a water leach nor a single extraction gastric leach test can fully predict the potential fluoride toxicity (Cronin et al., 2003; Stewart et al., 2016).

The timelines of the deaths of farm animals are also variable after each case study eruption (Craig, 2015; Cronin et al., 2003; Stewart et al., 2016). It is pointed out in Cronin et al. (2003)

that the Hekla 1970 volcanic ash had highly soluble fluoride (Georgsson & Pétursson, 1972; Óskarsson, 1980). The 7500 animal deaths that occurred in the aftermath of the Hekla eruption of 1970 was easily attributed to acute short-term fluorosis due to the high F^- leached soil (Georgsson & Pétursson, 1972; Óskarsson, 1980). Óskarsson (1980) measured an ash-to-water ratio of 1:50 that yielded 1100µg g^{-1} F^- after 300 minutes, compared to 11.2µg g^{-1} soluble F^- from the 11 October 1995 Mt. Ruapehu eruption (Cronin et al., 2003). The differences in the soluble concentrations of fluoride that were leached influenced the thinking about the hazards to animal health in the Mt. Ruapehu and the Cordón Caulle 2011 eruptions where the occurrence of animal deaths was not anticipated (Cronin et al., 2003; Stewart et al., 2016). The animal deaths of Mt. Ruapehu and Cordón Caulle are more analogous with chronic fluorosis (Flueck, 2016b; Stewart et al., 2016). The time of eruption in regard to season needs to be considered. In the 11-12 October 1995 Ruapehu eruption, it was at the end of winter when feed was already low quality and the animals had high energy demands so were forced to eat the low quality feed that they may not have otherwise touched.

The 2000 sheep that died were also pregnant and lactating, increasing energy demands further (Cronin, Lecointre, Palmer, & Neall, 2000). Since feed is often of poor quality at the end of winter the increasing ingestion of soil increases animals to further ingestion of fluoride. The 9-day gap between deposition and death has been attributed by Cronin et al. (2003) to be due to the other physical impacts of volcanic ash deposition and general lowered resistance. The leachate geochemistry of the fluoride of Mt. Ruapehu may also be a factor, and the phreatomagmatic nature generated slowly soluble F^- compounds (CaF_2, AlF_3 and $Ca_5(PO_4)_3F$ (Stewart et al., 2016). Stewart et al. (2016) suggested also that multi-decade applications of phosphate-based agricultural fertilisers to New Zealand agricultural soils. This is an issue that has been expressed in New Zealand agricultural soils in the Waikato region, which have a high F content, and it may have pre-exposed livestock to significant F accumulation prior to exposure to the Mt. Ruapehu volcanic ash (Taylor & Kim, 2010; Taylor et al., 2012). In the aftermath of the eruptions in South America many animals refused to eat contaminated feed resulting in starvation estimated at 1,000,000 individuals (Craig, Wilson, Stewart, Villarosa, et al., 2016). The Cordón Caulle 2011 eruption presents interesting parallels. Flueck and Smith-Flueck (2013) explained that the volcanic ash was considered to be low in fluoride, which proved to be an under-estimation. In November 2012, red deer (*Cervus elaphus)* fluoride in bones was 5,175ppm, but by 2014 had reached a maximum of 10,000ppm (Flueck, 2016a, 2016b; Flueck & Smith-Flueck, 2013). These studies occurred in the semi-arid Patagonia region where volcanic ash re-suspension, together with conserved leaching due to low rainfall, is theorised to have increased the fluoride problem.

The detrimental chemical impacts of volcanic ash deposition on animal health have been well publicised in the scientific literature. Less exposure has been given to the potential benefits that volcanic ash may have on animal health. The influence on dry matter yields and vegetation chemistry of sulphur, calcium and potassium have been expressed (Cronin et al., 1998; Cronin et al., 1997). Another observation from Cronin et al. (1997) is that pasture selenium concentrations were elevated for 7 weeks after the 11 October Mt. Ruapehu eruption. Selenium is not essential for plants, although is important for the health of young growing animals where deficiencies have been associated with infertility and ill-thrift (Fordyce, 2013). The science of bio-fortification involves using vegetation grown on soils high in a desired trace element. Leachate and soil tests have also found enrichments of copper, zinc, iron and selenium and these are all important elements for the health of both vegetation and animals (Olsson, Stipp, Dalby, & Gislason, 2013). This is a potentially unstudied beneficial impact on animal health that has not been fully looked at. Zinc in New Zealand agriculture protects against fungal infection. Anderson, Robinson, West, Clucas, and Portmann (2012) found that bio-fortified fodder grown on soil with elevated zinc concentrations resulted in increased zinc duration in sheep as opposed to drenching. If research such as this was transferred into ash covered land this could provide a bio-fortified fodder of high trace element nutritional value.

1.2 Controlling factors of environmental impact

1.211 Components of eruptions

It is important to recognise that, once expelled, the fragmented magma evolves into pyroclasts in an eruption plume. The dynamics are dependent on particle morphology and atmospheric conditions. Terminal fall velocity (TFV) of individual particles is used to express the balance between gravity and the drag of the volcanic ash particle (Wilson & Huang, 1979). Explosive eruptions in addition to volatile gases expel variable amounts of black glass (Tachtylite) and light glass (Sideromelane), lithics, free crystals and volatile gases from the vent conduit, influencing the shape and the particle size distribution, (Cas & Wright, 1987; Fisher & Schmincke, 1984; Sparks & Walker, 1977; Zimanowski, Wohletz, Dellino, & Büttner, 2003). Alfano, Bonadonna, Delmelle, and Costantini (2011) found the TFV calculated for particle size diameters up to 125µm are not significantly impacted by particle shape and componentry, resulting in a similar TFV for this size fraction. The mode of particle size distribution decreases in grain size diameter from the vent (Bagnato et al., 2013; Rubin et al., 1994; Witham et al., 2005). Large particles preferentially settle with a high TFV near source (Folch, 2012). The TFVs of 0-125µm are influenced by aggregation causing preferential settling/deposition. Deposited particle size distributions exceeded the calculated TFV for the individual particles in several important case studies for large Plinian eruptions (Brown, Bonadonna, & Durant, 2012; Textor et al., 2006), including Mt. Hudson, from 12-15 August 1991 (Scasso et al., 1994) and MSH on 18 May 1980 (Durant, Rose, Sarna-Wojcicki, Carey, & Volentik, 2009; Sarna-Wojcicki, Shipley, Waitt Jr, Dzurisin, & Wood, 1981).

An eruption column contains abundant volatile gas species in addition to volcanic ash particles (Ayris & Delmelle, 2012a; Brown et al., 2012; Delmelle, Lambert, Dufrêne, Gerin, & Óskarsson, 2007). In an eruption plume, the dominant volatile gases released are water vapours called ‘hydrometers’ (Lathem et al., 2011; Textor et al., 2006), and gases of lower concentrations include SO_2, HCl and HF (Rose, 1977). These gaseous compounds are considered to be originators of salt and liquid acid aerosols (Mather, Pyle, & Oppenheimer, 2003). Volcanic aerosols have particle size distributions up to 1µm and are derived from a range of microphysical ash/volatile gas interactions: nucleation, condensation, adsorption and aggregation processes (Belosi, Santachiara, & Prodi, 2011). In a short duration eruption, plumes undergo temperature gradients from 1000°C to an ambient temperature. The Eyjafjallajökull 2010 eruption presents the best studied recent eruption plume. This eruption highlights the duration and the distance of aerosols compared to volcanic ash in the atmosphere. Compositions of in-plume aerosols sampled by Andersson et al. (2013) were dominated by products of sulphur dioxide oxidised to sulphate aerosols and lesser HCl and HF. Detections of an aerosol plume above background levels were found at Mt. Cimone, Italy at a distance of 3000km from Eyjafjallajökull (Sandrini et al., 2014). Eyjafjallajökull was a relatively minor Plinian eruption (Mereu, Marzano, Montopoli, & Bonadonna, 2015), demonstrating the far-reaching impact of even small explosive eruptions several hundred kilometres from their source.

1.212 Adsorption of volatile gasses in the eruption plume

Table 3: Table of leading hypotheses of adsorption of volatile gases by volcanic ash (also featured are the leading experiments on the adsorption of the primary anion donors)

	Temperature	**Overall plume model**	**Furnace experiment** **(Ayris, Cimarelli, et al., 2015)**		**HF = experiment**
	Eruption plume zone	**Óskarsson (1980) hypothesis**	**Ayris et al. (2014) (HCl)**	**Ayris et al. (2013) (SO_2)**	**Óskarsson (1980)**
Salt formation	600 >1100°C	Cl^-, F^-, S^{2-} + metallic volatiles Formation of salts leads to reaction with ash	Limited Cl^- dehydroxylation +(OH^-) decreased sustained uptake/exchange	SO_2 adsorption @ Ca-O Diffusion of Ca^{2+} - SO_4 Initial $CaSO_3 \rightarrow CaSO_4$ (>600°C)	Decreased HF due to dehydroxylation on (F^-) means CaF_2 complexes
Surface adsorption	<600°C	Halogen gases leads to direct interaction with particle	Adsorb HCl = Cl^- salts + chloride minerals: Na^+ exchange	Disproportionation (<600°C) = $CaSO_3$ = $CaSO_4$ & CaS	Increased efficiency aerosol adsorption NaF, CaF_2
Condensation dew point	338°C	H_2SO_4 condenses (190-200°C)	Surface adsorption continues	Oxidation SO_2 to H_2SO_4 aerosol @ (190°C - 200°C)	~
	120°C	Halogen acids condense: HCl, HF	~		~

It has long been known that the interaction of volcanic ash and volatile gases produces soluble leachable elements. The first known study was published from the 1906 eruption of Mt. Vesuvius where it was found that pristine volcanic ash leached soluble elements (Lacroix, 1907). The first study that produced a plausible model on the origin of soluble leachable elements from volcanic ash was proposed by Óskarsson (1980), who proposed that condensation, sublimation and adsorption of the volatile gases on the surfaces of volcanic ash particles occur in three main temperature regimes (Bagnato et al., 2013; Witham et al., 2005), (Figure 1). Óskarsson (1980) evaluated the results of the earlier studies (Rose, 1977; Taylor & Stoiber, 1973), and those from laboratory experiments, and studied the 1970 sub-Plinian Hekla eruption in Iceland. The main evidence is from leachate studies and gas adsorption experiments finding soluble compounds leached by solvents (Witham et al., 2005). The model that is proposed by Óskarsson (1980), however, has some slight methodological errors, but it has remained the main eruption plume model of leachate adsorption for 37 years as at 2017. In Table 3, the main temperature perimeters of the three-stage temperature dependent model. Each zone is associated with a specific type of chemical reaction involving the state of acidic magmatic gases (Cronin et al., 2003).

The first zone of the temperature model is considered to be above 700°C, which is at the very core of the eruption plume near the vent (Óskarsson, 1980), (Figure 1). This zone is characterised by magmatic temperatures and is often referred to as salt formation zone (Delmelle et al., 2007). This extends down to the magma fragmentation zone, (Figure 1).

Delmelle, Gerin, and Oskarsson (2000) explain that aerosols of microscopic crystals react directly with volcanic ash to form sublimates of halite and sulphide salts such as NaCl and $CaSO_4$. Although little direct evidence of the chemical reaction has been found, Naughton, Lewis, Hammond, and Nishimoto (1974) sampled directly above the Mauna Ulu lava pool in Kilauea Volcano. They found sulphate (SO_4^{2-}), chloride (Cl^-) and fluoride (F^-) in the high temperature low oxygen environment in the form of salts and increasing oxidation of sulphates with increasing exposure to oxygen. However, considering Naughton et al. (1974), it could be argued that it is not necessary to call this a separate temperature regime as the study focused on small basaltic eruptions and may not reflect the conditions of the larger explosive (e.g.) Plinian eruptions. However, an important finding of the study is that the elements start in the form of volatile gases, which react and evolve with volcanic ash particles in reducing conditions, near the fragmentation zone during subsequent oxidation and cooling in the atmosphere (Naughton et al., 1974).

One of the main processes of gas-particle interaction is thought to be the direct adsorption of gases at temperatures zones between 700°C-338°C (Óskarsson, 1980), (Figure 1). This is known as surface adsorption where HCl, SO_2 and HF acid magmatic gases react with volcanic ash (Armienta, De la Cruz-Reyna, Morton, Cruz, & Ceniceros, 2002; Cronin et al., 2003). It is thought to be the key reaction where cations leach. Cations react according to their position within the silicate network of the volcanic ash particle. The specific origins of major cations still causes some controversy (Bagnato et al., 2013). Most research into the origins of cations can only be done through gas adsorption experiments, Table 3: Table of leading hypotheses of adsorption of volatile gases by volcanic ash (also featured are the leading experiments on the adsorption of the primary anion donors) of Óskarsson (1980) experimented with HF-H_2O fumes at 1100-150°C. Finding HF adsorption low at 700°C (CaF_2), however, increased linearly below 600°C (CaF_6Si) to 1500ppm. Ayris et al. (2013); Ayris et al. (2014), conducted SO_2 and HCl adsorption experiments on Tephrite, Phonolite, Dacite and Rhyolite glass compositions between 200°C-800°C, respectively. HCl adsorption (He-SO_2 and CO_2) is sustained by the diffusion of Na^+ from the glass surface exchanging and being replaced with $H^{+,}$ resulting in NaCl salts on the glass surface (Ayris et al., 2014). Maximum efficiency of uptake had a range between 400°C-600°C, whose upper limit is controlled by Cl^- dehydroxylation, while its lower limit is governed by aerosol condensation. In comparison, Ayris et al. (2013) experimented on sulphur dioxide (SO_2), which has a maximum uptake at 600°C-800°C with diffusion of Ca^{2+} forming $CaSO_4$ (Gypsum/Anhydrite). Adsorption below 200°C is limited by the dew point temperature where H_2SO_4 forms instead (Mather et al., 2003).

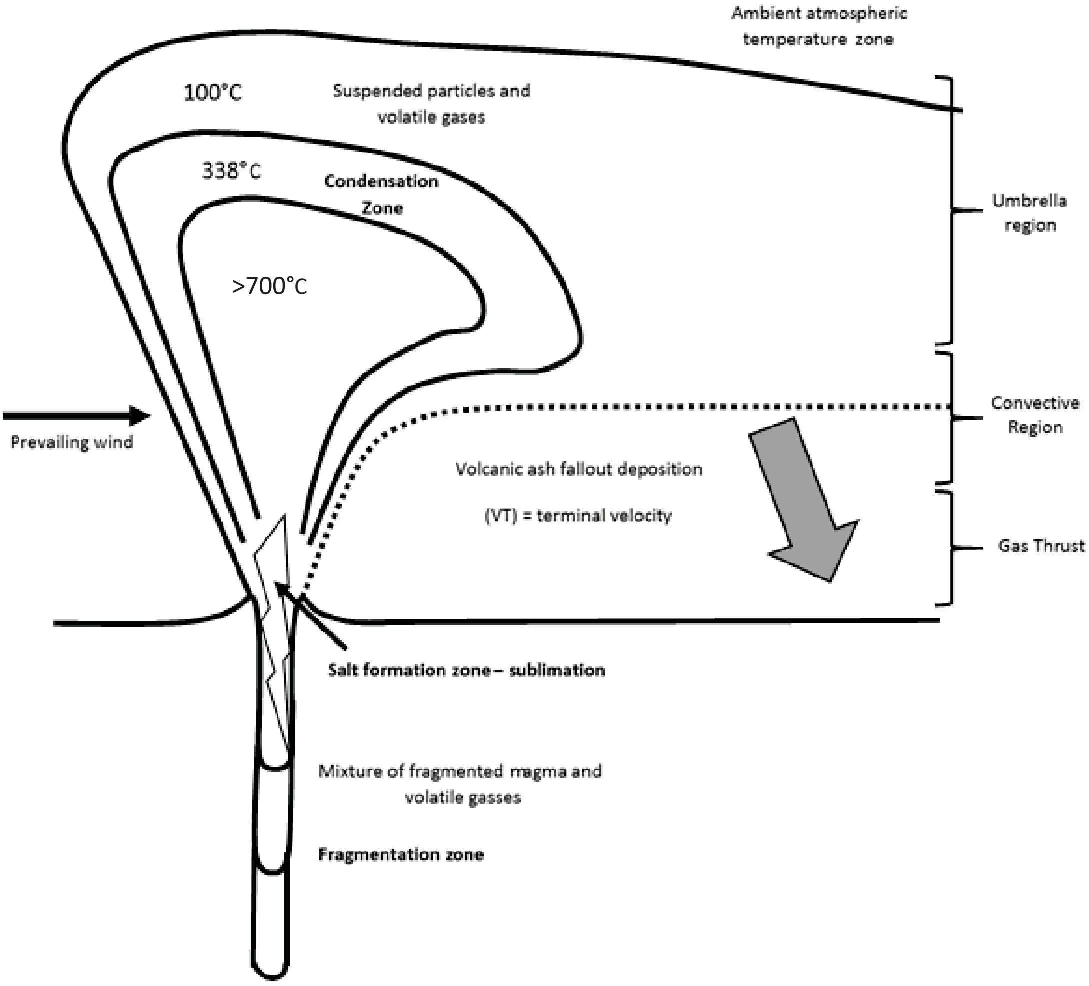

Figure 1: Schematic diagram of the three temperature zone model that was proposed by (Óskarsson, 1980). Modified and redrawn from: (Cronin, Neall, Lecointre, Hedley, & Loganathan, 2003).

The process zone that has the most influence on the leachate content of the volcanic ash is still controversial in the scientific literature. Rose (1977) postulated in Central America that leached soluble elements originating from the dissolution of the volcanic ash particle. It was concluded that the leached material was deposited during the eruption via precipitation of volatile liquids and gases as aerosols. Rose (1977) suggested that aerosols of acid 'attach themselves' to ash particle surfaces and react with the volcanic ash surface (Cas & Wright, 1987). Óskarsson (1980) calls this the 'condensation zone' in the atmosphere. In ambient temperatures below 338°C an anion such as H_2SO_4 sulphuric acid is the first volatile gas to condense into an aerosol followed by the halogen acids below 120°C. These anions combine with hydrometers to form aerosols (Cronin & Sharp, 2002). The most well-known of these aerosols is H_2SO_4, where the SO_2 gas forms H_2SO_3, which rapidly oxidises to form H_2SO_4 (Ayris et al., 2013; Naughton et al., 1974). In this zone of formation, the largest particles of volcanic ash cool slower if they have not preferentially fallen out of the eruption cloud (Gilbert & Lane, 1994; Scasso et al., 1994). The condensation of acidic liquids on fine particles occurs as they cool quicker and remain longer in the eruption plume and have a larger surface area. Thus, on a general basis, major cation concentrations such as calcium and sodium have been found to increase linearly from the source, which indeed occurred in Eyjafjallajökull in 2010 (Bagnato et al., 2013).

Analysis of volcanic ash by X-ray fluorescence has found liquid phases on the surface of volcanic ash. The analysis of the recent eruption of Eyjafjallajökull agrees with the theory that the condensation of acidic anions dissolves the particle surface, thus being the key origin of cations (Bagnato et al., 2013). The process of aerosol condensation onto volcanic ash was postulated by Óskarsson (1980) to be driven by precipitation onto volcanic ash particles due to a decreasing ambient temperature. However, this neglects the role of water in the volcanic plume, which is the dominant volatile gas. Mueller (2017) conducted an interesting study on the effects of water, atmosphere and aggradation on ash leachate compositions. The deposition of liquid aerosols in the condensation zone also dissolves existing salts on particle surfaces (Mueller, 2017); Mueller, Kueppers, Ayris, Jacob, and Dingwell (2016). Capillary forces will naturally result in the liquid travelling to particle contact points, and subsequent precipitation will cement the particle aggregate. Also explained in Durant et al. (2009); Textor, Graf, Herzog, and Oberhuber (2003), is that H_2O in a liquid form nucleates and condensates around ash particles which freeze between $^{-}$23.15°C to $^{-}$13.15°C. This is also influenced by the conductivity and acidity of the liquid, making the freezing and precipitating temperature highly variable. Therefore, an individual particle will have been through multiple adsorption and reaction processes before reaching the ground (Bagnato et al., 2013).

1.213 Origin of trace elements

In comparison, the origin of the trace and minor elements is much less clear cut, and literature on the concentrations of trace metals is generally rare or absent from the scientific literature (Armienta et al., 2002; Bagnato et al., 2013; Delmelle et al., 2007). Ash leachate trace metals form predominately from volatile magmatic gases or diffusion from the volcanic ash particles and form compounds. For example, cadmium (a volatile trace element) may form CdCl or CdS although this is challenging to prove due to low detection levels and almost certainly with strong Cl, F or S compounds. Moune, Gauthier, Gislason, and Sigmarsson (2006) in a study about the 2000 Hekla eruption found through stoichiometry that ash plumes rich in fluoride have enhanced rare earth element enrichment in the deposited volcanic ash. Experiments using enrichment factors (EF) by Bagnato et al. (2013) found that copper and zinc were the most enriched trace elements. However, their transport is difficult to distinguish (Moune et al., 2006; Naughton et al., 1974) and the most probable origins of zinc and copper are via ZnS, CuS and $ZnCl_2$ compounds.

Selenium in leachate concentrations has been reported in environmentally significant concentrations in the Mt. Ruapehu eruptions (Cronin et al., 1998; Cronin et al., 1997). These are theorised to be derived from magmatic gases rather than diffusion by acid aerosols (Floor & Román-Ross, 2012). Bia, Borgnino, Gaiero, and García (2015) found that the speciation and release of arsenic on ash surfaces was via the aluminium-silicate glass structure. The content of the mobile fraction arsenous acid $As(OH)_3$ is consistent with surface enrichments, although volatile acids can dissolve the main structural arsenic. Iron is another element that has garnered attention in the scientific literature. Ayris et al. (2014) found in their experiments that HCl adsorption forms soluble iron salts, which is significant as iron has been known as an element with low volatility at magmatic temperatures (Ayris & Delmelle, 2012a). In this case the pH of any liquid is believed to control aqueous iron dissolution from the silicate structure (Hinkley, 1987; Jones & Gislason, 2008). However, the composition of the eruption as well as the amount of volatile elements released in an eruption has primary control over the release of soluble trace elements.

1.3 Current leachate methodology and its benefits to hazard research

1.311 Current laboratory analysis techniques

The main laboratory methodology for the analysis of water and acid soluble elements on volcanic ash is done through batch leaching extraction tests of volcanic ash samples. It is clear from recent reviews of the scientific literature on the leaching of volcanic ash by Witham et al. (2005) that the wide variety of leaching perimeters and techniques used negates any credible comparison between studies. Stewart et al. (2015), from the International Volcanic Health Hazard Network (IVHHN), present an overall protocol for analysing the soluble volcanic ash. First, the collection of the volcanic ash is important and they carefully note the conditions especially if it is pristine and has been rained on (Hinkley, 1987). Splitting of the bulk sample into weighed sub-sample proportions for analysis needs to be done with a Jones splitter to prevent the settling of grains of different sizes. The ash is added to centrifuge tubes where the leaching solution is then added with an automatic pipette, deionised water or HCl for a gastric leaching experiment. Recommended rations of ash (g) to solution (ml) are 1:20 and 1:100. Stewart et al. (2015) explains that both of these ratios have drawbacks because there is a compromise between elemental detection limits, saturation and re-precipitation of secondary mineral phases. To ensure complete contact between the solution and sample, the centrifuge tubes are placed onto an end-over-end shaker for 60 minutes, termed ‘contact time’. Then are put in a centrifuge for 3 minutes at 3000-5000 RPM to settle the samples. Immediately either vacuum or syringe filtration is then prepared through 0.45µm filters. The resulting filtered sample is analysed for pH, conductivity, major cations, anions and trace elements. Lessons learned from Cronin et al. (2003) mean that two to three re-extractions are necessary to ensure the prevention of incomplete extractions to counter any drawbacks due to the short contact time.

The leachate methodology protocol of Stewart et al. (2015) remains the only published proposal put forward for a unified methodology. However, reviews by Ayris and Delmelle (2012b); Ayris, Delmelle, et al. (2015); Witham et al. (2005) comparing multiple studies have advocated for its inception. Witham et al. (2005) identified many major differences across the methodologies in the published literature. This includes, but is not limited to, contact time or agitation ranging between 3 minutes to 24 hours. Some studies do not report agitation at all. The ratio of volcanic ash to water is also of significant importance. For example, Ruggieri et al. (2012) used a ratio of 1:10, which is viewed by Stewart et al. (2015), with the results potentially skewed by saturation problems. Differences also apply across the published literature on the same volcanic eruption.

In the past, there has been literature on the inadequate accounting of sampling procedures, weather conditions, plume spatial characteristics, PSD and componentry (Witham et al., 2005). The best example is the 1980 MSH eruption that still holds the highest number of studies after any volcanic eruption. Ayris, Delmelle, et al. (2015) conducted a retrospective analysis of leaching results on abundances of Ca, Cl, Na and S. A total of ten studies were published on the leaching of the volcanic ash from MSH. However, only 20% of the dataset of the 10 studies totalling 302 analyses were able to be used together. Ayris, Delmelle, et al. (2015) encountered inadequate reporting and descriptions of the sampled volcanic ash deposits. To date, there has only been limited uptake of the new Stewart et al. (2015) methodology in the published literature. This could be in part due to the small number of scientists studying the topic as much as reluctance. Where the Stewart et al. (2015) methodology has been used, for example, Te Maari, 2012 (Cronin et al., 2014) and in South America (Craig, Wilson, Stewart, Outes, et al., 2016; Craig, Wilson, Stewart, Villarosa, et al., 2016; Stewart et al., 2016), the results have proven concise. The most important mechanism is to note in detail what was done even more than the results themselves.

1.312 Scientific relevance: applications of leachate studies

Ash leachate studies, in addition to answering questions on environmental impacts and the processes and origins of adsorption, have been used as proxies for in-plume gas compositions (Witham et al., 2005). The compositions of volcanic ash leachates are related to volcanic activity in a non-linear manner not fully understood in the scientific literature (Bagnato et al., 2011). Evaluations are universally done through evaluating S: Cl: F ratios, to determine changes in plume chemistry and eruption style (Rose, 1977; Smith et al., 1983). Bagnato et al. (2013), in a study about the 2010 Eyjafjallajökull eruption, compared the results of direct sampling of gases in the eruption plume and leachates. Bagnato et al. (2013) found that ash leachates are not representative of the gas concentrations of the eruption plume. Also reactions between S: Cl: F, although certainly volcanic in origin, are gas-specific (Armienta et al., 2002). Fluorine in the form of hydrofluoric acid in the eruption plume reacts three times faster than sulphur and chlorine. Also, evaluating fluorine reactions in the eruption plume has proved difficult, Ayris, Cimarelli, et al. (2015). However, it is known through experiments that glass dissolution increases 10-fold in the presence of fluoride compounds in acid geochemistry (Wolff-Boenisch, Gislason, & Oelkers, 2004; Wolff-Boenisch, Gislason, Oelkers, & Putnis, 2004).

Nonetheless, ash leachate tests reveal a lot of information from leaching volcanic ash with either water or acid. Although not fully representative of the eruption plume dynamics individually, studies about Mt. Ruapehu, South America and Indonesia show that ash leachate compositions are important to ascertain environmental impacts (Anda & Sarwani, 2012; Ayris & Delmelle, 2012b; Craig, Wilson, Stewart, Villarosa, et al., 2016; Cronin et al., 1997). On a general basis most of the soluble salts leach almost immediately from volcanic ash when contact occurs with water, either in the form of precipitation or in an open water body (Olsson et al., 2013; Ruggieri et al., 2012). Time is a critical component when volcanic ash leachate results are applied to the geochemical impacts on an environment. Studies such as Cronin et al. (1998); Cronin et al. (1997); Stewart et al. (2016) can only estimate the total input of elements through leaching or soil and vegetation sampling. There have been a small handful of experiments published where leaching with columns has been used rather than bulk leaching in centrifuge tubes. These studies calculate chemical fluxes in the laboratory (Jones & Gislason, 2008; Olsson et al., 2013; Ruggieri et al., 2012).

These experiments use a single pass continuously flowing with a plug flow-through reactor, using a methodology first used by (Frogner, Gíslason, & Óskarsson, 2001). In the Jones and Gislason (2008) study, their aim was to investigate the geochemical impact of eight different volcanic ash samples into aqueous environments such as into lakes or oceans. Initial experiments ran for 8 hours and some continued for 24 hours. Ruggieri et al. (2012) used samples from the 2008 Chaitén Rhyolitic Volcano where column experiments were used to evaluate the temporal mobility of soluble toxic trace elements and estimate its environmental availability. Their column was similar to that of Jones and Gislason (2008). They called the results the 'environmentally available amount' and estimated the total mass of each element that has entered the environment. Lastly, Olsson et al. (2013) used volcanic ash from the 2008 Grímsvötn eruption in a flow-through reactor similar to the methods of the following studies (Frogner et al., 2001; Olsson et al., 2013). Their conclusions were similar to other studies (Jones & Gislason, 2008; Ruggieri et al., 2012) where the rapid dissolution of surface salts gave way in time for the dissolution of crystals and glass itself. Although, these experiments reveal a lot of information, it needs to be noted that the solute flow in this methodology is continuous. This is ideally suited for simulating the impacts on water sources of weather on a lake, river or ocean where this flow in mimicked well. However, on land within the soil profile, the water flow processes are considerably different. Water flow is not continuous, but is a process of filling, saturation and rapid drainage as rainfall occurs.

1.313 History of the soxhlet reactor

Research was conducted into defining a methodology where the chemical weathering of rocks and other natural materials was occurring in the 1960s. The two experimental conditions were absolutely essential for the validity of this methodology to approximate natural conditions, maintain atmospheric pressure and to maintain a temperature less than 30°C. The main problem facing Pedro (1961) was that the human lifespan is relatively short in comparison to the chemical weathering process. The answer was to increase on a simulated basis the time and thus the speed it took each natural geochemical process to occur within a laboratory setting. Pedro (1961) used the principle of water as the main solute in free drainage conditions as it takes place in the natural environment. A Soxhlet reactor apparatus, with a set-up drawn in Figure 2, proved to be the ideal tool for simulating weathering in natural conditions. The Soxhlet reactor itself is not a new invention, as it was first used in 1879 by Franz von Soxhlet for the determination of fat in milk (Soxhlet, 1879).

The operating principle of a Soxhlet extractor is where a sample is leached by renewed/distilled water (Pedro, 1961), Figure 2. The deionised water in the reservoir continuously boils and evaporates. The water vapour ascends till it condenses inside a condenser attached to the Soxhlet extractor. Then the water drips down into the sample till the water reaches a level where it is the same height as the syphon, then it discharges back into the reservoir where the cycle begins again. The flow rate is a function of the temperature of water in the reservoir and the Soxhlet reactor. The set-up can be manipulated to control the temperature and flow rate (Yao et al., 2010).

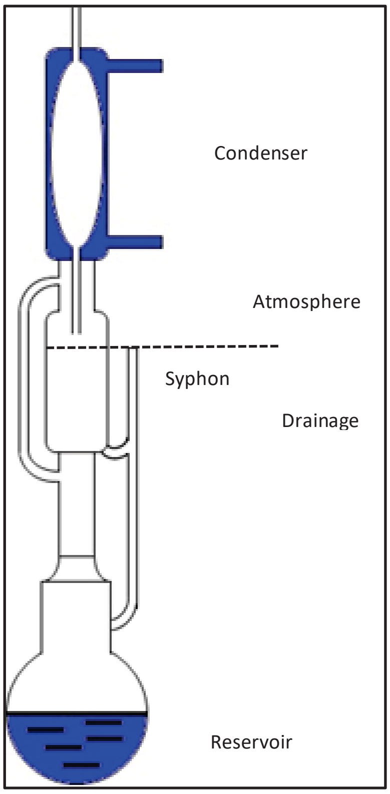

Figure 2: Schematic diagram of the original unmodified set-up of the Soxhlet reactor in experiments during research in the 1960s. Recent experiments highlight variations of this method. Modified after (Pedro, 1961).

1.313 Geoscience applications of soxhlet reactors

Despite the ground-breaking nature of the research by Pedro (1961), the succeeding literature has not been possible to obtain beyond limited citations. Despite an exhaustive search little was found for 36 years until Humez, Humez, Juste, and Prost (1997); Humez and Prost (1999), published papers on evaluating the durability and mobility/kinetics of elements from solidified/stabilised waste. Yao et al. (2010) similarly used the Pedro (1961) methodology to evaluate the release kinetics of biochar made from sewage sludge. Humez et al. (1997) modified the Soxhlet reactor so that the water temperature was between 14°C and 18°C rather than the 30°C used by Pedro (1961); Yao et al. (2010). This is the approximate temperature of the soil profile (Aldridge, 1982; Aldridge, 1983), although there Is a cosine variation throughout a typical day.

Humez et al. (1997); Humez and Prost (1999), studied the processes behind the kinetics of the weathering of waste material. They found that the geochemical process of elemental release begins with the dissolution of soluble salts and compounds, transitioning into the diffusion of the matrix surface reactions taking place in the long term. Humez et al. (1997); Humez and Prost (1999), emphasised the importance of the surface area of a sample as a key perimeter that dictates the reaction capacity of a sample in addition to its mass (Delmelle, Villiéras, & Pelletier, 2005). In addition, the term 'equivalent time' was first used (Humez et al., 1997; Humez & Prost, 1999). Equivalent time is defined as the time that a sample in a Soxhlet reactor under laboratory conditions would take to be released in the natural environment (Humez (1996). Mathematically, it is the idea used in Humez (1996) and (N. Humes, Personal communication, 12 October 2016) to compare and evaluate the amount of leached elements. This means that in addition to the physical and chemical properties of the volcanic ash sample the climate can be studied.

Chapter 2 Methodology

2.0 Preparation of volcanic ash

Table 4. Table of samples of volcanic ash collected for this project suitable for further analysis. Information about the details of the 1995-96 Mt. Ruapehu eruption sequence as well as the three international samples are presented.

Sample Name & Source	Location – Distance	Eruption Style	Date
(95/5) Lower Layer	Mangatoetoenui Quarry – *15 km*	Phreatomagmatic – Magmatic	11-12 October 1995 – *(25 x* $10m^3$*)*
(95/5) Upper Layer			
(95/8) Ruapehu	*18 km*	Dry Magmatic	14 October 1995 – *(5 x* $10m^3$*)*
(96/7) Ruapehu	*85 km*	Phreatomagmatic-Magmatic	17 June 1996 – *(5 x 10* m^3*)*
(96/46) Ruapehu	*8.7 km*	Strombolian	20 July 1996 – *(0.01 x* $10m^3$*)*
Weathered Ruapehu	Pit – *30 km*	Assumed 11 October	1995 - 1996
Sakurajima	Kagoshima Prefecture, Kyushu Japan – *10 km*	Vulcanian	18 August 2013
Kelut	East Java, Indonesia – *210 km*	Phreatic – lava dome	14 February 2014
White Island	NE Crater Rim – 300m	Phreatic – vent clearing	28 April 2016

2.1 Obtaining volcanic ash samples

The foremost task was to obtain suitable samples of volcanic ash from relevant eruptions. The criteria of a volcanic ash sample included that it needed to be in a suitable amount and had appropriate preservation without post-collection processing. The preference was that samples be collected immediately after a volcanic eruption within hours. Time was of the essence because environmental factors soon altered the preservation of deposited volcanic ash. The volcanic ash samples which were considered suitable are outlined in Table 4. Furthermore, since the writing of this thesis in 2016 and 2017 there has been a quiescence of sizable eruptions within mainland New Zealand. Therefore, it was necessary to rely on samples that had been previously collected after past eruptions and were in storage rather than collected directly from the field.

The volcanic ash samples used in this project were from the Mt. Ruapehu eruption sequence between 1995 and 1996. This was both the most recent and the largest volcanic eruption in mainland New Zealand. The suitable volcanic ash samples pertaining to this eruption were found at Massey University. The identifiable details of the volcanic ash sample sachets in two storage containers were from Cronin et al. (2003). The sample labelling in this project is hence modified after those of (Cronin et al., 2003), (Table 4). The unique aspect of the 1995-1996 Mt. Ruapehu eruption sequence is the variability in eruption styles from the same source, detailed in Table 4. A Mt. Ruapehu eruption of significant note is from the largest one on 11-12

October, referred to as sample (95/5) Lower and Upper Layer in this project (Table 4) for recording purposes. These samples appeared unprocessed after collection.

The larger amounts of volcanic ash samples stored at Massey University about the Mt. Ruapehu eruptions were from the 1996 series of volcanic eruptions. The skewing in the amount of 1996 samples meant that volcanic ash from eruptions on 18 June 1996 and 6 July 1996 were not required in this project. Furthermore, much of the volcanic ash deposited onto the roads surrounding Mt. Ruapehu during the eruption sequence was dumped into a pit in the vicinity of Lake Otamangakau (A. Moebis, Personal Communication, 15th September 2016). This had been collected by Massey University for another unrelated summer scholarship project in 2016. This particular sample had been leaching in the natural environment for the 20 years since deposition. Since the experiments have considerable reference to time, having a sample with a known time component will validate some experimental hypotheses.

For the purpose of comparison to contrast the impacts of the differing volcanology between volcanic eruptions, three samples that were erupted in overseas eruptions were also used in this project, Table 4. The unique nature of the volcanic ash from White Island made this an ideal sample to use in this project. The source of the volcanic ash was the eruption on 28 April 2016. The sample itself was collected from the North East rim of the crater by GNS scientists, Table 4. Dr Carol Stewart, a Senior Research Fellow at the Joint Centre for Disaster Research with (Massey University/GNS), obtained 70g of sample to be allowed for use in this project. Two other overseas samples were collected from Professor Shane Cronin from Kelut and Sakurajima, Table 4. The Kelut sample was originally obtained from a distal sample in Yogyakarta City early on the day of 14 February 2014 from the roof of the National Department University in Yogyakarta for the study (Blake, 2015). This was approximately 210km from the source at Mt. Kelut. The Sakurajima sample was obtained from the roof of the Department of Earth and Environmental Sciences at Kagoshima University in Kagoshima City, a distance of approximately 10km from the vent. The recent nature of these eruptions (Table 4) within the last three to four years also provided a unique opportunity. To evaluate the different properties of the volcanic ash would draw out any different or unique results in the planned experiments.

2.112 Initial sample processing

In this thesis the samples of volcanic ash (Table 4) that were used in the experiments were in large bulk packages. Other volcanic ash samples originating from the eruptions of Mt. Ruapehu prior to 11 October 1995 had been processed into different grain sizes. Therefore, these potentially valuable and rare samples were unable to be used due to inadequate labelling (A. Moebis, Personal Communication, 15th September 2016). Furthermore, the processing required to split the bulk samples that were originally at Massey University into amounts suitable for the analysis was done by using two Jones splitters, which were ideal to prevent a bias from occurring to the grain size distribution of a sample if it became graded in the sample bag. These Jones splitters were of different sizes, Figure 3. The large Jones splitter was used in splitting bulk samples into sub-samples for particle size distribution, componentry and Soxhlet experiments. Another issue always occurring with splitting is the constant danger of loss of sample and contamination. Loss of sample was due to the fine-grained nature of volcanic ash causing it to become airborne due to air turbulence. In addition, contamination by foreign trace elements is also a hazard of volcanic ash samples for this project as well as those of other laboratory users. This was rectified in this project by using makeshift dust covers with cardboard, Figure 3. This was important because some of the samples were small and could ill-afford to be carelessly lost.

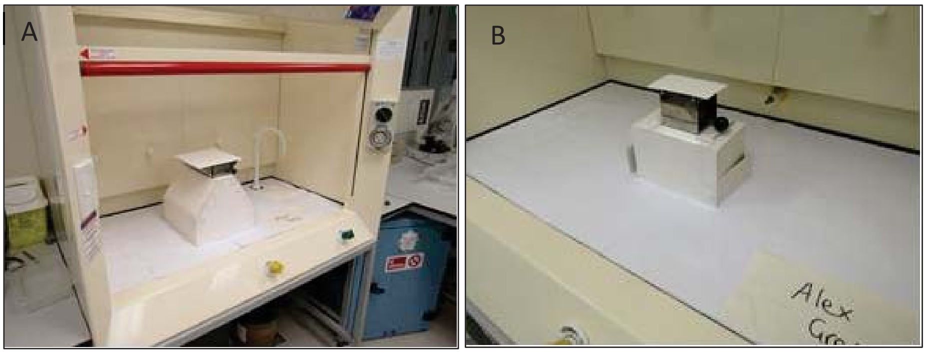

Figure 3: The Jones splitter in (a) was used to take sub-samples from the original large sample, (b) was used for smaller splitting requirements including grain size distribution analysis and preparing of Soxhlet samples. Both have dust covers to minimise loss of fine volcanic ash particles.

2.2 Describing volcanic ash samples

2.211 Particle size distribution (PSD)

The sieving was conducted by on a general basis sieving by hand with the brass volcanology hazard solutions sieves in ½ Φ phi intervals from 16000µm down to 500µm. The samples that were below the 500µm grain size fraction were put into the laser particle analyser (LPA). This sieving was conducted in a way to prevent to the best of my ability loss of additional sample. As soon as shacking done, it was left it for at least 3-4 minutes to allow the agitated dust that was stirred by the shacking motion to settle before dismantling the sieves. A small brush was used to clean each sieve to ensure as much of the fine ash particles as possible were not lost. As with the Jones splitter, splitting with a sieve was done in the same fume hood, Figure 3, to prevent contamination of both the project samples with free-floating dust as well as those of other users of the laboratory.

The shacking for sieving was in a side-to-side rotating motion. This was found through trial and error to be the best way to handle the sieves while also not developing repetitive strain injury. Once a sieve fraction had settled after the shaking, they were collected into an additional sieving pan. The sieve was placed onto the pan upside down to make sure any grains still stuck in the wire grates were not lost. Then the sieved fraction was poured into pre-weighed pink top (50ml) containers and immediately weighed again on a two decimal place set of scales. The weight of the ash could then be subtracted from the empty weight of the pink top. The weighing was done immediately, ensuring insufficient record keeping did not compromise the grain size distribution. It was also to ensure that the data was collected accurately and that there was no accidental mixing of the results.

Although the methodology of the sieving the course fraction (16000-500µm) was identical for all nine subsets of volcanic ash samples there were some differences. Furthermore, the whole sample was sieved in ½ Φ phi and even less when only the 0-2000µm was counted. This is because 2mm is categorised in the literature as the boundary between volcanic ash and lapilli (Cas & Wright, 1987). This was dependent on the amount of sample that was available; 5g was required for the ICP-MS and 25g for the Soxhlet reactor. The 95/5 upper and lower samples had a maximum of 40g bulk available (unsieved), the small size of the whole sample required it to be sieved down to 500µm. All other volcanic ash samples that were going to be analysed further needed to be split because of the volume for both analyses – between 30-35g was needed. The remaining seven were split again with Jones splitters into P35 containers, with leftover material to be used as a reference sample for future use. The Weathered Ruapehu ash was only sieved >2mm fraction. That this sample did not require splitting and grain size analysis as the information revealed would not be scientifically credible.

2.212 Laser particle analyser (LPA)

The samples that were split below <500µm were put through an LPA, specifically, a laser scattering particle size distribution analyser (LPA) LA 950V2 manufactured by the Horiba company based in Japan**.** This instrument is designed to analyse particles between 0.01-3000µm (Horiba, 2017). The fundamental way an LPA works is a particle will scatter light from a laser beam in a specific way that corresponds to the size of that particle. According to Horiba (2017); (Moebis, 2011) a small particle (<0.01µm) has wide angles and large particles (>0.01µm) have small angles. The angles of this scattered light are calculated into a partial size distribution using the Mie theory of optical principles. Therefore, a refractive index is also required and this is an important setting that has to be set in the LPA. For the majority of the volcanic ash samples that were dark grey in colour a refractive index of 1.56 was used in the LPA. The visibly lighter Kelut and White Island samples were analysed with a refractive index of 1.53 instead.

The LPA required a very small amount of volcanic ash. To ensure accuracy, each of the eight volcanic ash samples was replicated in the LPA three times. The resulting data in the form of a Nonogram puzzle file was exported from the LPA program as a text file. The resulting text files were then saved as in the excel file format as a comma separated values file. The data was processed from these files into eventual particle size distributions.

First, the frequencies of the three subsets from each volcanic ash sample were averaged together forming eight datasets. Then the course tail (16000-500µm fraction) that was hand sieved in ½ ɸ phi fractions in the form of weight (g) classes. A problem arose because the LPA averaged results (4000-0.11µm) were in ¼ ɸ phi and the coarse results were in ½ ɸ phi. In excel the solution was to add the ¼ ɸ phi together to form a ½ ɸ phi, such as 0.5 ɸ + 0.25 ɸ in (¼ ɸ phi) would be equal to 0.5 ɸ in (½ ɸ phi). The next task required the coarse tail results to be added to the fine LPA results. The coarse tail was calculated to equal the weight percentage of the sample weight taken over to the LPA. The LPA results were in the percentage of the fine sub-sample, not the total sample. Therefore, the LPA value in (½ ɸ phi) was multiplied by the weight percentage of everything lower than 500µm then divided by the sum of all of the LPA results below <500µm. This is because 500µm is the maximum grain size fraction. However, because of the needle shapes of amphiboles and pyroxenes there was an overlap in the results. It was decided to truncate all of the LPA results above the 355µm category. Finally, a histogram of the grain size distribution allowed for comparison and interpretations of the data.

2.213 Geometric surface area – SSA_{GEO}

Data parameters gathered from volcanic ash samples, in addition to leaching concentrations, are critically important in placing the leaching results into context and aiding in the eventual interpretation. Parameters include grain size analysis and point count componentry. The particle size distribution (PSD) of a sample of volcanic ash was among one of the easiest to measure in a laboratory. The scientific consensus is that the finer the mean of the particle size distribution the more the soluble material will leach. This is because of the higher surface area of particles of smaller diameter and the consequential increased residence time inside the plume and the atmosphere. However, calculating the surface area of volcanic ash is one of those complicated things in volcanology. The default method of calculating the surface area is via the adsorption of gas in molecular layers onto the surface of an individual particle; this is called BET (Brunauer, Emmett, & Teller, 1938). Stewart et al. (2015) emphasise using the time-consuming and costly BET method to calculate the surface area. Delmelle et al. (2005) reveal that this method of the calculation of surface area has unintended complications and volcanic ash readily absorbs water higher than predicted by nitrogen gas. This facilitates the need for careful consideration of the methodology and the results pertaining to the surface area calculations.

The method of using a Soxhlet reactor in this project for the analysis of volcanic ash means that the texture of the particle size distribution and, consequently, the surface area has a significant influence on the results (Humez & Prost, 1999). In the scientific literature, PSD is frequently applied in a qualitative intellect rather than in a quantitative mathematical calculation. However, a relatively uncommon calculation was found called the geometric specific surface area (SSA_{GEO}) (Ayris, Delmelle, et al., 2015; Bagnato et al., 2013). This is a promising new calculation that could create a less complicated way to calculate an estimated surface area. The equation to SSA_{GEO} was initially complicated to find the formula, due to its sparsity and lack of explanation in the scientific literature. Elena Maters (Personal Communication, 8 April 2017) was one of the co-authors of Ayris, Delmelle, et al. (2015) and recommended (Brantley, White, & Hodson, 1999; Wolff-Boenisch, Gislason, & Oelkers, 2004) as detailed references. First, Equation 1 gives the effect of particle diameter *(deff.)* of each bin in the PSD in m^2. Then Equation 2 provides the geometric surface area within one bin. The density was estimated from the average of volcanic glass and was measured in grams per metre cubed. The final step was to multiply the overall SSA_{GEO} and each bin by the weight of each sample particle size bin, individually from each volcanic ash sample. This gives the total geometric surface area in meters squared. In this case, for PSD the particles are assumed for simplicity, to be cubes. The geometric surface area is one number that can be used to calculate the flux of elemental release, thus accounting for the sample methodology more accurately than any other currently known method.

$$deff. = {}^{(D\max - Dmin)}\Big/_{In\,(\frac{Dmax}{Dmin})} \quad \text{Equation 1}$$

$$SSA_{GEO} = {}^{6}\Big/_{((26\,\times 10^{6}) \times deff))} \quad \text{Equation 2}$$

2.214 Componentry of volcanic ash

An important aspect of describing volcanic ash in addition to the grain size distribution is evaluating the amounts of ratios of juvenile fragments (volcanic glass), free crystals and lithics. Point counts of volcanic ash samples used in the Soxhlet reactor experiments are of significant importance. The abundance of glass, lithics and free crystal fragments in comparison to each other manifest themselves directly in the results of the Soxhlet reactor experiments. The exact rations and content of the constituents depend on the eruption and fragmentation processes occurring in the eruption. Juvenile fragments are derived from chilled melt and are almost directly from the erupting, fragmenting magma. These are differentiated into black coloured glass (Tachylite) and light coloured glass (Sideromelane) (Cas & Wright, 1987; Fisher & Schmincke, 1984). Free crystals or pyrogenic crystals (Fisher & Schmincke, 1984) represent the crystallisation that took place prior to fragmentation. Lithics fragments are differentiated into cognate lithics (from previous eruptions) or accentual lithics (from the sub-volcanic basement).

In this thesis, point count componentry analysis is conducted in full phi Φ fractions from 2000µm down to 125µm. The original plan was to conduct componentry point count analysis concurrently with the grain size distribution work. As the volcanic ash samples would already be split, this was a mistake where a small fraction of grains from the samples could have been taken, especially if they had been put into full Φ phi prior to them all being put together. However, 5g ICP-MS samples needed to be prepared and sent as soon as possible to Hills Laboratories as analysis duration was approximately 2 weeks. The sieving for the componentry analysis was done using a set of small sieves in full Φ phi. Altogether eight of the samples were split into their full Φ phi components. As illustrated in Table 4, the majority of the volcanic ash samples had a sufficient amount left over for componentry. For the 95/5 samples this was not the case; the 95/5 Lower Ruapehu sample 7.54g had to be split from the Soxhlet sample. For the 95/5 Upper Ruapehu layer there was 8g of sample leftover that was suitable. After the sieving was completed the split full Φ phi fractions were sealed in small size plastic Ziploc® bags and then put inside one large bag per volcanic ash sample (eight altogether).

The method that was used to conduct the point counts themselves was to line them up on the glass plate and count them that way. Any organic material is not counted in this analysis and is to be removed from the sample. It was discovered that the White Island, Kelut, 96/7 and the 95/5 upper and lower samples required washing to remove clay-sized grains adhering to the grains. This hindered identification of the component. Each fraction was placed in a 100ml beaker and filled with deionised water then placed in an ultrasonic bath. Successive 3 minute washes were done until the water remained clear. It has been statistically proven that a representative sample needs to have counted 300-500 individual grains. If a size fraction has less than 300 grains available it is still important to note how many and the components observed. The componentry point counting methodology itself was the first to use a metal spatula to scoop a few out of a plastic packet and onto a glass pane. Once all of the grains have been sorted into their components the next step is to begin counting them. This was done with the aid of a Leica WILD MZ8 low power binocular microscope with a SCHOTT KL1500 lighting source. Also a Watson Victor Ltd NZ Swift Model F point counter helped to keep track of these point counts.

2.3 Soxhlet reactor experiment

2.31 Soxhlet reactor preparation

In the experimental methodology using the Soxhlet reactor there are two main parts that require careful attention and handling. The first is the preparation of the volcanic ash sample as it is loaded into a cellulose extraction thimble. This process must be done carefully and did not change throughout the course of this experimental methodology. The second area is the sampling leachates from the Soxhlet reactor which are conducted at pre-planned times measured by the duration of the initial cycle which is called Time = 0. This cycle is always longer than the others as it has more space to fill as it is saturating the sample from a completely dry state. Similar to the methodology of Yao et al. (2010), this sample was treated separately. In this experimental sequence there were two main methods by which this was conducted.

The preparation of the volcanic ash sample before placement into the Soxhlet apparatus is an important aspect of this experimental methodology. As outlined previously, how the 25g of volcanic ash material is obtained from the original sample is of vital importance. A mass of 25g of volcanic ash was used to enable a ratio of 1:10 to deionised water, although in hindsight maybe more research into an optimum ratio of sample to solvent should have been continued. The correct procedure to obtain a sub-sample of 25g of volcanic ash is to use a Jones splitter. This ensures as much as possible to maintain a grain size distribution similar to the bulk sample. The less time-consuming method was to use a small spoon instead. This was done with the Sakurajima and the Kelut samples. However, when processing a bulk volcanic ash sample into a sub-sample a spoon should never be used (A. Moebis, Personal Communication, 15 September 2016). Also the grain size of volcanic ash is limited to <2mm. Therefore, wire mesh sieves were used to filter out larger lapilli and ballistics (Cas & Wright, 1987). However, in the rest of the sample these mistakes were not completed, with splitting and sieving occurring as part of preparing the samples for grain size analysis.

Once a sample of 25g of volcanic ash, stored in a pink top container, was obtained that had been sieved to filter out the grains larger than 2mm it was time to transfer the sample into a cellulose extraction thimble. This was done in an isolated weighing room with the aid of a three decimal place scale, Figure 4. Also seen is a plastic cover on the scales, and this was because a constant problem was the air circulation causing unstable and inadequate readings. This served to shelter the sample and substantially improved stability. The first step was to place a new 50ml pink top container onto the scales and then zero them. This was important as these cellulose extraction thimbles have a round bottom and thus putting them in an open pink top bottle would help hold them. Then the thimble was weighed and subsequently recorded. Then while still on the scales a small plastic funnel similar to the one in Figure 5 was placed in the cellulose extraction thimble. This aided the next step of adding the volcanic ash, which was done by pouring the ash from the pink top, with the funnel helping to minimise spillage of the sample. A small spatula was used to tap gently on the outside to encourage the sample, although it would sometimes become clogged. A small brush would then ensure the smaller fine grains were not clinging to the side of the funnel.

Even with the funnel some of the fine grains would cling to the sides of the thimble, and again a gentle tap from the metal spatula would encourage them to fall to the bottom. Again the resulting weight was recorded. Then a small amount of glass wool was taken from a Ziploc® bag and put into the top of the cellulose extraction thimble. Then a pair of plastic tweezers was used to push the roll of glass wool to ensure it was next to the sample of volcanic ash. In this step the only opportunity arose where possible compaction would take place, and there was no set agenda in the methodology to compact the volcanic ash samples. However, this was not the aim of this methodology in this experiment and all efforts were taken to ensure this was not the case, as freshly deposited volcanic ash (as was attempted to be replicated here) would not have been compacted either.

Figure 4: The three decimal place scales used for preparation of the volcanic ash sample in the cellulose extraction thimbles. Note the plastic case on top of the scales.

Figure 5: The set-up and measurement of 250ml of deionised MilliQ® water into a boiling flask with the aid of a funnel as seen above.

2.31 First version of soxhlet reactor experiment

The first methodology began with the preparation of the sample of volcanic ash as has been outlined previously. In this methodology, the initial preparation phase consisted of filling and pre-boiling the available (round bottom) boiling flasks with 250ml of deionised water, Figure 5. At the beginning of this experiment six boiling flasks were available. This number decreased during the course of this experiment due to the cracking of the borosilicate glass. It was initially thought that using deionised water unheated straight from the measuring cylinder and pouring it straight into the Soxhlet would be suitable. It was expressed that the thermal shock with the cold water and the hot boiling flask may be enough to break the glass as happened previously. Therefore, to ensure the temperatures of the empty boiling flasks and the incoming water were as equal as possible the 250ml measuring cylinder ensured that volumes remained consistent. Three or four anti-bumping granules were added to each boiling flask, ensuring a calm bubbling to reduce instability. To pre-boil the flasks they were placed on a long heater set to high in a fume hood. A water condenser held by clamps prevented the loss of sample in this process through evaporation. While the pre-heating preparations were happening the clamp was undone and the cellulose extraction thimble placed in the Soxhlet reactor sleeve with the volcanic ash sample inside.

In light of the previously mentioned issues that arose due to the broken 250ml boiling flasks, and the fact that there was not an inexhaustible supply, the need arose to develop a methodology that ensured the equipment was kept intact as well for health and safely. The issue to devise a safer method change for the boiling flasks was also a factor. There was no easy method to remove the boiling flasks themselves. It was duly suggested by the laboratory technicians that using a pump to suck out the sample may be the most ideal method. The idea of using the boards to remove the flasks themselves after an experiment was suggested by Graham Freeman. The previous trailed method involved lifting up the whole Soxhlet apparatus and sliding the heater out and quickly substituting it for a lab jack – a two-person job fraught with hazards. It was enough for the heater to be 20mm lower to be slipped out from under the Soxhlet set-up safely, Figure 6. The clamp was moved to the bottom of the three-way intersection so the boiling flask would be held in location.

An old pump originally used for vacuum filtration was sitting on the bench adjacent to where the Soxhlet reactor was set up, Figure 7. A few further modifications were made, including setting up moisture traps and later a bath of cool water in the red tray. The moisture trap prevented moisture from entering the pump and causing serious damage to the mechanism of the pump. The moisture traps consisted of a pair of Büchner flasks with another to collect the sample.

Originally only one moisture trap was set up, although the high amount of condensation in the single trap in pre-experimental trials prompted a back-up moisture trap to be added. To put in a new pre-boiled sample the glass stopper on the top-middle of the three- way intersection was removed and, with the aid of a plastic funnel, poured in the fresh deionised water. The 250ml of deionised water was left to boil, taking an average of 46-60 minutes. So planning this step ahead of time was essential. However, it is also important to note that the first initial Time 0 sample is expected to have a longer cycle time than succeeding cycles. The Time 0 was the only sample not pre-heated, remaining at room temperature (20°C). This was when the sample underwent saturation, so thus it was hypothesised it would take longer than successive cycles. As the Time 0 cycle is the determinant cycle for when other samples were taken there was little point in pre-heating. However, this did not turn out to be the case even though fresh samples were boiled beforehand and were poured in as there was still cracking of the flasks. When this methodology was used for the Sakurajima volcanic ash sample there was the constant sound of glass shattering and cracking every time a new sample was poured.

When the deionised water level inside the Soxhlet reactor sleeve had reached the level of the siphon, the water drained to the boiling flask. This was the time in the experiment of the schedule which called for it to collect the sample. The leachate sample was collected using the pump. This process was identical for all samplings that were conducted with this first methodology. A glass tube was attached to the pump via rubber tubing and the Buchner flasks.

The rod was placed through the middle of the three-way intersection, shown in Figure 6, and this allowed the bottom of the glass rod to reach the bottom of the boiling flask.

Teething problems persisted as the old heater cycled for an average of 12 minutes and ran hotter than the new Thermolyne, Type 1000 heater that cycled in 20 minutes. This was difficult to fix as the emphasis was on maintaining a constant temperature of 20°C +/- 2°C in both reactors. Also the purpose of having two similar heaters was they would perform at similar specifications and allow for replications. This was also why the newer Thermolyne, Type 1000 had two layers of time foil wrapped around the boiling flask to try to increase efficiency and to make them more even in cycle time. Since this was no longer the case, the decision was made to just use one of the heaters. The experimental methodology where the pumps and two heaters were used was only successfully used with the Mt. Sakurajima volcanic ash sample. Also this was the only time where two Soxhlet reactors were used.

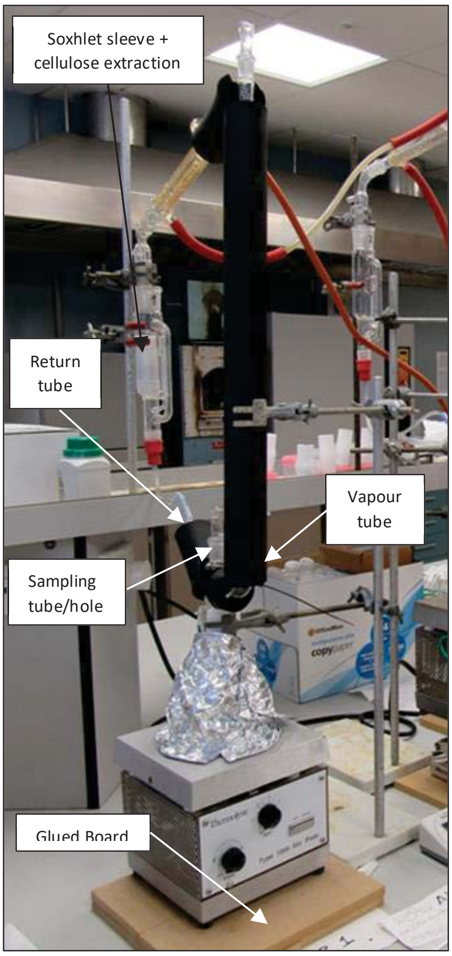

Figure 7: Original pump configuration. Note the white circle indicating placement of clamps on the retort stand.

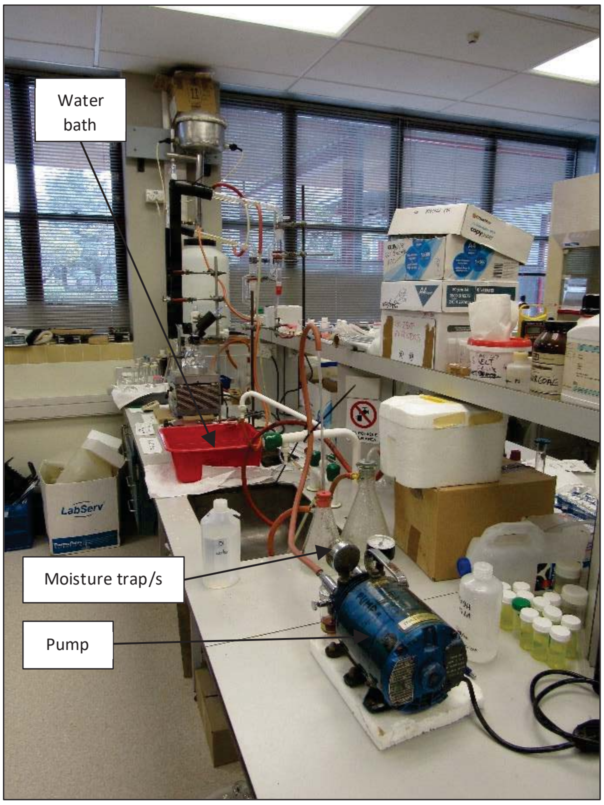

Figure 6: Illustrates the configuration used in the first methodology with the use of the pump.

2.32 Second methodology of the soxhlet reactor experiment

The second methodology as outlined previously has some significant modifications based on the first methodology. However, the beginning preparation of the volcanic ash sample remained consistent throughout the nine samples that were tested. This methodology was used with the remaining eight volcanic ash samples. The main modification in this second methodology is how the leachates were sampled. Instead of pumping from the boiling flask, the Soxhlet apparatus was modified so that the heater was placed on a laboratory jack. This methodology was designed to prevent the problems with breaking boiling flasks through thermal shock as was found in the first methodology. Some of the specificatons on the first methodology remained the same, especially in the preparation phase. As in the first methodology, the first step was to fill the 250ml boiling flask with 250ml of deionised water and then put it in the fume hood to reach boiling point. Also another boiling flask was filled with 250ml of deionised water at room temperature as was done with the initial Time 0 in the first methodology. This boiling flask was placed in the Soxhlet underneath the three-way intersection and tightened with a clamp. The laboratory jack, which was in the down position, was then wound up so that the aluminium hotplate sat snug against the boiling flask. Note that only one heater (the new Thermolyne, Type 1000 heater) was used in this methodology. The heater was set to a dial setting of 6, as this corresponded to a temperature of 20°C water dripping into the sample using a thermocouple, Figure 8.

The initial Time 0 sample was treated in the same way as in the first methodology where it was collected separately and the time of sampling dictated subsequent samples. However, the time regime sampling was changed slightly where instead of something every cycle in the first hour sampling on the first day it was done once every hour after Time 0 to 6 hours. The sampling regime continued normally once daily as in the first methodology. However, as mentioned previously collecting the samples was different. When our sampling cycle had completed and it was time to sample, the first task was to wind down the laboratory jack isolating and separating the heat and thus stopping the cycle, Figure 9. Then using a thick wool glove the boiling flask was removed after undoing the clamp and placed in a 500ml beaker filled with cold tap water. This was a two-fold function, first to cool down the sample, and secondly to serve as a holder before the well-known next step was completed. The next step was to remove the two layers of tinfoil that acted as insulation which in turn acted to increase efficiency of heating. Again, using the wool glove a fresh sample was collected and preheated from the fume. This was placed in the Soxhlet reactor in the same identical method as was the first time 0 sample – the only difference was that this sample was already preheated. The laboratory jack was then wound back up and the cycle allowed to proceed. The last step was to replace the two layers of tinfoil around the boiling flask in the soxhlet reactor which had been removed.

Figure 8: The thermocouple used in monitoring the temperatures of the water dripping into the Soxhlet reactor holding the volcanic ash sample.

Extra insulation plus zip tie added (right-hand side)

Figure 9: Two different methodologies, 1st on the left, modified 2nd methodology on the right. Note, Black line shows the 10cm needed to raise the modified methodology.

2.314 Sampling regime over experimental time via time

The sampling regime for the first methodology had an emphasis on time. For the first 2 hours of sampling the brine, the frequency was for every cycle. Therefore, it was essential for maximum efficiency and turnaround time to have as many 250ml boiling flasks with fresh samples being pre-boiled. While this step ensured the cycles were kept timed for the 2 hours keeping up with the demanding regime sometimes resulted in mistakes being made. This is the case with the first methodology when the Sakurajima volcanic ash was trailed because there were two Soxhlets going at the same time. The probability of unforced errors increased with the demands of two Soxhlets to sample. Although in theory spacing the two Soxhlets 10 minutes apart should have prevented any double-ups, but the faster running time of the old heater made this a repeating recurrence. This rapid sampling regime made it vulnerable to missing sampling. In fact, on the first day that the first methodology was tried, mistakes were made to the degree where the data could not be considered for this experiment.

Once the two hours were concluded the sampling frequency decreased significantly. In the first methodology sampling took place in the succeeding 2, 3, 4 and 6 hours after the first Time 0 cycle had been sampled. Then sampling was done on a daily basis until the total 168 hour time was completed. However, the frequency of the sampling could not be extended more than 24 hours apart. A continuing loss of sample occurred to the extent that the final brine sample ended losing 150-100ml of water over 24 hours. Therefore, decreasing the frequency between sampling would have resulted in a complete loss of sample. During the second methodology (Figure 12), the sampling regime was modified during the first day. From 24 hours onwards, the brine sampling regime remained identical.

After each sampling of the soxhlet reactors when it was convenient the pH as well as the electrical conductivity was measured. First, the samples were removed from the chiller room where they were stored temporarily. The samples were then allowed to warm to room temperature before any analysis had begun. The electrical conductivity is a direct measure of the dissolved salts that may be present in the sample. In this experiment a Hanna Instruments HI 2300 EC/TDS/NaCl meter was used. The probe for this instrument is a little different in that it does not sit in any solution, rather it is left in open air. This was the first meter used before the pH meter, because the pH probe leaches Cl^- to obtain a soluble pH reading. The radiometer analytical model: PHM210 interlab was the standard pH meter that was used. This was also one of the reasons that one of the P35 35ml containers of sample was kept apart specifically to measure the electrical conductivity and the pH. In the case of measuring the Soxhlet samples, it was in the period before the measuring for the Ion Chromatography.

2.4 Analysis of volcanic ash leachates

2.411 Total recoverable metals (ICP-MS)

In addition to the leaching of water soluble elements from volcanic ash samples, it is also important to know the percentage of element that was leached compared to the total amount that is available to leach. This test is called a ‘total recoverable metals test’ (TRM) conducted at Hills Laboratories in Hamilton, New Zealand. An inductively coupled plasma mass spectrometry instrument was used. Hills Laboratories used a methodology that was recommended by the United States Environmental Protection Agency (Creed, Brockhoff, & Martin, 1994; Martin, Creed, & Brockhoff, 1994) where volcanic ash is digested with nitric and hydrochloric acid. Hills Laboratories required to be prepared: 5g of volcanic ash sample split from the sub-samples with the small Jones splitter, Figure 3. In addition, the samples were sieved to <2mm diameter in accordance with the categorisations of volcanic ash (Cas and Wright (1987); Fisher and Schmincke (1984). Finally, each sample was put into a P35 container to be sent to Hills Laboratories. The only sample that did not require a Jones splitter was the Weathered Ruapehu sample, only sieved to remove grains >2mm. This was because the already unknown nature of the sample made a grain size scientifically irrelevant (A. Moebis, Personal Communication, 28 September 2016). This was due to the fact that the sample had been disturbed periodically from when this particular ash was scraped from the main highways.

Stewart et al. (2016) explain that TRMs are representative of the maximum possible immediate elemental input released by volcanic ash deposits (Cronin et al., 1997; Ruggieri et al., 2011). However, the terminology of TRM needs to be checked carefully. This issue was initially debated, however, as this problem in reality was found to be much simpler and easily explainable. It lies in the terminology and the assumptions made based on TRM concentrations. This was initially thought to mean the total concentration of each of the 17 elements analysed and each of the nine volcanic ash samples. It was clarified that this was the total acid soluble elemental concentration, not the 'total' concentration (C. W. N. Anderson, Personal Communication, 2nd February 2017). It was pointed out that a similar situation occurred at the Waikato Regional Council. This was the reason that the organisation had opted for a very strict classification on the term 'total recoverable metals' test. Applying this new assumption to the Hills Laboratories results provides a satisfactory explanation of the results exceeding 100%. It was only the method of using a Soxhlet reactor and applying the second objective of putting a time constraint on volcanic ash leaching that brought about this finding.

2.412 Microwave Plasma Atomic Emission Spectrometer (MP-AES)

The MP-AES model: 4200 was manufactured by Agilent Technologies, Figure 10 In this analysis of the trace elements and the major cations there were four separate planned analysis runs. The sample preparation required was to filter with Whatman #42 ash-less 110mm diameter filter papers.

In order to reduce the amount of pre-analysis labelling and increase the efficiency of the process the sample labels that were categorised in order of volcanic ash sample were substituted for numbers. The same order of numbers and samples were maintained throughout the analysis. These were easier to write and thus would be more legible on the computer that operated the MP-AES instrument. The filtered samples from the P35s were later poured into 10ml polyethylene test tubes that were placed in the auto sampler. There was 2% HNO_3 required in order to clean the sampling probe of the instrument and this had to be periodically refilled. There were four separate analyses conducted with 14 different dissolved elements that tested for in the MP-AES. Once the preparation was done the test tubes were placed in the auto sampler. If the MP-AES worked to its specifications then that was all the work that was needed to be done before the completion of the analysis.

In order to ensure the methodology of the elemental analysis was accurate, some of these elements required further preparation than the filtering. This was the case with the major cations in Run #4. All of these elements (Ca^{2+}, K^{+}, Mg^{2+} and Na^{+}) are known to interfere with the major wavelengths. This distorts the ability of the MP-AES to read the concentration accurately. The solution to use an ion suppressant was necessary in order to suppress any unwanted wavelengths that can interfere with the MP-AES reading the solution. An ion suppressant Sr, Cs & Cl solution, with a 10,000ppm concentration had to be amended in the samples. This was done through using a pipette to form a mixture of 9ml of original filtered sample and 1ml of the ion suppressant. To ensure accuracy, two different pipettes were used, one for each sample. A pipette was calibrated to 9ml for the original sample and a smaller 1ml pipette was calibrated for the ion suppressant.

Figure 10: MP-AES instrument in the foreground and the automatic sampler in the middle nest to the computer.

2.413 Ion Chromatography (IC)

Ion Chromatography was the instrument that was used for the analyses of the anions, (Figure 11). Here there was a significant amount of preparation that was required before the analysis of the leachates could begin. The Ion Chromatography instrument itself is a DIONEX AQUION model manufactured by Thermo Scientific with a DIONEX AS-HV auto sampler also manufactured by the Thermo Scientific Company. It was an alternative to MP-AES which measures the wavelengths that each element emits, thus requiring ion suppressants for major cations that are not required with the IC which is a direct measurement. Instead, in summary an eluent (opposite charge) is combined with a sample of anions, which are separated in a column according to their electric conductivity (EC $\mu S\ cm^{-1}$). A subsequent detector measures the EC after a suppresser reduces the eluent background noise and increases that of the sample anions. The eluent used in this analysis is bicarbonate, HCO_{3^-} and it is the default eluent for anion analysis. As in the suppresser, carbonic acid (H_2CO_3) is formed and this carries the fully dissociated anions (increased in sensitivity) to the detector. Thus, the carbonic acid results in a low pH 4 eluent and a high sample pH will therefore increase retention so detection results in the end.

The only reference was from similar analysis that some of the environmental soil scientists had conducted. It was speculated that Cl^- & SO_4^{2-} should not be affected by a pH alteration and neither would NO_3. Fluoride is an uncertainty, although it is regularly adjusted to pH 8.5 for ion electrode F measurements in soil science, so F^- should not be a problem. A key note here though is that none of these conclusions were from other ash leachate analysis. This is instead of plants and soil, which have little resemblance to the primary products of volcanic ash. Further concern was expressed with the Fe and Al and how they will change as the pH of the sample is adjusted, where the phosphate may be precipitated out of solution. The calculated iron concentrations went to the IC manufacturer to evaluate what would constitute a high amount as this had not been previously stated.

The most important anions in this study were fluoride (F^-), chloride (Cl^-) & sulphate (SO_4^{2-}). At the time of the analysis the other elements (nitrogen, bromide and phosphate) were not considered to be important. This was also reflected in the results. Low amounts of these elements were detected, except for White Island which will be discussed later. Furthermore, due to the high (pH 6-7) requirement to be able to analyse the volcanic ash leachate samples because of the eluent, the general agreement reached on dealing with this issue was to raise to either a pH 7 or pH 8 with a 0.1 M $NaHCO_3$ solution. The original pH of the unaltered volcanic ash leachates samples were as low as between (pH 2-5). However, all other avenues of methodology were explored before this step was taken. Furthermore, no other reference to a similar occurring situation in the scientific literature was found, so the effect on the anion concentrations when the pH was raised is unknown.

The final step was to filter the samples that had their pH raised to the optimum of (pH 6-7). It would be considerably more difficult and not a good use of time to do the adjustments after filtering. The filtering itself was conducted with a 0.45µm size syringe filter with a 10ml syringe. First, the new syringe filter was rinsed with deionised MilliQ® water. Then 4-5ml of raw sample was put through the filter 1ml and then put into waste to ensure the filter was accurately saturated. The filtered samples were put into 10ml polyethylene test tubes. The raising of the pH and the filtering represented the most labour-intensive part of the IC analysis. These test tubes were transferred to the auto sampler, Figure 11. The first IC run analysed the first 50 leachate samples collected during the course of sampling from the Soxhlet reactors. The second run took care of the remaining 87 samples.

However, a third run was required when it was discovered that the results of the standards run with the second analysis had exposed drifting of 10% from the first sample to the last standard analysed on the second run (J. Hanley, Personal Communication, 17 January 2017), while a final third run occurred for samples that were inaccurate. Once the computer was set with the samples and the start time selected the process of analysis was almost completely automatic. After the analysis of the samples with the Ion Chromatography instrument the data was transferred from the computer controlling this instrument to an excel file with an external hard drive.

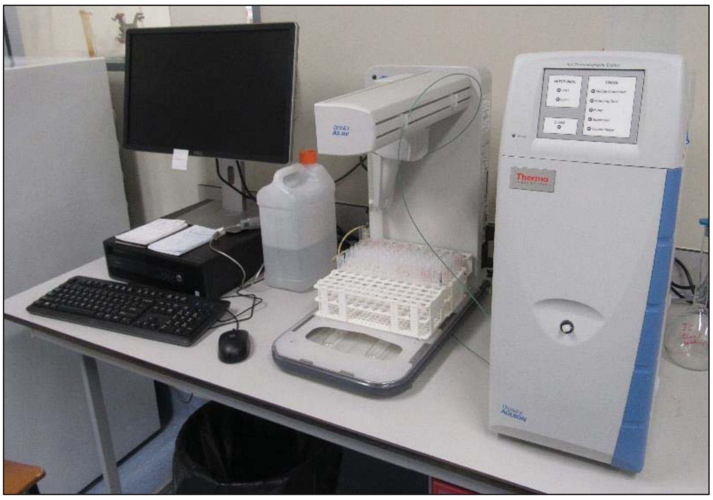

Figure 11: Photo of IC instrument, on the right is the instrument and next to it on the left is the automatic sampler.

2.5 Quality control

The quality control of the analyses of both MP-AES, as well as Ion Chromatography, are reported to ensure the validity of the end results. Therefore, there are several methods that were used in this analysis to ensure this was carried out throughout the analysis of all 137 samples that were tested.

The main method to maintain quality control with the MP-AES was to run five standards using standard reference material of increasing elemental concentrations and a method blank, which was 2% nitric acid. This was in order to calibrate the instrument to the elements while analysis was taking place. Throughout the analysis regular inserted samples of standard were used to ensure that the calibration curves of the relevant elements in each run were identical to that at the beginning. If the resulting concentrations of the standard reference material remained within a deviation range of 95-105% the MP-AES analysis was considered successful.

A similar method to maintain the validity of the samples was carried out in the Ion Chromatography analysis. Here there was one inserted sample standard for every 11 leachate samples, called S3. The standards consisted of standard reference material. These were particularly important when using the Ion Chromatography instrument as dangerous drifting was recognised in the 16/01 analysis used is this method conducted on 16 January 2017. Furthermore, the second analysis of the 87 samples also revealed that the value of standards changed significantly and it did not reflect the correct values.

2.6 Statistical analysis

Statistical analysis of the results after the analysis had been completed was also important for both the MP-AES and the Ion Chromatography.

Statistical analysis for the MP-AES results was particularly important because the raw results did not reflect the true concentrations of the sample. Therefore, a formula for the ($\mathrm{Correct}_{\mathrm{Value}}$) was used in Equation 3 to fine the correct value.

$$(Correct_{Value}) = Origional_{Value} \times \frac{250\ ml}{Sample_{Weight}} \text{ Equation 3}$$

The $Origional_{value}$ is the first reading of the MP – AES. The *250ml* value is the original volume of the sample that was used in each sampling cycle. The $Sample_{Weight}$ is the original weight of the volcanic ash sample from which the brine originated. In this case that was the weight of the volcanic ash weighed for each sample prior to the commencement of each Soxhlet experiment. Then this result was divided by a dilution factor, the amount of deionised water by which the original sample was diluted. 250ml was chosen as the dilution factor because that was the original amount boiled in the boiling flasks at the bottom of the Soxhlets. Although apportions holding the thimble/sample were not 250ml (75ml approximately) this cycled back into the 250ml boiling flask. The answer should then be an accurate depiction of the true concentration. Furthermore, four samples from the White Island experiment had to be diluted 10 times due to high sodium concentrations making the data unreadable. This was factored into the dilution calculations subsequently.

However, a number of problems associated with the drifting of the standards were discovered. In order to correct these problems statistical analysis had to be conducted to correlate the anions results with the drifting standards. The formulas is Equation 4 and Equation 5 were used to derive the original values had the drifting of the standards not occurred.

$$(\%\ of\ standard\ drift) = \frac{S3_{Last}}{S3_{First}} \text{ Equation 4}$$

The drifting in the results was fixed first by Equation 4, dividing the $S3_{last}$ which is the last standard value by the first standard measurement value in the analysis. This produced the percentage of drift throughout the whole analysis, Equation 4.

$$(Correct_{IC\ value}) = \frac{(\%\ of\ Standard\ drift - 1)}{injection\ no.} \text{ Equation 5}$$

The correct result derived from Equation 5 where the *(Correct*$_{IC\ value}$*)* was found by subtracting the *(% of standard drift)* from 1 and then dividing by the *injection no.* which is the ranked number that was sampled in the analysis. This provide an accurate way to estimate the amount of drift in each sampling analysis. This produced the correct values. For Ion Chromatography the drifting of the standards was the only statistical analysis required prior to the work beginning on the interpretation and discussion of the results.

In the Ion Chromatography analysis the issue of water loss also influenced the samples that were collected as they are always less than the original samples. This is due to the fact that the original sample volume is 250ml. It was discovered that the cation concentrations were already factored to the original amount of 250ml. Any water extractable dissolved analyte should remain within the water that is recovered from the Soxhlet reactor (S. Hall, Personal Communication, 17th March 2017). Therefore, the analyte concentration is higher in the recovered sample than if the preparation of the water had not occurred. The best way to compensate for the loss of sample was is to use dilation equations due to the loss of sample is still mostly water vapour.

$$\left(\frac{\frac{mol}{l} x\ H_2O\ collected}{H_2O\ lost}\right) = (C) \text{ Equation 6}$$

The original concentrations were converted from mg/L to molar mass, then calculate (C) using Equation 6 then converting the molar mass back into mg/L.

Chapter 3 Results

3.0 Granularity and componentry

The particle size distribution (PSD) is important to characterize the eight volcanic ash samples and to interpret aspects of the soxhlet reactor leaching results. The statistics outlined in Table 5 describe the individual particle size distributions, calculated with the Microsoft excel program GRADISTATE, Blott and Pye (2001) according to the principles of (Folk, 1954; Folk & Ward, 1957). The geometric surface area (SSA_{GEO}) of the particles was calculated by a formula defined by (Wolff-Boenisch, Gislason, & Oelkers, 2004; Wolff-Boenisch, Gislason, Oelkers, et al., 2004). The surface area is an important parameter to characterize the reactivity of volcanic ash within an eruption plume and also during the leaching. Released volatile gasses interact with the surface of volcanic ash particles. Since no surface area analyses were undertaken in the original studies of Mt. Ruapehu or the other overseas samples, the geometric surface area (SSA_{GEO}) must be calculated, (*see Methodology*).

3.01 Granulomentry

95/5 Lower and Upper Ruapehu (11/10/95)

The lower layer PSD has two modes, a fine mode at 302.5 µm plus a coarse mode at 3400.0 µm. The median diameter of the lower layer is 450.3 µm, this is considerably coarser grained in comparison with the upper layer, (Table 5). The histogram (Figure 12) has a negative skew towards the course grained volcanic ash.

There is one mode in the particle size distribution of the upper layer at 302.5 µm. The upper layer has a finer grained mean than the lower layer at 260.2 µm as well as a median of 318.8 µm. Furthermore, the histogram indicates that the mode though fine grained, has a larger weight percentage at is mean than the lower layer, Figure 12. The distribution is clustered around the mean than one would expect from a normal distribution. The resulting geometric surface area for the upper layer is considerably higher than the lower layer

Table 6), due to the difference in the mean values across the two samples.

95/8 Ruapehu (14/10/95)

There are two modes in the particle size distribution at 107.5 µm and another mode with a 15% value for the weight percentage at 427.5 µm. The corresponding mean is 84.78 µm while the median is 110.2 µm, Table 5. The PSD therefore, is very poorly sorted, even more so than the 95/5 samples. Overall, the distribution is clustered around the median value, similar to the 95/5 Upper layer. The difference is that the distribution is considerably more finely skewed and multimodal. The geometric surface area is reflective of the fine median value as well as the fine multimodal skewing,

Table 6. The 95/8 sample has the second highest value of the nine samples where the surface area is calculated.

96/7 Ruapehu (17/6/96)

There are two modes in the particle size distribution of the 96/7 sample, at 37.72 µm and again a larger mode at 302.5 µm with a 20% weight percentage value. The corresponding weighted mean is 97.00 µm with a median at 175.1 µm, Table 5. The main difference compared to the 95/8 sample is that the multimodal distribution and the negative skewing of fine grained material is exaggerated by the higher weight percentage contained in the second mode. This is reflected in the median of the 96/7 sample which is higher than the 95/8 geometric surface area. The SSA_{GEO} of 2.9 m^2 is a value of 0.5 m^2 lower than the 95/8 geometric surface area.

96/46 Ruapehu (21/07/96)

In the 96/46 volcanic ash sample, two modes have been identified at 18.86 µm and at 215.0 µm, Table 5 . The corresponding mean is 54.67 µm with a median value of 60.16 µm. This median is the finest value that has been found for all eight volcanic ash samples analysed for the particle size distribution. The histogram is also unique in that modes are relatively flat with a weight percentage of 10% the maximum. Overall, the 96/46 sample is not comparable to any other Mt. Ruapehu sample. The geometric surface area value is 4.1 m^2, Table 6.

Mt. Sakurajima (18/08/13)

Mt Sakurajima volcanic ash sample contains one mode at 215.0 µm with a corresponding mean of 164.9 µm and a median of 192.8 µm. The one mode contains a value of 23% weight percent of the total grainsize distribution, the highest of the eight samples analysed, (Figure 12). Furthermore, the histogram shows that there is a high clustering around the median value with a slight fine grained skew. The corresponding geometric surface area for the Sakurajima sample is 0.7 m^2, Table 6. This geometric surface area is the lowest of all eight samples. Although the median is not the highest the clustering around the mean and an absence of a large fine skewing results in a low surface area.

Mt. Kelut (14/02/14)

The Mt. Kelut volcanic ash sample has two modes; the fine one at 13.3 µm has the largest weight percentage at 15% while the coarse mode is 605.0 µm (Table 5) with a weight percentage of 6%. The PSD corresponds to a mean of 49.7 µm and a median value of 28.63

µm. The median value here is the finest of all eight volcanic ash samples. The histogram also reveals that there is a large positive skew towards the course component, Figure 12. The geometric surface area is a value of 3.9 m^2, Table 6. This is the second to highest surface area, only to the 96/46 sample. The main reason for the high surface area is that the bulk of the 60% cumulative weight percentage is overwhelmingly clustered around the median. A positive skewing results in a low weight percentage of the fine component.

White Island (28/04/16)

The White Island sample has three modes, the largest is at 1700.0 µm where the corresponding weight percentage is 13%, with another two modes are at 76.3 µm and 13.3 µm, (Table 5). The overall particle size distribution corresponds to a mean weight percentage of 130.3 µm and a median value of 101.1 µm. The mean and median values are in the middle the comparison to the other 8 volcanic ash samples, (Table 5). The multimodal nature of the sample makes this sample unique. Very poor sorting of the particle size distribution and the relatively high proportion of fine- grained material results in a high geometric surface area, (Table 6). Note that the mean 130.3 µm is considered to be course. The large variability in the types of grains explains why the PSD is the poorest sorted with the largest range, Table 6.

Table 5: Table showing the main statistics of the grain size distributions measured for the 6 Mt. Ruapehu volcanic ash samples. Selection is based on (Moebis, 2011). Based on GRADISTAT V8.0: (Blott & Pye, 2001) – Method of Moments.

Volcanic ash Sample	**Mode σ (µm)**	**Mean (µm) Weight**	**Median D_{50} (µm)**
New Zealand			
95/5 Lower Layer	302.5, 3400.0	509.3	450.3
95/5 Upper Layer	302.5	260.2	318.0
95/8 Ruapehu	107.5, 427.5	84.8	110.2
96/7 Ruapehu	37.7, 302.5	97.0	175.1
96/46 Ruapehu	18.9, 215.0	54.7	60.2
Overseas Samples			
Kelut	13.3, 605.0	49.7	28.4
Sakurajima	215.0	164.9	192.8
White Island	13.3, 76.3, 1700.0	130.3	101.1

Table 6: Table of geometric surface area for the soxhlet reactor volcanic ash samples. Rounded to four decimal places.

Sample	**SSA_{GEO} (m^2)**
Sakurajima	0.6958
Kelut	3.8913
Weathered Ruapehu	0.9457
95/5 lower Ruapehu	0.9803
95/5 Upper Ruapehu	0.9849
95/8 Ruapehu	3.4189

96/7 Ruapehu	2.8914
96/46 Ruapehu	4.1128
White Island	2.9674

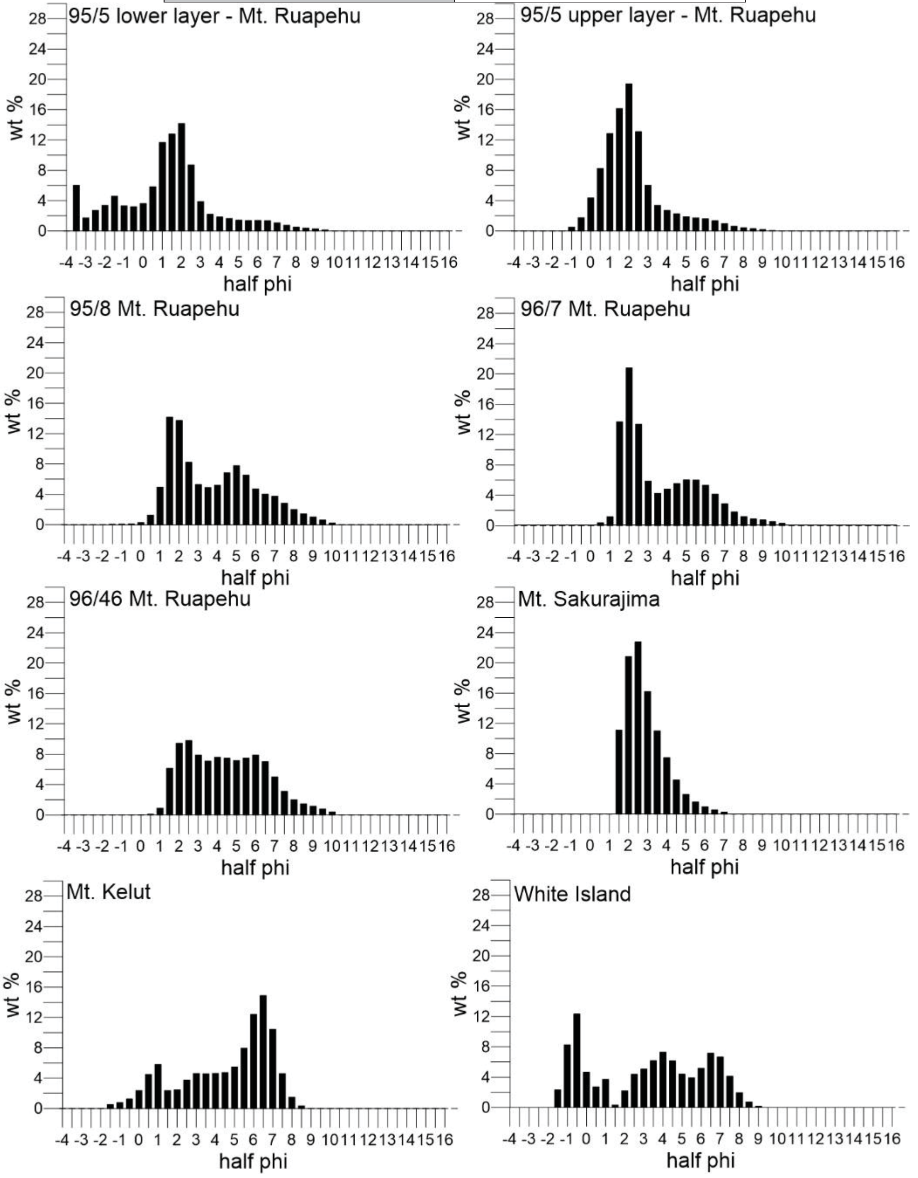

Figure 12: Grain-size histograms showing the half phi size fraction versus the weight percentage of eight of volcanic ash samples that were analysed.

3.02 Componentry analysis

The minerology of the volcanic ash is dominated by glass followed by free crystals and lithics. As echoed in Moebis (2011), the different colours of the bulk volcanic ash samples prior to processing are due to the varying types of light glass and dark glass. In the following section, the main characteristics of componentry point count analysis will be summarised. Point count componentry analysis under an optical microscope was conducted was conducted for the fractions 125µm, 250µm and 500µm. Components in fractions, lower than 125 µm were not possible to identify with a microscope. The grains greater than a diameter of 1000 µm although noted, did not contain enough grains to ensure reporting of an accurate statistical analysis.

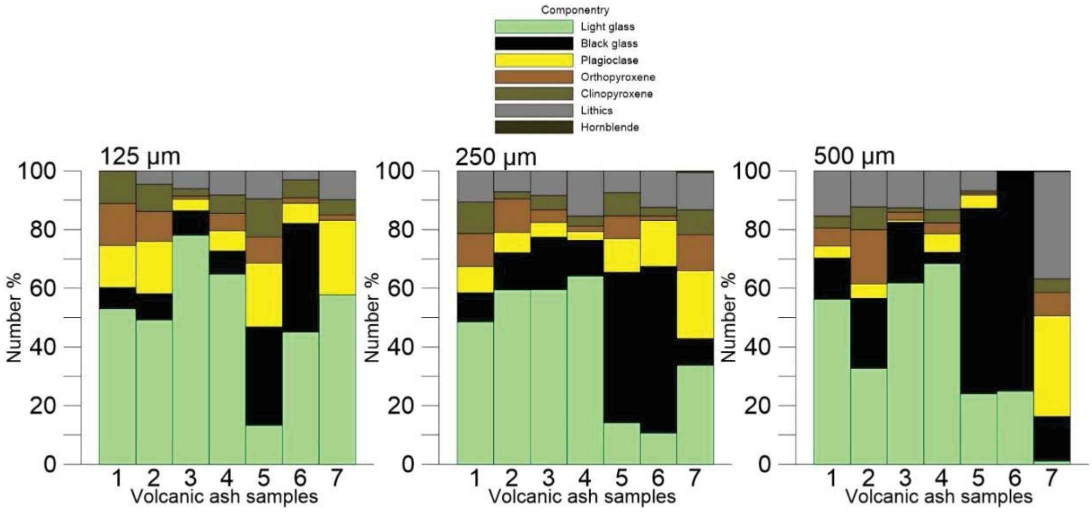

Figure 13: The percentage of componentry for the grain size fractions; 125 µm, 250 µm and 500 µm of (1) 95/5 lower layer, (2) 95/5 upper layer, (3) 95/8, (4) 96/7, (5) 96/46, (6) Mt. Sakurajima, (7) Mt. Kelut.

Volcanic Glass

The appearance of the volcanic glass component is strongly dependent on eruption style (Moebis, 2011; White, 2015; Wohletz, 1986). Volcanic glass comes in two main forms, black glass (Trachyte) and light glass (Sideromelane). The 1995-96 Mt. Ruapehu eruption samples are dominated by light glass in all three size fractions as well as the 96/7 sample, (Figure 13). An important observation is that the 95/8 and the 96/7 samples have a higher percentage of light glass than was found in the 95/5 samples. The observed light glass is primarily beige coloured, as small vesicles and is elongated, making them distinct under an optical microscope. The black glass in comparison, is observed to be blocky to sub-angular, opaque and has little to no vesicles. Microlite inclusions of plagioclase were also observed in the larger black glass fractions of the 96/46 sample. This black glass of the 96/46 sample was predominant in comparison to the other Ruapehu samples, (Figure 13).

In the Mt. Kelut sample light coloured glass was dominant, (Figure 13), black glass was only found in the 250 µm and 500 µm fraction. The light coloured glass in Mt. Kelut was white to translucent. With some grains having small opaque mineral microlite inclusions. The black glass was blocky, non-vesicular and had adhering dust that made identification difficult, even after repeated ultrasonic washes. The Mt. Sakurajima sample had in the 125µm fraction, black glass and light glass of equal abundance. In the 250 µm fraction, the light glass decreased to 10%, was grey to brown coloured with rear opaque mineral inclusions. The black glass increased to 57% in the 250 µm fraction and was non-vesicular to semi-angular with some plagioclase inclusions observed.

Free crystals

The free crystals were found in the eight volcanic ash samples were plagioclase, clinopyroxene, orthopyroxene and rare amphiboles. Plagioclase was found in all of the Mt. Ruapehu samples analysed across the three size fractions. The most abundant were in the 95/5 lower, upper layer and in the 96/46 sample, (Figure 13). The percentage of plagioclase decreases as the size fraction increases. Moebis (2011), explains that this is due in part because of the natural size of the crystals as well as the degree of fragmentation. All plagioclase across the samples was translucent, angular and platy, due to how the mineral breaks down its 90° cleavages. In the Mt. Kelut sample, there was 23 to 25% plagioclase in both the 125µm and 250 µm fractions. Sakurajima in comparison has less than 10% plagioclase. Pyroxene compared to plagioclase is more vulnerable to breakdown through increasing size fractions.

The mineral pyroxene is found as clinopyroxene and orthopyroxene, across the volcanic ash samples, (Figure 13). In A. Moebis (personal communication, 2017) it is explained that clinopyroxene breaks down earlier than orthopyroxene. While clinopyroxene breaks down into cubes orthopyroxene has a more random breakdown component. This occurrence is apparent when the pyroxenes are split, in the 250µm and 500µm fractions. In the 95/5 and Mt. Kelut samples clinopyroxene has less abundance than orthopyroxene. This is not visible for the other Mt. Ruapehu samples and Mt. Sakurajima possibly due to the different types of pyroxenes that are beyond the scope of this project. The breakdown of clinopyroxene is the reason why the proportions of clinopyroxene and orthopyroxene are similar or opposite in the 125µm fraction. Overall in Figure 13, there is a noticeable decrease in the percentage of free crystals with reference to the Mt. Ruapehu 1995-96 stratigraphy.

Lithics

The lithic component of the volcanic ash observed in these samples are derived from the basement geology. These have been 'piggybacked' onto the ascending magma as it fragments and erupts, (Moebis, 2011). In the Mt. Ruapehu samples greywacke from the Mesozoic era is the interpreted rock type. The observed grains are often mid-grey in colour with visible granularity and porphyritic texture, often rounded to sub-angular fragments. In some cases this material could also have been recycled from previously erupted material near the vent, especially in the case of the phreatic and phreatomagmatic eruptions (Sigurdsson, 2015). In Figure 17 it is observed in the 1995 Mt. Ruapehu samples that the content of lithics increases with the grain fraction. Approximately 4% - 9% in the 125µm and 250µm fractions, increasing to 15% on average in the 500µm fractions. In the 96/46 samples the lithic content decreases with increasing grainsize; 9% in 125µm to 4% in the 500µm grainsize fraction.

Recycled lithics are a white, orange or a red colour (Moebis, personal communication, 2017), highly altered by iron oxidation. This alteration creates challenging determinations of the original mineral componentry. Both Sakurajima and Kelut have high lithic contents. Sakurajima has 3% (125µm) - 12% (250µm) compared to Kelut where there is 9% (125µm), 12% (250µm) and 34% in the 500µm grainsize fraction, (Figure 13). Both, Mt. Sakurajima and Mt. Kelut have the most highly altered lithics. Mt. Kelut in particular a large percentage of lithics that are 'rotten' (Moebis, personal communication, 2017). The eruption of Mt. Kelut, a lava dome driven by gas overpressure has a low juvenile glass component.

White Island

The componentry point count analysis from the sample of White Island proved challenging. Because of the complexity of the volcanic ash grains encountered. These grains contrasted from any of the other samples observed in this project. Therefore, the categorisation of componentry was only completed based on texture and colour characteristics. A high clay component was also visible in the bulk sample that was a light green colour requiring extensive washing of the sample before componentry could begin. Michael Rosenberg (personal communication, March 22 2017) explained his interpretations on several unidentifiable clear, crystalline and opaque white coloured grains. These were difficult to differentiate into any component. The crystalline white semi-translucent cloudy coloured grain could be either altered plagioclase or the calcium sulphate minerals anhydrite or gypsum.

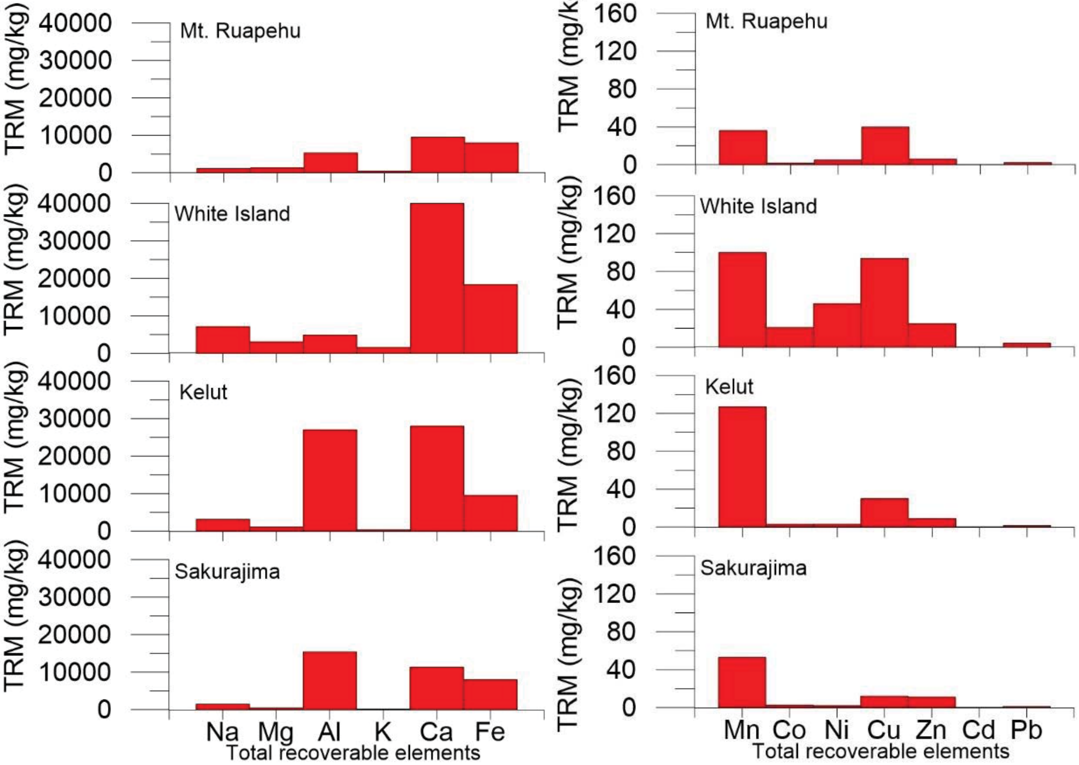

Figure 14: Bar graph of the total recoverable metal concentrations ordered according to the atomic number of the element detected. These have been split with cations of high concentrations on the right and trace elements on the right-hand side (A) Mt. Ruapehu eruption on the 17th of June 1996, (B) White Island from 28th April 2016, (C) Kelut from 14th February 2014 and (D) Sakurajima from the 18th August 2013.

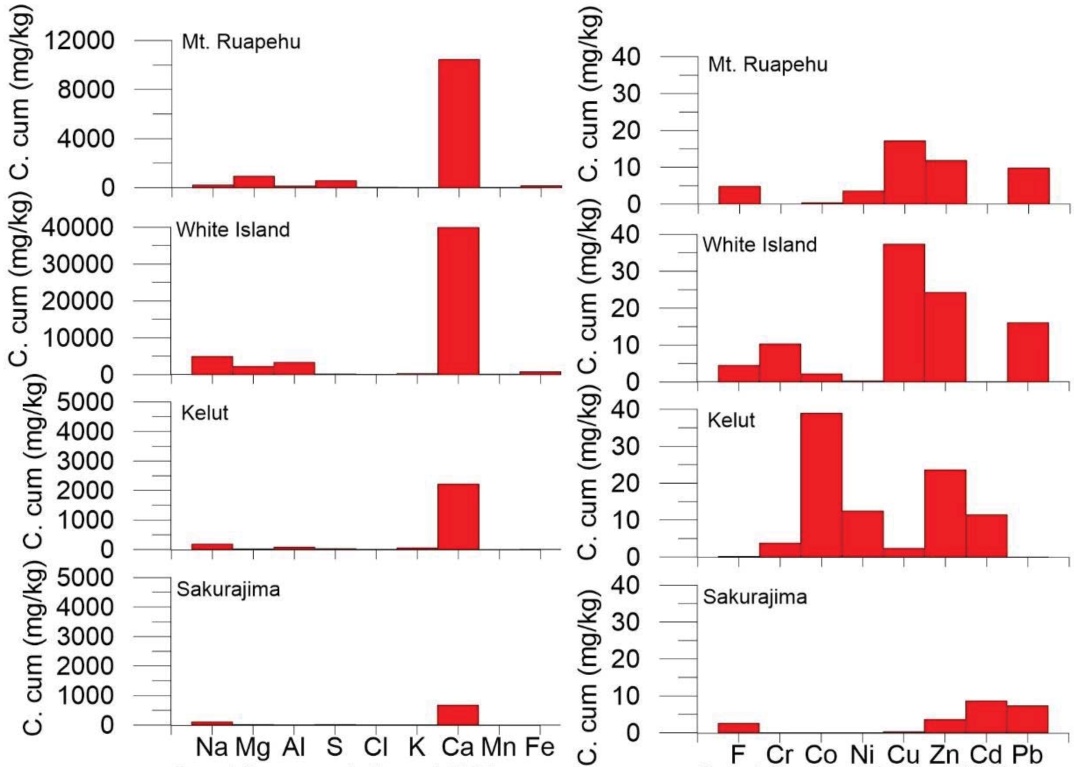

Figure 15: Graph of cumulative concentration of elements leached after 168 hours, ordered according to the atomic number, (A) Mt. Ruapehu eruption on the 17th of June 1996, (B) White Island from 28th April 2016 has been scaled up due to the high calcium, (C) Kelut from 14th February 2014 and (D) Sakurajima from the 18th August 2013.

3.1 Acid and water leaching: characterisation and differences of brine composition

3.11 Acid leaching

Initially, the acid recoverable concentrations of elements (Figure 14) leached from four different volcanic ash samples were analysed to attain an overview of the total and relative elemental abundance. Overall, out of the elements sodium to iron; the highest concentrations are that of aluminium, calcium and iron. The Absolute concentrations are variable among the volcanic ash sources. Figure 14 shows that White Island sticks out as being very high in calcium and iron. Mt. Ruapehu on the other hand has low concentrations, in particular that of calcium (4,800 mg/kg) and iron (3,700 mg/kg) in comparison to the other samples. White Island in comparison has the highest concentrations of iron (18,300 mg/kg) and Mt. Kelut has the highest concentrations of aluminium.

For all of the sources (Figure 14) the highest trace element concentrations are in copper, followed by zinc and nickel for all of the samples. However, the absolute concentrations differ strongly from sample to sample. Overall, the highest trace element concentrations are in the White Island sample. For instance, with copper having a concentration of 94 mg/kg, in comparison to Mt. Ruapehu of 40 mg/kg, Mt. Kelut of 30 mg/kg and Mt. Sakurajima of 12 mg/kg.

3.12 Water leaching

Elemental concentrations in water-leached brines are sometimes lower than those in acid-leached brines (Figure 15). In this overview, we report the brine concentrations after 168 hours of water-leaching (i.e. at the end of the soxhlet reactor experiment). These data points also include fluoride, chloride and sulphate which could not be tested for in the acid recoverable tests. The relative abundance of elements in acid and water leaching situations differs. Calcium is overwhelmingly the largest major element that is leached in water. However, in terms of the relative abundance there is less calcium leached by water. For instance White Island leaches 39,954 mg/kg of calcium in water comparison to 40,000 mg/kg in acid.

The leaching for trace elements is also lower in the water than for acid. The general behaviour is also differing. Overall, the relative ratios of trace elements in each eruption is different between the acid solution and the water solution (Figure 15). For instance, in the Mt. Ruapehu sample the concentration of zinc in the acid solution is 6 mg/kg compared to 12 mg/kg in the water solution. Mt. Kelut has a large enrichment of cobalt 5 mg/kg, zinc 12 mg/kg while copper 2 mg/kg, the opposite of the relative ratio for the acid solution (Figure 14).

3.2 Water digestion: characterising time variant of ash leaching for soxhlet reactor experiments.

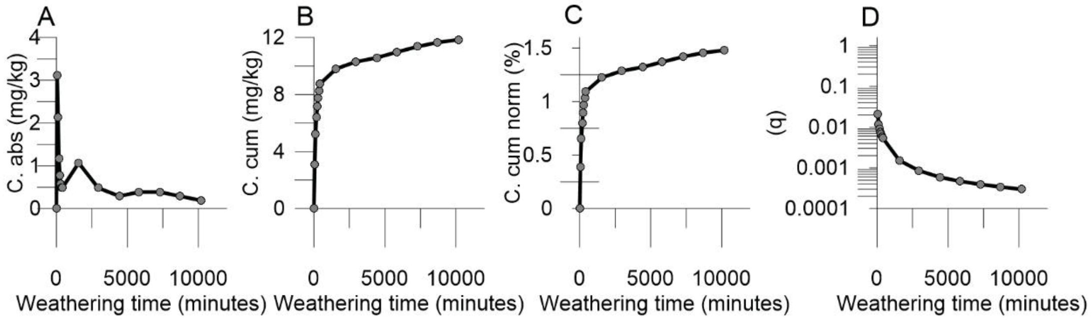

Figure 16: Graph illustrating the four different ways of plotting the brine concentration results, (A) is the absolute concentration (C. abs), (B) the cumulative concentration (C. cum), (C) cumulative concentration normalised (C. cum. norm) metal concentration, (D) Volcanic flux (q) into brine into the brine normalised with the effective surface area of the volcanic ash.

The soxhlet reactor experiments (Figure 16) provide data for the water digestion of volcanic ash over experimental time. An example of the time-variant absolute concentration of a leached element in a brine sample is shown in (Figure 16A). The brine sample is replaced with fresh deionised water in each step. The individual concentration explains only the concentration since the last sample replacement and the absolute concentrations are not representative of the total element leached. Therefore, it is meaningful to analyse the data in cumulative form (Figure 16B). The dataset is created by adding each new sampling concentration to the sum of the concentrations of the previous brine samples.

The third way of plotting the dataset is the normalisation of the time series of cumulative concentrations with the total recoverable metal contents. The objective was to evaluate the total cumulative concentration of an element to determine its future potential of the brine with reference to experimental time. However, this approach did not yield meaningful results due to differences in the leaching of acid compared to water as outlined before. An example is illustrated in Figure 16C, where in an experimental time of two to three hundred minutes, the cumulative concentration has exceeded 100% of the total concentration (presented as 1 in Figure 16C). Therefore, this normalisation to the total recoverable concentration will not be discussed further.

The fourth way of plotting the dataset explored here is to look at the volumetric flux of an element into the brine. Mathematically, this represents the first derivative of the cumulative concentration data, which for simplicity was computed as finite differences of the cumulative concentration time series. A strong dependence of the leaching rate on the particle size distribution and the geometric surface area was observed. Data will be discussed where it is normalised to the effective available surface area by the following Equation 7.

$$(q) = \frac{\left(\frac{TimeMax-TimeMin}{ValueMax-ValueMin}\right)}{SSA_{GEO}} \text{ Equation 7}$$

The flux in Equation 7 is defined by Humez and Prost (1999), as the amount of dissolved element per milligram of sample, during a set experimental time. In the soxhlet reactor experiments, the initial time zero result ($TimeMin$) and the initial time zero concentration result ($\mathrm{ValueMin}$) is subtracted individually in the 12 subsequent sampling points ($\mathrm{Time\ Max}$) in the experiment as well as their corresponding cumulative concentrations ($\mathrm{ValueMax}$). This was done to account for the replacement of the brine samples, yet the continual leaching of the sample itself over the experimental duration.

3.21 Pattern of time variant behaviour

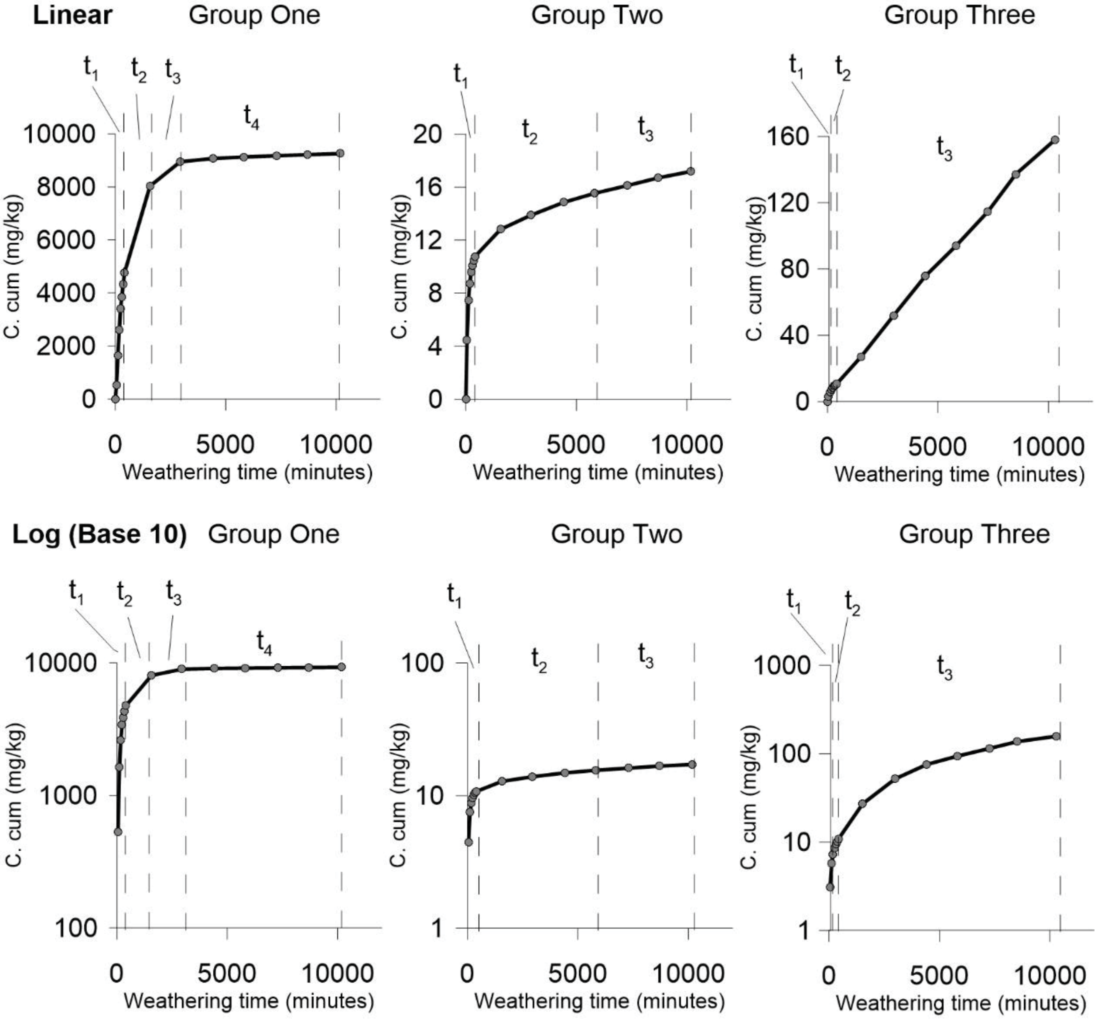

Figure 17: Diagrams showing typical examples of the three groups of time-variant element release plotted with a linear y – axis (top) and a log (base 10) y – axis (bottom), (A) group 1 – calcium, (B) group 2 – copper (C) group 3 – iron. The dotted lines represent the approximate temporal boundary separating phases of strongly contrasting leaching rates.

The soxhlet reactor leaching experiments revealed highly variable and quantifiable time-variant leaching behaviour for the different volcanic sources and elements. Despite the range of observed behaviours, there are three main groups of temporal pattern of leaching. Figure 17, shows examples of these three groups of time-variant leaching time variant leaching behaviours which are described below.

Group one is defined by brief initial period of high element release (a high and approximately constant leaching rate), transiting into a long final phase of strongly decreasing leaching rate approaching low to zero element release into the brine (low to zero leaching rate). Elements that fall into group 1 behaviour differ in their temporal transition towards zero leaching rate.

Group two is also characterised by a fast initial leaching rate, which, however, transitions into a long final phase of intermediate and almost constant leaching rate.

Group three is characterised by almost constant element release over time, which is depicted by the cumulative concentration plot on linear scales in Figure 17. However, a log-linear plot of group three behaviour reveals that (Figure 17), group three does not obey perfect constant leaching rates, but a mild exponential decrease in leaching rate over time.

An example of an element that has a group one release is calcium, a group two example is copper and group three behaviour is only found for the case of iron. The important point of Figure 17 is that the group behaviour is primarily controlled by the element and not by the individual sample of the source volcano. For this reason it is possible to place all seventeen of the elements analysed into one of the three release groups, presented in, Table 7.

Table 7: The table shows where each of the elements have been categorised in relation to their release groups.

Group One	Group Two	Group Three
aluminium	cobalt	iron
manganese	lead	
magnesium	chromium	
chloride	nickel	
calcium	cadmium	
sodium	potassium	
	zinc	
	copper	
	sulphate	
	fluoride	

Table 8: Table illustrating some of the typical ranges for each release phase of the cumulative concentration of the soxhlet reactor over experimental time.

	$t_0 - t_1$	$t_1 - t_2$	$t_2 - t_3$	$t_3 - t_4$
Group 1	1.0 – 4.0%	0.5 – 54.0%	-	42.0 – 98.0%
Group 2	1.0 – 3.0%	3.0 – 57.0%	42.0 – 97.0 %	-
Group 3	3.0 %	3.0%	94%	-

The three groups of leaching behaviour can be further characterised by the occurrence of transient phases of common temporal variation in the leaching rate. Here a minimum of four such phases is suggested (Table 8). Phase 1 characterises a high and almost constant leaching rate. Phase 2 characterises intermediate values of leaching rate progressively decreasing with time. Phase 3 characterises a low and almost constant, but, non-zero leaching rate. Phase 4 characterises very low to zero leaching rates. Phase one typically lasts for 1% to 4.0% of the duration of the experiment time and has a relatively small range across release classes, (Table 8). Phase two can last between 0.5% and 57% of the experiment. Phase three for groups two and three is between 42.0% and 97% of the entire experimental duration and can extend for as much as 98.0% of the duration of the experiment. Examples of the duration of leaching phases are presented in Figure 17, with dotted lines representing the boundaries of the approximate changes in phase over experimental time.

The origins of the release pattern of elements is due to the manner in which they are bonded in the sample of volcanic ash. If the bonds of an element are initially week with the surface area of the volcanic ash particle, then all of the available element will be released. This will leave just a very small amount of the element that will be slowly released as the chemical weathering takes effect. If the release trend is constant over time then the source is from the minerals or glass within the volcanic ash particle. If the release class is a mixture of group two and three then the elements will be bonded via a combination of sublimation and the surface area to the particle. In the discussion the principle sources for these released elements are identified. This in-turn, might indicate in principle, that there variable processes occurring that relate to the origin of each element. Overall, it will be a mixture of a process of sublimation and surface area dissolution of the crystal or mineral matrix. In the following the actual cumulative concentration data will be shown for elements in each group.

3.212 Examples of time-variant leaching behaviour for certain elements

In the following section the time-variant leaching behaviour of some elements of environmental importance will be illustrated further. The previously introduced leaching groups 1, 2 and 3 (Table 7) and their characteristic phases of common leaching rate behaviour (Table 8) will guide the explanation.

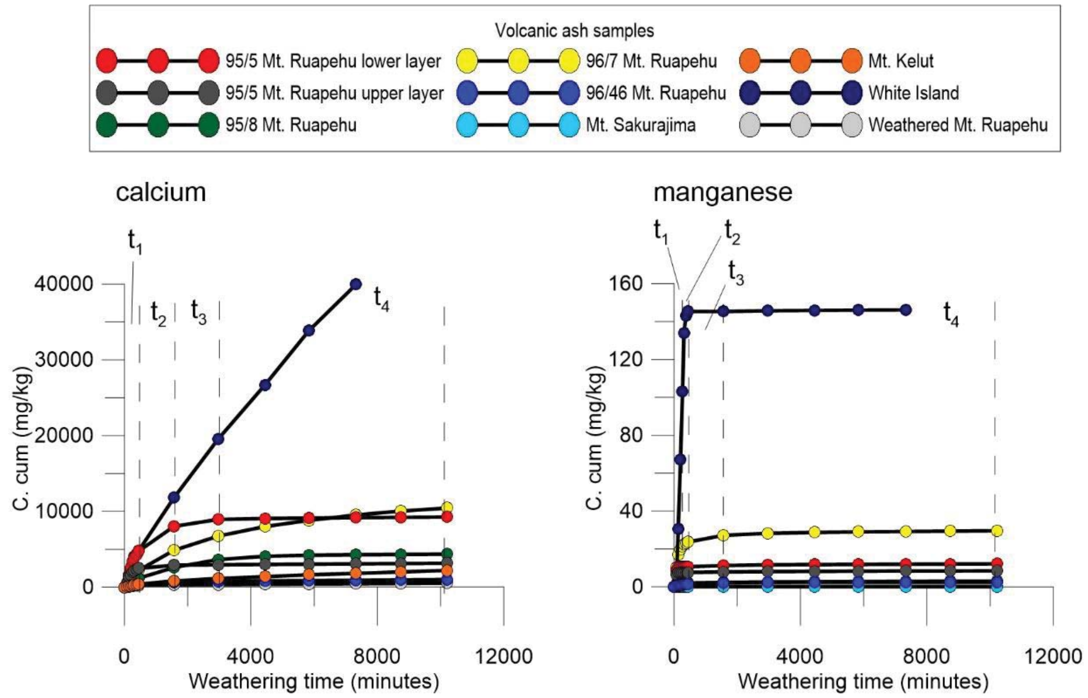

Figure 18: Presents the cumulative concentration of calcium and manganese. Examples elements that display the release behaviour of group one. The dotted lines highlight the boundaries between the approximate release phases of each element.

Group one is characterised by an initially high element release into the brine. However, different elements differ in the typical duration of leaching rate phases 1 to 4, Figure 18. The elements calcium and manganese are an example of the variability that is existing in group one. The duration of the phase 1 release for calcium is approximately 4 % of the experiment, phase two of 11%, phase three is 15%. The last fourth phase is 70% of the experiential duration. For manganese the first phase is 3%, though the 1% duration of the second transitional phase is in stark contrast to the long transition time of calcium. The fourth phase of the magnesium cumulative concentration is 86% of the experiment.

Lead and zinc are two examples of group two, whose time-variant leaching behaviour for the different ash-samples is shown in Figure 19; lead has a phase 1 and 2 duration of 3%, 0.946 %, respectively. Zinc has a phase 1 and 2 duration of 5% and 39%, a significant difference in the experimental durations of the phases 1 and 2. This results in a relatively long duration of phase 3 for lead of 95% compared to zinc that has only 56%. Therefore, the elements in group two illustrate the differences from element in their long-term experimental phase. However, the increasing linear nature of phase 3 means there is still continued release of element.

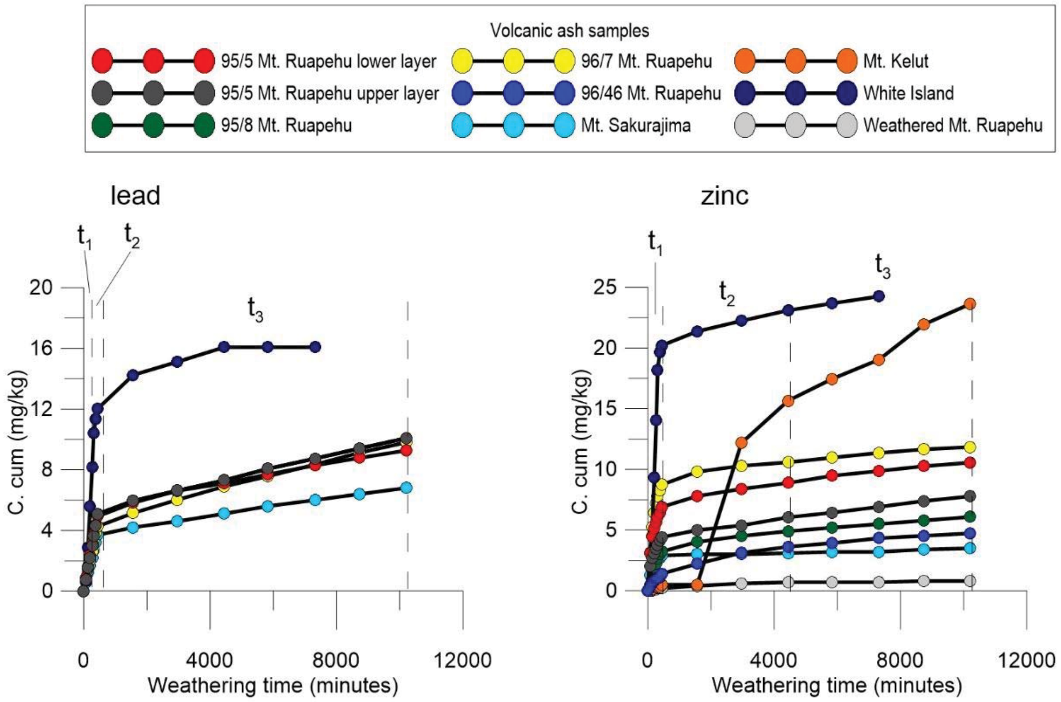

Figure 19: Presents the cumulative concentrations of lead and zinc. Examples of elements that display the cumulative release behaviour of group two. The dotted lines represent the boundaries of the different phase changes.

The group three release pattern is unique in that it is the only pattern of cumulative iron release, Figure 20. The duration of phase 1 is 3%, phase 2 is 3% while the final, third phase is 94% of the experiment duration. Iron is unique in that it has relatively little observable transition from a high release rate to a low release rate.

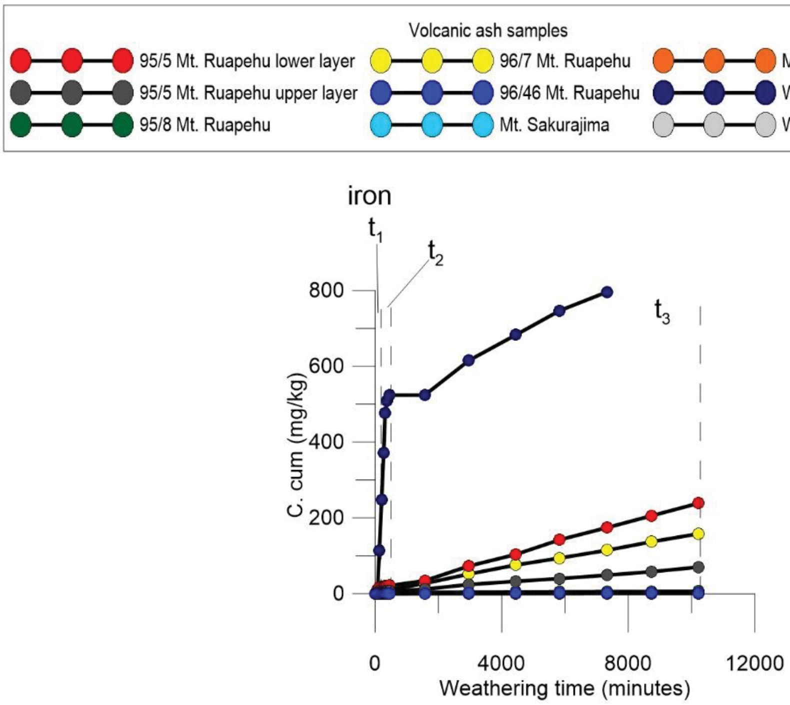

Figure 20: Presents the cumulative concentrations of iron. This is an example of the cumulative release pattern for group three. The dashed lines represent the boundaries between the different release phases with experiential time.

Each of the elements fall into one of three defined groups of element release, (Figure 17). However, some unique element release behaviour has been observed among individual volcanic ash samples. For instance, the sample from Mt. Kelut shows a delayed release in zinc (Figure 19), in comparison to the other elements that have a group three release pattern. Another sample that shows unique behaviour is White Island. In almost every cumulative element concentration result the White Island by far, leaches the highest concentrations of almost every element.

The three groups of element release each show unique characteristics for each cumulative element release, even within each element release group. To get an idea of whether these different experimental times refer to short or long-term behaviour in the real world, it is necessary to approximate how long these experimental times equate to real time.

3.3 Characteristics in time-variant leaching behaviour for ash-samples of the 1995-96 Mt. Ruapehu eruption episode

Eruptions of Mt. Ruapehu have been regularly recorded since human settlement began in the central north island more than 100 years ago (Kilgour, Blundy, Cashman, & Mader, 2013). Historically, the crater lake of Mt. Ruapehu together with an active hydrothermal system has been a significant influence of past (Christenson & Wood, 1993). The 1995-96 eruption sequence started in September 1995 as a series of small phreatomagmatic eruptions, culminating on the 11th of October 1995 in the largest eruption of this sequence which erupted through the Crater Lake, and resulted in the complete emptying of the lake. A smaller eruption occurred on the 14th of October 1995 through the now dry vent. A lull in activity ensued over the winter of 1995-96 allowing the crater to be partially refilled. This resulted in another phreatomagmatic eruption on the 17th of June, which graded into more strombilian eruptions including one of the last eruptions of this sequence on the 20th of July 1996.

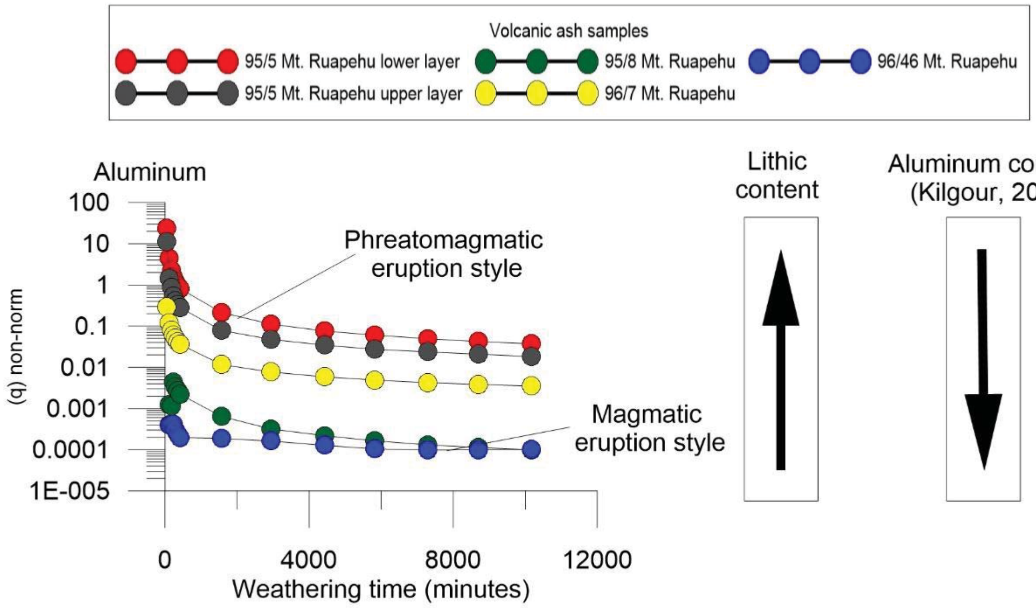

Figure 21: Graph showing the non-normalised flux ((q) non-norm) of aluminium for the volcanic ash samples of the 1995-96 Mt. Ruapehu eruption sequence. Opposite is the relative lithic componentry content and the relative aluminium bulk chemical content from Kilgour et al. (2013).

Aluminum. When plotting the volumetric flux of aluminium into brine over experimental time, it is noted that at any time during the soxhlet experiment there is an almost systematic decrease in aluminium in stratigraphic order (Figure 21). The only outlier of this trend is the eruption from the 14th of October 1995 (the first dry magmatic eruption in the sequence). This suggests that the relative abundance of aluminium in brine is strongly influenced by the eruption condition, and in particular the existence of a Crater Lake and hydrothermal system. In fact, time series of the aluminium flux show consistently high values for phreato-magmatic eruptions, and low values for magmatic eruptions. These trends are in line with the relative abundance of non-juvenile lithic material (as quantified in section 3.112), which increase with concentration of aluminium in the brine at any (experimental) time. Most of these lithic components are altered pyroclasts from the hydrothermal system and Crater Lake floor. It is also noted that the actual concentration of Al_2O_3 in bulk rock analysis of juvenile particles of the eruption sequence is displaying an opposite trend (Figure 21). Possible explanations are presented in chapter 4. Other elements that show similar behaviour to aluminium are zinc and copper.

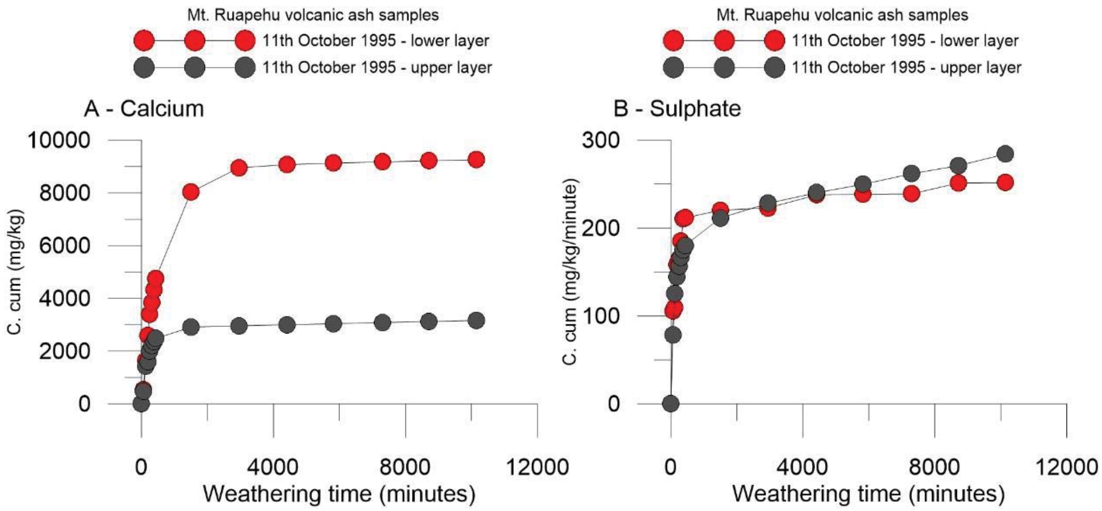

Figure 22: Graph showing the cumulative concentration of (A), calcium and (B) sulphate for the lower and upper layer samples for the 11th of October Mt. Ruapehu eruption.

Upper and lower ash layers. An important finding of syn-eruption sampling of the 1995-96 eruption sequence is that the fall deposits of phreatomagmatic eruptions are typically composed of a lower and light-coloured ash and an upper darker ash (Hodgson, Lecointre, & Neall, 2007; Pardo, Cronin, Palmer, & Németh, 2012). Similar two-particle sequences have since been identified in many volcanic ash deposits of the Tufa-trig formation (c. last 2000 years of Mt. Ruapehu activity) as well as in fall sequences from the Mt. Ngauruhoe and Red Crater (Moebis, Cronin, Neall, & Smith, 2011).

There are important differences in the leaching behaviour of the lower and upper layer of the 1995-96 eruption sequence. For instance, calcium, at any time, is much more enriched in brines from the lower layer than in the upper layer (Figure 22A). The same trends occur for sodium, magnesium, aluminium zinc and copper (see appendix).

By contrast, the brine composition of some elements is extremely similar for some other elements. One such case is sulphate (Figure 22B). Other examples include chloride, and potassium. These findings are further discussed in Chapter 4.

Chapter 4 – Discussion

4.0 An attempt to relate the soxhlet experimental time to natural weathering times

Time-variant leaching data introduced in the last chapter was presented in various forms of the concentration of certain elements leaching into brine as a function of experimental time. A key result from these analyses is that temporal changes of the brine composition for almost every element detected are strongly non-linear. For instance, almost every element shows a brief initial phase of very high elemental flux into the brine, which is followed by longer periods of lower and typically progressively declining fluxes. In order to understand the environmental significance of these findings it is interesting to estimate the real-world duration that is equivalent to the duration of the soxhlet reactor experiment (i.e. 168 hours).

As a first order approximation of real-world time equivalents the methods of Humez (1996); Humez et al. (1997); Humez and Prost (1999) were followed. This analysis relies on two assumptions: first, the long-term weathering flux of a volcanic ash sample should be approximately a power decay curve; and, rainfall is assumed to be the primary agent of weathering the volcanic ash. In these situations, the equivalent real-world time T_{equiv} in years corresponding to the duration of the soxhlet experiment is given by:

$$T_{equiv} = \frac{H_{SOX}}{H_{RainAnnual}} = \frac{V_{SOX\_total}}{A_{SOX}} \frac{1}{H_{RainAnnual}} \quad \textit{Equation } 8$$

where $H_{RainAnnual}$ is the average annual rainfall height in millimetres for an ash accumulation location of interest, H_{SOX} is an equivalent rainfall (or water) height in millimetres for the experiment, and is defined as the ratio of the total volume of water percolated through the soxhlet reactor, V_{SOX} (volume of water in reactor times number of cycles) over the cross-sectional area of the soxhlet reactor, A_{SOX}.

For the experimental conditions used, T_{equiv} for the 168 hours of experimental time equates to approximately 18 years, with only minor differences between different samples due to slight variations in sample volume, bulk solid density, and grain-size distribution. In order to evaluate this result, the computed equivalent time is compared to leaching results performed on two different ashes from the 95/5 Mount Ruapehu eruption.

The first sample is a pristine sample obtained directly after the eruption at a sampling distance of c. 15 km from source. The second sample was collected from a medial site at c. 30 km from source, where the 95/5 ashes were dumped after the eruption clean-up and where it has been freely weathering for 19.5 years before sampling.

Figure 23 shows the area-normalised flux q against equivalent time of both samples for calcium, a group one element with a typical power decay characterising long-term leaching behaviour. For the weathered 95/5 sample, the total equivalent time is sum of the computed equivalent time and the actual weathering time of 19.5 years. For the long-term quasi-power decay phase, data of both samples collapse onto a single line in the log-linear plot. This result indicates the simple estimate of equivalent time via equation 8 is fairly accurate.

Somewhat surprising, the leaching time-series of the weathered sample also contains a brief initial high flux phase, somewhat similar (albeit not nearly as high) to any of the non-weathered samples. An interpretation of this finding is somewhat difficult in the limit of conducted analyses. One possible explanation could be that the leaching flux is not only controlled by water volume, but also by the conditions of the sample. This finding may be relevant to the interpretation of the time-variant leaching data, but further control experiments are needed to shed light onto this issue.

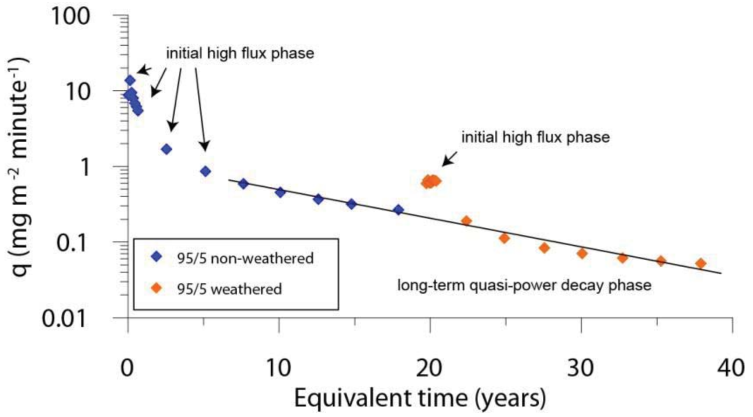

Figure 23: Surface area-normalised volumetric flux of Ca into brine against total equivalent time for the non-weathered and weathered 95/5 Ruapehu ash samples. For the weathered sample, the total equivalent time is the *Tequiv=HSOXHRainAnnual=VSOX_totalASOX1HRainAnnual* Equation 8*) and the weathering time of 19.5 years.*

4.1 Beneficial and detrimental thresholds of brine composition

In the following section the concept of equivalent time will be applied to several examples of elements from each group of time-variant leaching behaviour. The volcanic ash samples from the Mt. Ruapehu eruption sequence of 1995-96 will be the primary focus in this section. This is due to the ability to compare and contrast the samples from the same source in different eruption styles. The environmental implications of the input of each element will be discussed in terms of an example the probable behaviour of the element once it e00nters the soil profile.

4.11 Group 1

4.111 - Calcium

Calcium is an example of an element with *group one* release behaviour where Figure 24, illustrates the release behaviour over estimated real-world time. There is a high initial flux of Ca into brine for the first 262 days, rapidly exceeding the maximum acceptable hardness value of 200 mg/kg for calcium (MoH, 2008) and a gradual decline until c. 4.5 years. After c. 4.5 years, the flux enters a period of very low and continually declining fluxes. This behaviour is seen for all Ruapehu ash samples except for sample 96/7. The 96/7 was a phreatomagmatic eruption that occurred on the 17th of June 1996. It is still releasing significant amounts of calcium into the brine after 18 years. Generally, the brines of phreatomagmatic eruptions have higher concentrations of calcium at all times than those of the magmatic samples.

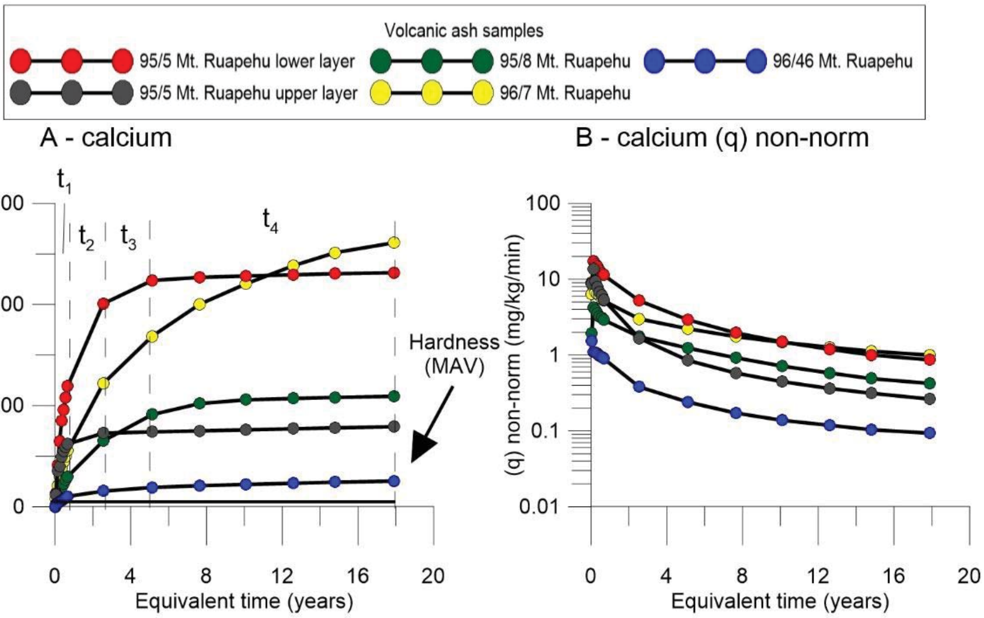

Figure 24: Calcium an example of the group 1 element release behaviour, (A) shows the cumulative concentration for the Mt. Ruapehu 1995-96 volcanic ash samples (MAV) is the maximum acceptable potable drinking water value for calcium, (B) shows the flux (q) non-norm (mg/kg/minute).

The fate of calcium in a dissolved form once entering a soil profile is dependent on the clay content and the drainage characteristics of a particular soil. In a sedimentary alluvial parent material the coarse texture and rapid drainage of the soil profile will result in a rapid loss of calcium into the subsoil or into the groundwater. However, an important part of the behaviour of calcium in the soil profile is the moisture content. If the soil is well drained but, with low moisture content calcium will not migrate any significant distance from its point of origin.

On the other hand in an allophanic soil with a moderate to well drainage pattern, calcium is more likely to be retained on the soil itself. This is due to negative charges of the clay and organic surfaces causing an electrostatic attraction to positively charged calcium. However, this absorbed calcium is highly mobile and is easily displaced by other elements. In soil that is well drained through will result in increased loss of dissolved calcium as it can be displaced from exchange sites due to the replacement of hydrogen and aluminium derived from increased chemical weathering of the minerals soil profile.

Calcium in the natural environment is an essential macronutrient for the growth of both plants and animals. Specifically, calcium is essential in plants for the functioning of root tips. Plants require an almost constant supply of calcium in order to remain functioning (Loneragan & Snowball, 1969). Calcium in the plants is also transported to the upper parts of the xylem. Root growth appears to cease almost immediately upon loss of the supply of calcium. Even in soils with a low pH the acidity has very rarely induced full calcium deficiency in plants (Kirkby & Pilbeam, 1984).

Regarding the leaching results of the well-drained soil, the increase in the dissolved calcium in the soil is liable to induce its luxury uptake only in the short-term period of 262 days during the period of a high flux of calcium into the brine. In the long-term after c. 4.5 years the well-drained soil is not going to see any further benefits from the input of dissolved calcium. In comparison the moderately drained allophanic soil with the high organic matter and clay contents has the ability to store the leached calcium before it is lost deeper into the soil profile for the later demand by plants. This results in an enhancement of the benefits that the moderately drained soil is going to get from the calcium leaching.

4.112 – Manganese

Another example of *group one* leaching behaviour is Manganese, whose time-variant leaching behaviour in estimated equivalent time is presented in Figure 25. There is an initial high flux for the first 262 days that exceeds the maximum acceptable drinking water value (0.05 mg/kg) for manganese and then a very rapid decline in the flux for the next c. 2 years. After the period of c. 2 years the flux of manganese enters a period of very low and declining flux values. All of the Mt. Ruapehu samples show a similar behaviour. As with calcium, the only exception in the 96/7 sample (Figure 25). Also similar to Ca, at any time, samples of phreatomagmatic eruptions are characterized by higher fluxes than those of magmatic eruptions. Of the three phreatomagmatic eruptions, the 17th of June 1996 sample has the highest flux of Mn overall.

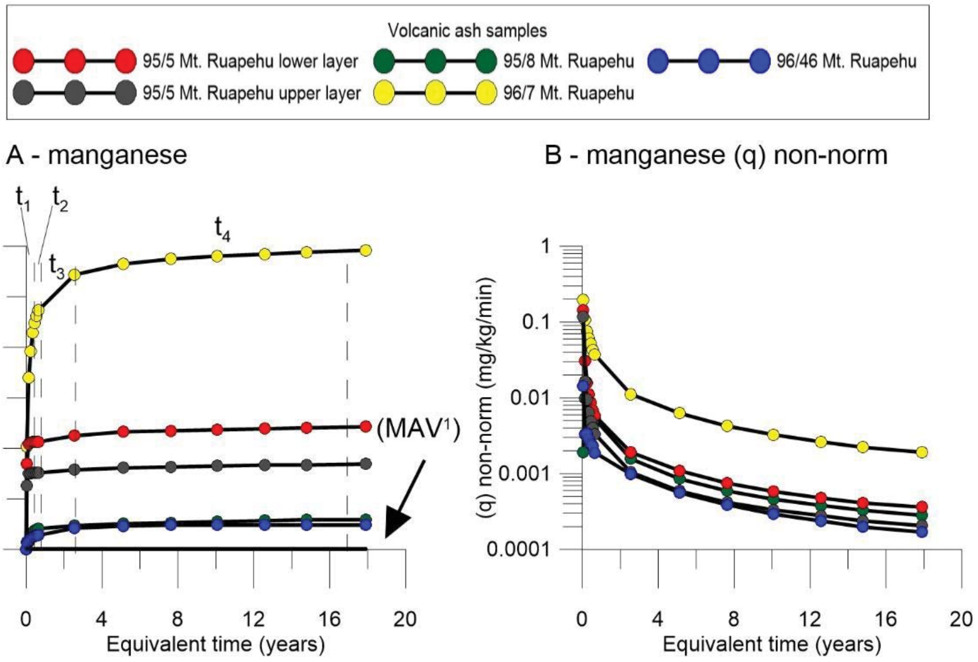

Figure 25: Manganese is an example of the group 1 element release behaviour, (A) shows the cumulative concentration for the Mt. Ruapehu 1995-96 volcanic ash samples (MAV^1) is the maximum acceptable potable drinking water value for manganese, (B) shows flux (q) non-norm (mg/kg/min).

An explanation of the behaviour of manganese within the soil profile is complex due to large variation in the reactions of manganese that can take place. In a well-drained soil profile, manganese can be found in its higher oxidation states of Mn^{3+} and Mn^{4+} within the phases of oxide and hydrous oxide minerals (Kabata-Pendias, 2010). These phases are relatively insoluble, making them unlikely to become remobilised and leached once Mn has been in an oxidising environment (Norvell, 1988). This is also likely to be the fate of any additional manganese that is leached into a well-drained soil profile from volcanic ash.

In a poorly drained, waterlogged soil with anaerobic conditions, water soluble Mn^{2+} is released. This is due to the oxidation of organic materials (Norvell, 1988). Furthermore, since Mn^{2+} was attached to iron oxides and hydrous minerals, other micronutrients including Fe^{2+} are often absorbed onto the same material. Therefore, increases in soluble manganese concentrations are often analogous with soluble phases of copper, zinc and cobalt.

Manganese in the environment is an important micronutrient for the function of plants. The most important process that manganese participates in, is as a catalyst for the initial reactions of photosynthesis (Burnell, 1988). Despite all of the different forms that Mn can exist in within the soil profile, plant roots preferentially take up Mn in its soluble Mn^{2+} form. In a similar way to calcium (Kabata-Pendias, 2010). Furthermore, the interactions of the roots of plants with microorganisms can result in the oxidisation of the soluble Mn^{2+} back into the insoluble Mn^{3+}.

Figure 25, illustrates that the manganese beneficial impacts are in the short-term, i.e. within the first c. 2 years. However, manganese in a well-drained soil can quickly go into forms that are insoluble for plants, reducing the beneficial impacts of manganese to only the amount that the plant root can take up immediately. The long-term portion (i.e. the last equivalent c. 15.5 years) of the soxhlet experiment for manganese showed very little manganese flux for 15.5 years of the experiment.

4.12 Group 2

4.121 - Lead

Lead is an example of an element with *group two* element release behaviour. Leaching data of lead (in cumulative and flux forms) against equivalent time for the Mt. Ruapehu samples are shown in Figure 26. A high initial flux for lead continues for c. 260 days, where the maximum acceptable value for drinking water (0.07 mg/kg) is exceeded almost immediately, (MoH, 2008). After this initial period, there is a relatively abrupt transition into a second period of increasing cumulative concentration.

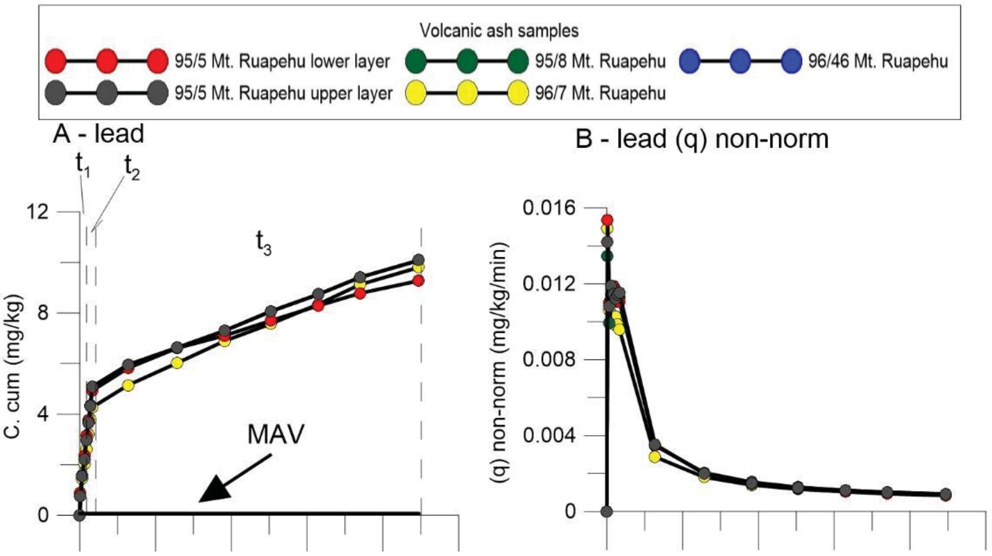

Figure 26: Lead is an example of the group 1 element release behaviour, (A) shows the cumulative concentration for the Mt. Ruapehu 1995-96 volcanic ash samples (MAV) is the maximum acceptable potable drinking water value for lead, (B) shows the flux (q) non-norm (mg/kg/min).

During these next equivalent c. 17.3 years, the flux of Pb into brine is exponentially declining. All of the Mt. Ruapehu volcanic ash samples follow a remarkably similar flux for the duration of the soxhlet reactor experiment.

The behaviour of leached lead in the soil profile is dependent on the abundance of clay and iron-manganese hydroxides (Kabata-Pendias, 2010). Furthermore, soils with a high content of soil organic matter such as in well-drained allophanic soils have been shown to have a significant role in the adsorption of lead near the soil surface. Another factor that influences the solubility of lead in the soil is the soil acidity. High soil pH decrease the solubility of lead significantly. However, the scientific literature is dominated by the impacts on plants by toxic levels of lead pollution from contaminated sites (Sabti, Hossain, Brooks, & Stewart, 2000).

Lead in its natural state occurs in plants, though it is not known for its importance to the functioning of any plant species (Kabata-Pendias, 2010). However, there have been some studies that have highlighted the beneficial effects on the amount of plant growth with the supplication of Pb salts. However, these studies have not isolated all of the potential factors that may result in this plant growth. Lead in plants inhibits several important enzymes that govern plant growth, as well as damage the soil biological functions.

There is a high flux for the first 260 days. Figure 26, shows that the long-term impacts of lead from the Mt. Ruapehu volcanic ash is going to be relatively constant from c. 3 to 18 years of estimated real world time. However, lead is not very mobile in the soil and is often held in organic matter and iron hydroxide complexes irrespective of the drainage profile of a soil.

4.122 – Zinc

Figure 27, presents leaching data for zinc, another example of an element with group two release behaviour, against equivalent time. There is a high initial flux for zinc until c. 0.9 years, it is after this time that the flux exceeds the (5 mg/kg) EPA secondary standard (EPA, 2002) for zinc in drinking water. Zinc changes into a period of decreasing flux over time until c. 8 years. From c. 8 years onwards, the flux changes into an approximately constant and low release over time. Time-variant cumulative concentration data for zinc shows an interesting relationship with the style of eruption. The sample with the highest flux is the phreatomagmatic sample of 96/7 that is followed by the 95/5 lower layer. The other three samples, dry magmatic in eruption style except for the upper layer of 95/5 sample are all clustered together. The 96/46 strombolian style sample shows the lowest cumulative concentrations (and fluxes) and does not exceed the EPA value at any time.

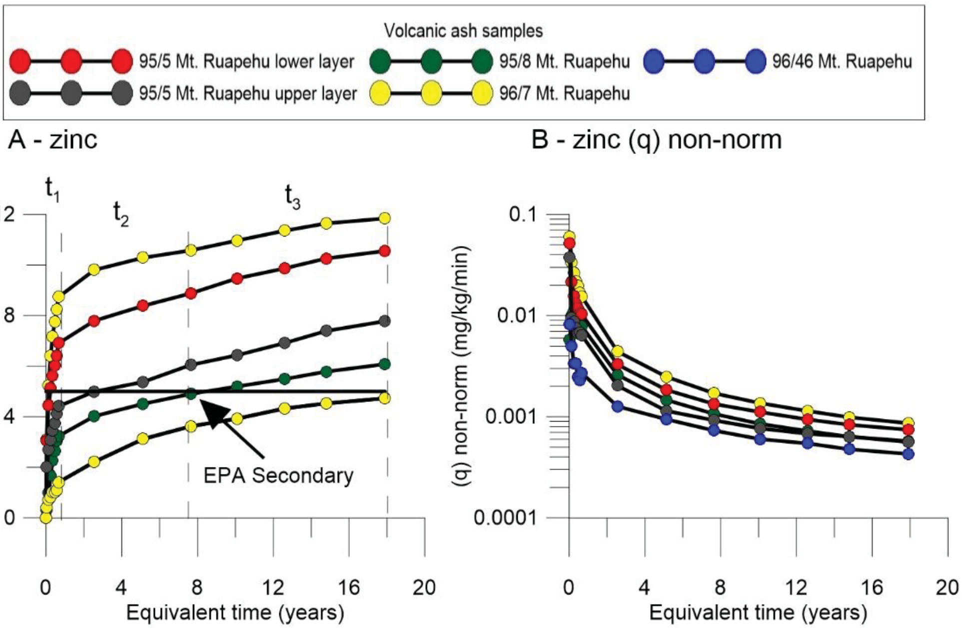

Figure 27: Zinc is an example of the group 2 element release behaviour, (A) shows the cumulative concentration for the Mt. Ruapehu 1995-96 volcanic ash samples (EPA secondary) is the maximum acceptable potable drinking water value for zinc, (B) shows the flux (q) non-norm (mg/kg/min).

In the soil profile the most common form of dissolved zinc is in the form of free ions (Zn^{2+}). The behaviour and the storage of zinc in controlled by the soil pH as well as the forms in which the metal is added. Although zinc is known to be mobile on most soil profiles, soils with high clay content and organic matter such as a well-drained allophanic soil are the most efficient at holding zinc. Within the soil profile there are two main mechanisms of zinc adsorption. The first is the cation exchange sites similar to the way in which calcium is stored in the soil. The second way is the adsorption by organic ligands in the soil. There are also the iron, aluminium as well as manganese hydroxides in the soil profile that adsorb zinc within the soil profile (Kabata-Pendias, 2010).

In plants, zinc has an important function in a variety of enzymes. The basic function of zinc in a plant is the metabolism of carbohydrates. In the scientific literature, there have been some studies expressing concern at the use of zinc based fertilisers that are increasing the toxicity of the soil profile. Zinc is also used extensively for the protection of livestock against biofortified Zn willow may have be a potential method to reduce fungal infection (Anderson et al., 2012). In the aftermath of the Mt. Ruapehu eruptions zinc was also found to be supplied to plants in small concentrations partially by the deposition of volcanic ash (Cronin et al., 1998).

As illustrated in Figure 27, the impacts of zinc are high in the short-term until c. 0.9 years. Then the flux of zinc will increase further in the long-term for 8 years. After 8 years the flux of zinc will be relatively constant and low. This could be an explanation for the findings of Cronin et al.

(1998), inferring that there were small amounts of zinc supplied by input from volcanic ash from the 1995-96 eruption sequence.

4.13 Group 3

4.131 - Iron

Figure 28 presents time-variant leaching data for iron, the only example of an element with group three release behaviour. The flux of iron until c. 1.08 years leaches into the brine in a non-linear flux rapidly exceeding the EPA secondary value for dissolved iron in drinking water (EPA, 2002). After c. 1.08 years the iron changes rapidly into an approximately constant or only slightly decreasing flux that continues for the rest of the soxhlet reactor experiment. The flux of the phreatomagmatic samples of the 1995-96 eruption sequence show the highest constant fluxes of iron compared to the 96/46 strombolian style sample that shows the lowest fluxes in the long-term leaching.

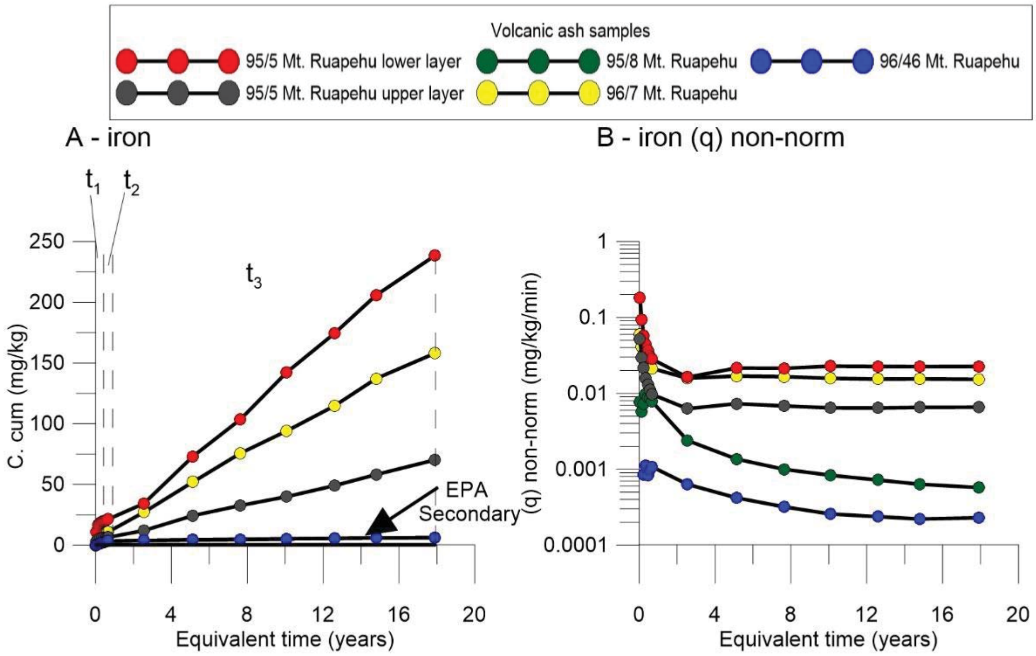

Figure 28: Iron is an example of the group 3 element release behaviour, (A) shows the cumulative concentration for the Mt. Ruapehu 1995-96 volcanic ash samples (EPA secondary) is the maximum acceptable potable drinking water value for Iron, (B) shows the flux (q) non-norm (mg/kg/min).

In the soil profile, iron is an important element. The most common Fe mineral in the soil profile is goethite. It is involved in influencing the behaviour of several other trace elements within the soil profile including copper, zinc, cobalt, lead manganese and cadmium, specifically their adsorption into the soil profile (Kabata-Pendias, 2010). In an acid or a reducing environment, the precipitation of iron compounds is promoted as oxides and hydroxides. In moist soil conditions iron has a tendency to form organic complexes and chelates (Kabata-Pendias, 2010). It is these compounds that are responsible for the loss of iron from the soil profile and soil solution.

Iron is an important element for both plants and animals due to its involvement in haemoglobin and its influence on the formation of chlorophyll. The deficiency of iron has been widely publicised in the scientific literature (Walter et al., 2002). Plants take up Fe^{3+} by reducing the ion to Fe^{3+} which is the fundamental ion that is adsorbed by plants. Ion deficiently has several important roles in plant physiological processes and results in the reduction of plant growth when iron deficiency occurs.

The immediate short-term impact of iron in the soil profile is low, especially within the first year. However, due to the approximately constant flux from c. 1.1 years onwards, the impact of iron leaching is important in long-term. In the soil profile irrespective of the drainage characteristics behaviour of iron is mainly governed by the Eh-pH geochemical conditions within the soil.

4.14 Fluoride

Figure 29, illustrates the release behaviour of fluoride as an example of a group one element over equivalent time. Over approximately the first year, all ash samples, except for the Strombolian eruption sample (96/46), show relatively high, but with time decreasing fluxes of fluoride. The Strombolian sample, in contrast, shows overall low and slightly increasing fluxes over this time period. After c. 3 years, fluoride fluxes decrease more gently with approximately power decay behaviour. Of all samples only the 96/7 phreatomagmatic sample exceeds the accepted fluoride level in drinking water (MoH, 2008), (Figure 29) already in the short term. The threshold is also crossed by the 95/5 upper layer phreatomagmatic eruption sample at c.

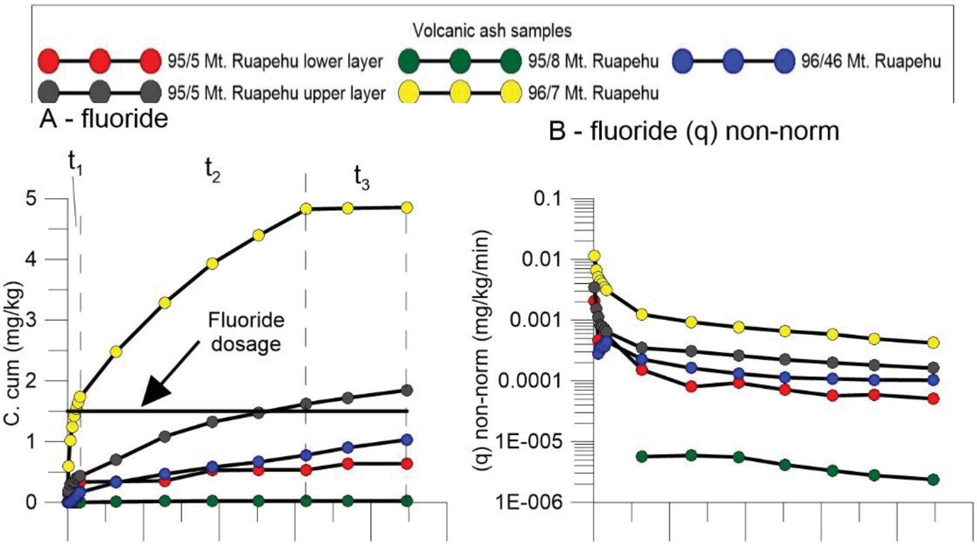

Figure 29: Fluoride is an example of the group 2 element release behaviour, (A) shows the cumulative concentration for the Mt. Ruapehu 1995-96 volcanic ash samples (EPA secondary) is the maximum acceptable potable drinking water value for fluoride, (B) shows the flux (q) non-norm (mg/kg/min).

12 years in the long term leaching. Two samples stick out of the general behaviour. The 96/7 eruption to its highest fluoride fluxes, and the 95/8 magmatic sample due to very low fluoride fluxes. A possible explanation for the high fluoride fluxes obtained in the 96/7 sample is given by the distal sample site of 85km from source. This means that the sample is very fine-grained with consequently high (highly reactive) surface area, and also means that the residence time of particles in the drifting plume is very long allowing for more efficient sublimation of fluoride aerosols to occur.

In the aftermath of the 1995-96 eruption sequence, the very low water solubility of fluoride was noticed (Cronin et al., 2003). This also contrasts with high water solubilises detected for eruptions at Hekla 1970 and Mount Hudson 1991 (Óskarsson, 1980; Rubin et al., 1994).

The release of fluoride from volcanic ash deposited onto soil is one of the most detrimental impacts on agriculture in the aftermath of a volcanic eruption. However, the soxhlet reactor experiments yielded relatively low fluoride concentrations. In order for fluoride to cause chronic fluorosis in cattle, an excess of 100 mg F/kg is required (Borgnino et al., 2013). Cronin et al. (1998); Cronin et al. (2003), both found that the fluoride from the phreatomagmatic Mt. Ruapehu eruptions was contained in slowly soluble phases. Furthermore, in leaching experiments with 1995-96 eruption samples (Cronin et al., 2003), found that dry magmatic samples were more initially water soluble with 85% of the total fluoride in a single batch leaching during 24 hours, compared to the phreatomagmatic eruptive samples leaching more than 200% in later extractions.

Fluoride within the soil profile is sparingly soluble and is immobile (Cronin et al., 1998; Loganathan et al., 2003). Fluoride forms stable bonds with allophane minerals as well as with iron and aluminium oxyhydroxides (Cronin, Manoharan, Hedley, & Loganathan, 2000; Delmelle, Delfosse, & Delvaux, 2003). In the aftermath of the 1995-96 Mt. Ruapehu eruption sequence, the ingestion of fluoride in the soil (Loganathan et al., 2003) and direct ingestion of volcanic ash by animals where the feed was of low quality proved fatal (Cronin et al., 2003). The long-term leaching experiments confirm the general observations of the short-term leaching experiments by Cronin et al. (2003) in that phreatomagmatic eruptions yield the highest fluoride concentrations. However, the results also show that long-term (i.e. after almost 12 years) detrimental effects can occur, particularly in medial to distal deposition areas where effects of aerosol sublimation and effective ash surface area are maximised. In these areas, however and countering this effect, ash deposition is typically low reducing the actual long-term detrimental effect considerably due to low total ash mass loading.

4.15 Sulphate

Sulphate, presented in Figure 30 is another example of an element with a group two release behaviour. For all samples, there is an initial high flux of sulphate in the first 200 days of equivalent time. After this, fluxes decline gently over the long-term with an approximately power decay form. The 96/7 phreatomagmatic sample (see also discussion for fluoride above) exceeds the 250 mg/kg secondary drinking water value for sulphate at around 5 years. The two other phreatomagmatic samples exceeded this threshold at around 20 years, while the magmatic eruption samples stay well below the threshold at all times.

The chemical form SO_4^{2-} within the brine can be directly taken up by the plant roots. In soils with a high content of iron, aluminium minerals hydroxides and 1:1 type clays, such as halloysite and allophane within the soil profile (Shoji et al., 1994) the soil will have a high anion retention capacity that will adsorb sulphate. Sulphate in allophanic soils is plant available meaning it is held less strongly than phosphate. This is the reason that sulphate is found to migrate preferentially into the subsoil (Ugolini & Dahlgren, 2002) due to less competition and lower soil pH (Metson, 1979).

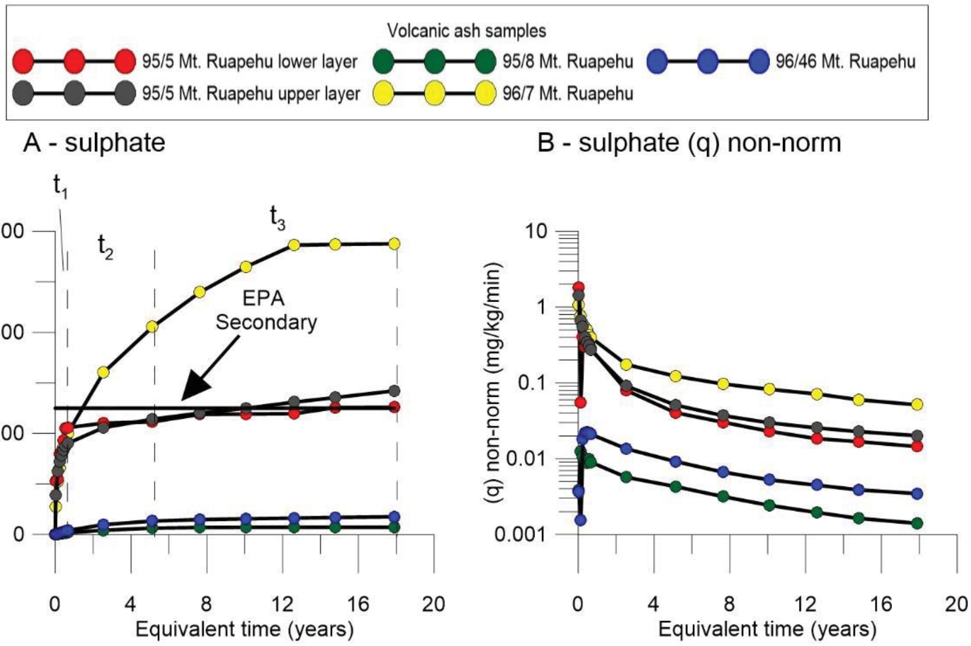

Figure 30: Sulphate is an example of the group 2 element release behaviour, (A) shows the cumulative concentration for the Mt. Ruapehu 1995-96 volcanic ash samples (EPA secondary) is the maximum acceptable potable drinking water value for fluoride, (B) shows the flux (q) non-norm (mg/kg/min).

Sulphate, is regarded as an essential macronutrient for the protein synthesis in plants and animals (Kabata-Pendias, 2010). The addition of large amounts of sulphate to soils during the Mt. Ruapehu 1995-96 is regarded as a beneficial impact on agriculture (Cronin et al., 1998). This is especially important as the soils impacted by the Mt. Ruapehu eruptions had naturally low levels in sulphate. Eight months after the deposition of 3mm of the volcanic ash from the

14th of October 1995 eruption soil tests were still registering an increase in total sulphur content of 25-40% in the top 7.5mm of the soil (Cronin et al., 1998). Furthermore, grazed pastures where more than 0.25 mm of volcanic ash deposited received their total annual topdressing sulphate requirements of (12 – 45 kg ha^{-1}). The here tested long-term leaching of sulphate particularly for the phreatomagmatic eruptions supports these findings of the short-term leaching tests.

4.2 Beneficial or detrimental elements to the environment: behaviour within the soil profile

In the previous section, the environmental fate of fluoride and sulphate, two of the most important macronutrient anions in agriculture was discussed. Elements dissolved in a brine solution emanating from volcanic ash have two long-term results either, adsorption or leaching. Upon infiltration into the soil profile cations with positive charges are attracted to sites of net negative charges such as allophane and halloysite clays. Therefore, soils with a high clay and organic matter content such as allophanic soils are well known for their ability to adsorb major cations (Shoji et al., 1994). This is the fate of the major elements that are leached from the volcanic ash which have infiltrated the soil profile. The addition of anions fluoride, chloride and sulphur into the soil profile has the effect of depressing the soil pH (Delmelle et al., 2003). The enhanced cation exchange capacity of volcanic soils is therefore, diminished. This can result in the displacement of alkaline cations through the soil profile. Soils interactions with minor elements, on the other hand, due to their overall low concentrations are adsorbed onto the iron and aluminium hydrous oxides within a soil profile. Instead of the negative charged clays (Kabata-Pendias, 2010).

Another important factor besides the chemical properties of the soil itself, are the physical properties of the substrate. Especially important is whether a soil has a well-drained or poorly-drained profile. For example, a well-drained allophanic soil with large pores is expected to have the brine from the leached volcanic ash pass through relatively quickly (Hewitt, 2010). This means that even if cumulative concentrations in the long term are high these concentrations are not effective and become diluted. In comparison, a poorly drained soil profile is expected to have the brine leached from the volcanic ash and remain within the soil profile for long times. This will result in an extended period of time where the leached elements can interact with the soil. Thus, future studies focusing on long-term effects of ash leachates should consider the substrate conditions in the region of interest.

In the New Zealand context, an excellent example is a case study in the Waikato region, where the soil profile is interspersed with volcanic ash deposits (Lowe, 1986). In a soil profile with a parent material predominantly of alluvium interspersed with volcanic ash will have a poor to an impeded drainage pattern. This will result in a ‘stagnant’ regime. This ensures that elements remain dissolved within the soil water, especially silica and aluminium. In the long-term this will favour the formation of halloysite. On the opposite extreme, a well-drained sandy soil profile means that dissolved elements will leave quickly and leach into the groundwater, promote loss of silica and increase the formation chances of allophane. This is a case study example of the influence of the soil profile on the drainage of elements leached from volcanic ash.

4.3 Origins of dissolved elements from volcanic ash

The origins of the release pattern of elements are due to the manner in which they are chemically bonded to the sample of volcanic ash. A three zone temperature release model currently best interprets the sources of the brine composition leached from volcanic ash samples (Óskarsson, 1980). The volatile gasses HF, SO_2 and HCl are emitted from the volcano during the degassing of the magma (Sigurdsson, 2015). In the atmosphere these gasses turn into acid aerosols and condense into liquid droplets. Via in-plume surface interactions these gasses interact with the surface of the particles of volcanic ash. This is the leading origin of the halide (F^-, Cl^-) and sulphate (SO_4^{2-}) salt compounds detected (Delmelle et al., 2007). These salts result from the acid dissolution of the volcanic ash surface and frees the monovalent and deviant cations in exchange for hydrogen ions. This is theorised to be followed by precipitation and crystallisation once the ambient temperatures decrease below 340°C.

4.31 Group One

The group one release pattern is characterised by a high and almost constant initial release, before transitioning into a long final phase of a declining leaching rate that is approaching low to zero element leaching into the brine. The elements aluminium, manganese, magnesium and chloride have a very fast transition into a zero release. This is interpreted as the dissolution of the elements that are weakly bonded to the volcanic ash via salt compounds. This would be characteristic of the salts of magnesium, sodium such as chlorides. The co-variance of chloride is consistent with this assumption. It is known that the source of aluminium is the dissolution of the Al-bearing aluminosilicate minerals in the volcanic ash (Oelkers, Schott, & Devidal, 1994). The acidic environment in the soxhlet would make both aluminium as well magnesium soluble.

The elements calcium and sodium display a more longer transition phase, proportional to the square root of time, transitioning into a flat gradient where no further elemental release is taking place. This is most likely a combination of the dissolution of the soluble salts. These would include chlorines and more sparingly soluble sodium and calcium species such as gypsum, alunite and natroalunite.

4.32 Group Two

The elements that belong to the release pattern of group two are characterised by an initial short-term, non-linear release curve. This transitions into a long-term lower release of approximately constant linear gradient that does not approach zero. Thus, in the long-term the elements are still being released into brine in a relatively constant pattern, rather than the very small amounts released in the long-term in group one. A possible interpretation is that the long-term behaviour of group 2 is controlled by the sparingly soluble species after the rapid initial dissolution of the soluble phases.

The increased quasi-linear long-term trend is due to a complex mixture of subaerial high temperature and low temperature heterogeneous chemical reactions, dissolving particle surfaces with decreased solubility than the salt compounds. This trend with the increased phase one and phase two durations are apparent for potassium, zinc, copper, sulphate and fluoride. However, in the case of cobalt, lead, chromium, nickel and cadmium, the phase one and two durations are considerably of shorter duration.

4.33 Group Three

The release pattern of iron is treated separately from those elements categorised as group 1 and two. This is due to iron having its own unique release pattern which is increasing and approximately linear for roughly 94% of the soxhlet reactor experiment. There are crystalline metals such as goethite that will scavenge metals once they are released back into solution

In the scientific literature the controls of iron solubility is understood to be the processes that occur within an eruption plume. Specifically, interpreted as iron being released from Fe-bearing silicate’s and iron oxide minerals (Ayris & Delmelle, 2012a). This source would result in (and thus explain) a constant linear cumulative concentration release pattern.

4.34 Further studies

Further studies into the processes of the solubility of elements leached from volcanic ash need to be conducted. This is in order to gain a full understanding of the origins of the soluble elements. This should be done in a two-fold methodological approach. First there needs to be continues studies on the leaching of volcanic ash over a period time. This has the potential to help isolate some of the processes that govern the solubility factors. Another promising methodology is in Ayris, Cimarelli, et al. (2015), where volcanic ash particle and gas interactions are simulated in an Advanced Gas-Ash reactor that atmospheres of different compositions and temperatures from 200°C to 900°C. One weakness is that hydrogen fluoride cannot be simulated due to risk of damage to quartz components. However, all of these methodologies need to be used in conjunction with surface analysis techniques such as; X-ray photoelectron spectroscopy and atomic force microscopy to image the surface structures of volcanic ash.

4.4 Influence of 1995-96 Mt. Ruapehu eruption parameters

4.41 Eruption style

The Mt. Ruapehu 1995-96 eruption sequence was the largest multi-stage eruption episode of the volcano. The main vent of Mt. Ruapehu is oftentimes covered with an acidic 8-10 million m^3 Crater Lake with a current pH or around 1 (Christenson, 2000; Cronin et al., 2003). The Crater Lake vent is host to an active hydrothermal system (Christenson & Wood, 1993). The effect of the acidic geochemistry of the Crater Lake on the eruptions are illustrated in Figure 31, where the pH of sample brines for the different ash samples is plotted against real-world time. The phreatomagmatic eruption samples are considerably more acidic than the dry magmatic eruption samples. However, the upper layer of the 95/5 sample is slightly less acidic than the lower 95/5 sample. This is the result of the higher influence of the 'long-lived' hydrothermal system on the lower layer. The point count componentry results also echoed this in the fact that there is a higher content of lithics (mostly from the acidic hydrothermal system) in the coarser grainsizes of the lower layer while there is a marked decrease in the

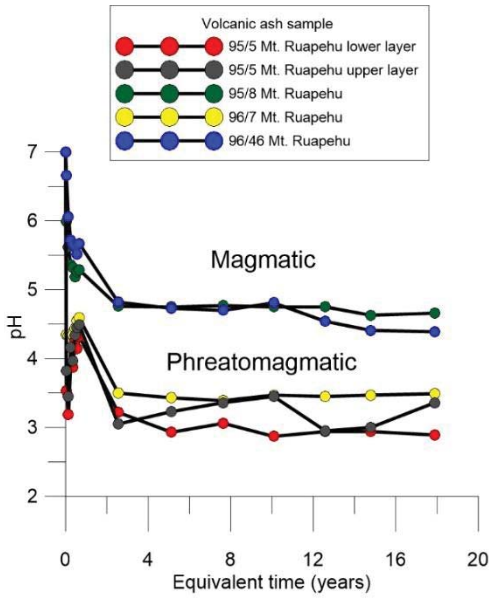

Figure 31: Graph of the pH measurements taken at the time of the brine sampling for each of the Mt. Ruapehu 1995-96 eruption sequence samples over experimental time.

upper layer. This is also interpreted to the fact that that the lithics are composed of altered non-juvenile material that has been influenced by the hydrothermal system of Mt. Ruapehu.

There is also a difference in the acidity between the first phreatomagmatic eruption on the 11th of October 1995 and the second one on the 17th of June 1996. The 17th of June 1996 sample has a higher overall pH, compared to the 11th of October 1995 samples Figure 31. This is interpreted to be due to the long lived hydrothermal system being largely cleared out by the eruptions that occurred prior to the 17th of June 1996 eruption, thus decreasing the amount of acidic hydrothermal material that could be erupted. However, there was still enough of the old hydrothermal system remaining along with the partial refilling of the Crater Lake to result in a significant phreatomagmatic eruption and an overall low pH.

The samples from the dry magmatic eruption that occurred on the 14th of October 1995 and the strombolian eruption on the 20th of July 1996 have pH values that are considerably higher than the other two phreatomagmatic eruptions. These dry magmatic eruption samples, despite the differences in the eruption style have a pH that is very similar, pH 4.5 – 5.0 in the long-term. The similarities in the pH highlights the influence that the acidic Crater Lake and the hydrothermal system have on the chemistry of an eruption. Both of these dry magmatic and strombolian eruptions occurred at a time when the water had been completely displaced from the crater.

Bulk aluminium concentrations measured in juvenile Mt. Ruapehu scoria by Kilgour et al. (2013), revealed that that the 1995-96 eruptions became more primitive with time. This implies a decrease in the aluminium content of the magmatic component. However, the decrease in aluminium content is overshadowed by the influence of the geochemistry of the Crater Lake. Since aluminium is amphoteric it will go into solution in highly acidic conditions. Such conditions are found in the oxidised part of the hydrothermal system at the floor of the Crater Lake of Mt. Ruapehu (Christenson, 2000; Cronin et al., 2003). Therefore, the phreatomagmatic eruptions including the 17th of June 1996 eruption will have a higher flux of aluminium than the magmatic eruptions that occurred later in the sequence.

The 11th of October eruption was sampled in two layers. These have been interpreted to represent two different phases of the same eruption (Moebis, 2011). The lower layer originated from the initial phreatomagmatic eruptive phase. This layer contains the fragmented contents of the pre-eruption hydrothermal system, explaining the enrichment in sulphur and aluminium. The upper phreatomagmatic layer has a lower content of lithic components and is instead enriched in juvenile components. This explains the changes in acidities of the brines, the lower layer being more acidic than the upper layer, (Figure 32). Figure 32, illustrates the differences between the lower and the upper layer for cumulative sodium and magnesium. The enrichment of the lower layer is inferred to be due to the increased hydrothermal system input compared to the upper layer.

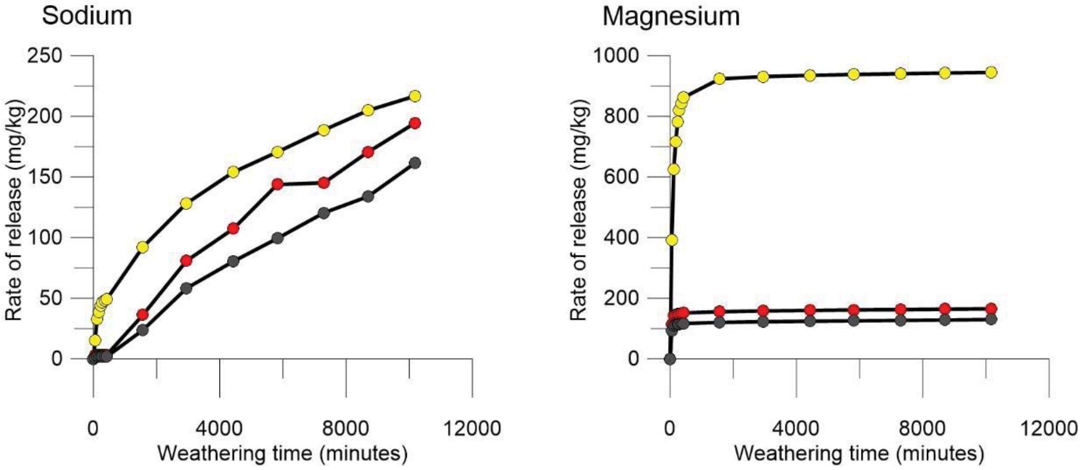

Figure 32: Graphs showing the weathering time of sodium and magnesium for the phreatomagmatic samples of Mt. Ruapehu.

The 17th of June 1996 cumulative concentrations show some unexpected long-term results that are higher than the 11th of October 1995 samples. This is in spite of the fact that the 17th June 1996 eruption was orders of magnitude smaller than the 11th of October 1995 eruption (Cronin et al., 2003). An example is for sodium and magnesium (Figure 32), the cumulative concentrations among these two elements are an order of magnitude different. The main point being the marked increase of the 17th June 1996 sample compared to the 11th of October sample, (Figure 32). Other elements that show this behaviour are fluoride, sulphate, zinc, manganese and to a lesser extent, calcium.

The trend of the enriched 17th June 1996 sample is unexpected because of the fact that the hydrothermal system, thought to contain an enrichment of environmentally important elements was emptied after the 11th of October eruption. Alternative, to the long-standing system from 1945, the last occasion the crater lake was completely expelled by an eruption was in 1945 (Kilgour et al., 2013). The 17th June 1996 eruption occurred through a partially refilled crater lake, with a hydrothermal system in existence during the quiescent period between 1995-96. Therefore, the 17th June 1996 eruption should not have had as much of an enrichment in cumulative elements as was observed in the soxhlet reactor experiments.

4.42 Eruption size and distance

In order to fully explain the 17th June 1996 sample, other sampling parameters have to be carefully considered. The 20th July 1996 sample originates from the smallest eruption in the

Mt. Ruapehu sequence, the grainsize is also the finest. In comparison, the lower and upper layers of the 11th of October samples from the largest eruption sequence have a coarse grainsize distribution. While the 14th October 1995 and the 17th of June 1996, despite being from two distinctly different eruption styles they have a grainsize distribution that is almost identical.

The distance where a volcanic sample is collected from the source can outweigh the influence that the style of a volcanic eruption can have on the cumulative concentration of a sample. For instance, the 20th July sample was the smallest eruption but, was collected 8.5 km from source, a very distal location for this eruption. In the case of the 11th of October 1995 eruption even though it had the largest volume, the sample was collected 15km from the source (Cronin et al., 2003). A very proximal sample with a short residence time when it is examined in conjunction with its eruption size. The 17th of July sample was collected 85km from source, a distal sample with the low total volume of the eruption. The volcanic ash from the 17th of June would have had an increased residence time in the atmosphere. Especially, where the ambient temperatures were below 340°C. This would allow for an increased interaction time with sulphuric and halogen acid aerosols. This explains the increased enrichment of some elements in this sample in comparison with the larger 11th October eruption.

4.43 Recommendations for improved hazard analysis

It is important to recognise that the analysed volcanic ash samples are a single snapshot into the processes and impacts that can occur in a volcanic eruption. In order to gain a full understanding of any volcanic eruption it is essential to carry out multiple collections of volcanic ash in separate locations distances from the source in both the longitudinal and latitudinal axis of the eruption plume. The Mt. Ruapehu eruption sequence has demonstrated that there can be multiple styles of eruptions within a very small period of time. This highlights the next recommendation, to ensure that there are continual details and observations carried out during any volcanic eruption periods. This step ensured that an adequate characterisation carried out of any potential external influences influencing its impact on the environment. The Mt. Ruapehu eruption sequence taught that even small eruptions such as the 17th of June phreatomagmatic eruption can cause widespread impacts after the climax of the eruption sequence has abated.

The soxhlet reactor experiments with the White Island and the Mt. Kelut samples have demonstrated that that there is no single factor responsible for the impact of an eruption on the environment. The soxhlet reactor experiments for White Island revealed repeatedly enriched cumulative element concentrations orders of magnitude over the other eruption samples. If this results was interpreted solely on the soxhlet reactor it would be assumed that this sample would have a significant impact on the environment. However, this sample came from a very small vent clearing eruption on an off sure island off the east coast of New Zealand. As well as the fact that this sample was collected 300 metres from the event is also important.

On the other hand the Mt. Kelut sample was collected approximately 210 kilometres from the source in east Java, Indonesia. Viewing the very fine grainsize might indicate that there would be a significant release of elements over the short-term. This is due to the fact that most gas-ash interaction models place significant emphasis on the finer grainsizes, releasing more elements that their coarser counterparts (D'Addabbo et al., 2015; Delmelle et al., 2007). However, in the soxhlet reactor experiments, despite its distal collection point and it’s comparatively larger size the cumulative element concentrations were relatively low. The fine grainsize and geometric surface area means that the dissolution of the glass and crystals are enhanced as seen with the delayed increase in Mt. Kelut cumulative concentration of zinc. However, the phreatic eruption involved the destruction of a lava dome, no crater lake was present. Hence, the relatively low cumulative element concentrations in comparison to its size.

4.5 Influence of the methodology

In the soxhlet reactor experiments, emphasis is placed on the attempt to correlate the results in the environment with real time. An issue that arose during the course of this project is the unexplained losses of recovered brine sample. One possible reason is that the high losses of water throughout the soxhlet experiments may be due to the design of the methodology (S. Hall, Personal Communication, March 17th 2017). Compensating water was designed to be maintained at a temperature of 20°C dripping into the volcanic ash sample. The temperature required in order to maintain this temperature was that the heater be set to 215° C. This was in order to propel the water vapour up the one metre length vapour tube. However, the large amount of water vapour escaping means a net water loss (S. Hall, Personal Communication, March 17th 2017).

Another issue picked up in the experimental design is the methodology of boiling 250 ml of water. In chemistry it is common practice to use 50% of the total volume of the boiling flask. In this soxhlet experiment this would have been 120 to 150 mL rather than the 250 mL refilled in each sampling. This resulted in a multitude of problems relating to the kinetics of boiling water. This method manifested itself when problems arose with the constant cracking of the borosilicate glass of the boiling flasks.

The evaporative water loss alone cannot explain the loss of water found in the experiment. A full explanation goes back to the porosity and permeability of the samples. Water infiltrates into a soil profile through the largest macropores initially, then down to the smaller micropores. Thus, the loss of water during the long-term part of the experiment beyond seven hours is likely the result of progressive filling between the grains of volcanic ash with water.

Conclusion

This project aimed at developing and testing a method to investigate the long-term leaching behaviour of volcanic ash. Previous research on various volcanic eruptions has demonstrated the strong environmental impacts of elements leached from volcanic ashes via simple batch leaching tests. What remained unknown is the long-term behaviour and impacts of potentially leaching volcanic ash deposits, as well as a deeper understanding of the elemental compounds of leaching brines. In particular, little knowledge existed on the minor and trace element composition of brines and their potentially beneficial or detrimental effects on the environment.

Research objectives revisited. This research was guided by three main objectives. These objectives are repeated here and the main conclusions of this research is summarised according to them.

Objective 1. The first objective was to develop or adopt a suitable methodology that can simulate the weathering of volcanic ash samples in a feasible time frame and to analyse the time-variant leaching behaviour of volcanic ash.

- The adaptation and variation of a soxhlet reactor experiment constantly flushing volcanic ash samples with deionised water was found a suitable method to simulate accelerated weathering of volcanic material.

- A number of shortcomings of the current method were identified during the course of this research and solutions for future research attempts in this direction were provided.

- The characterisation of the volcanic ash samples, in particular their componentry, grain-size distribution and effective surface area has proven to be of great significance to interpret long-term leaching results and should be recommended for future work also.

Objective 2. The second objective was to deploy this new method to characterise the time-variant leaching behaviour of volcanic ash samples from a variety of volcanic sources and eruption styles.

- To this end, nine individual ash-samples from four different volcanoes (Mount Ruapehu, White Island, Kelut and Sakurajima) could be analysed for their long-term leaching behaviour using the new soxhlet reactor.

• For the case of Ruapehu five ash samples from the 1995/96 eruption sequence could be analysed to elucidate the influence of eruption behaviours on the short- to long term leaching processes

• The analyses revealed the existence of a wide range of minor and trace elements in the leached brines, which are chromium, lead, cobalt, nickel, cadmium, zinc, manganese and copper

• Generally, all ash samples were found to release elements into brine over time in a strongly non-linear fashion.

• The time-variance of leaching was found to be primarily controlled by the element leached, while the volcanic source, eruption style and nature of the plumbing system has a primary influence on the absolute elemental concentration.

• This study defines three main groups of different time-variant leaching behaviour, named groups 1-3. These differ in their rates of concentration changes of the brine over time and in number of phases of characteristic concentration change, named phases 1-4.

• The study suggests that the elements aluminium, manganese, magnesium, chloride, calcium and sodium are of group 1, elements cobalt, lead, chromium, nickel, cadmium, potassium, zinc copper, sulphate and fluoride are of group 2 and the element iron is of group 3.

• For the 1995/96 eruption sequence, the study highlighted marked differences in the time-variant leaching behaviour of eruptions depending on their eruption style, existence of a Crater Lake and/or hydrothermal system, but also on the effective surface area of an ash sample (e.g. their effective grain-size influenced by eruption style, size and distance of ash sampling site from source).

Objective 3. The third objective was to attempt to relate the accelerated experimental weathering time to real-world time scales to define and interpret the short- and long-term beneficial and detrimental impacts of ash leaching processes and products for the environment.

• A simple method of relating the relative amounts of water percolation through experimental and natural ash samples to estimate the real-world time equivalent for the accelerated soxhlet experiment was adopted for the Ruapehu ash samples.

• The results of this method could be verified and showed that the 168 hours of the soxhlet experiment are equivalent to approximately 18 years of real-world weathering. This finding provided the confidence needed to interpret the non-linear time-variant leaching processes with respect to real time scales.

- In this respect, the brief initial high fluxes of most elements into brine, which can also exceed environmental and health threshold values, are found to occur in real durations of c. 0.2-0.7 years.

- Long-term effects (lead, zinc and copper) were found to last in part as long as the entire experiment

- Volcanic ash samples that have been derived from phreatomagmatic eruptions have a higher short- and long-term impact on agriculture than dry magmatic eruptions due to the increase of soluble elements that are leached.

- This study highlights the short-term (a few months to years) beneficial effects of the following elements: manganese, aluminium, calcium and magnesium; and the short-term detrimental effects of those elements: lead and fluoride.

- This study highlights the long-term beneficial effects of the following elements: zinc, copper, iron, potassium and sodium; and the long-term detrimental effects of lead and fluoride

This pilot study on accelerated weathering of volcanic ash samples and their potential short- and long-term beneficial and detrimental impacts provides a number of potential avenues for future more detailed research into the chemical, physical and environmental aspects of this field. The current results will allow interpreting observations of beneficial and detrimental effects of volcanic ash on the environment, the agriculture and health with more complexity.

Bibliography

Aldridge, R. (1982). prediction of soil temperature in New Zealand and application to the temperature regimes of'Soil Taxonomy'. *New Zealand Soil Bureau Scientific Report*.

Aldridge, R. (1983). *Estimation of soil temperatures at 0.1 m and 0.3 m depths*: Department of Scientific and Industrial Research.

Alfano, F., Bonadonna, C., Delmelle, P., & Costantini, L. (2011). Insights on tephra settling velocity from morphological observations. *Journal of Volcanology and Geothermal Research, 208*(3), 86-98.

Anda, M. (2016). Characteristics of pristine volcanic materials: Beneficial and harmful effects and their management for restoration of agroecosystem. *Science of the total environment, 543*, 480-492.

Anda, M., & Sarwani, M. (2012). Mineralogy, chemical composition, and dissolution of fresh ash eruption: new potential source of nutrients. *Soil Science Society of America Journal, 76*(2), 733-747.

Anderson, C. W., Robinson, B. H., West, D. M., Clucas, L., & Portmann, D. (2012). Zinc-enriched and zinc-biofortified feed as a possible animal remedy in pastoral agriculture: Animal health and environmental benefits. *Journal of Geochemical Exploration, 121*, 30-35.

Andersson, S., Martinsson, B., Friberg, J., Brenninkmeijer, C., Rauthe-Schöch, A., Hermann, M., . . . Zahn, A. (2013). Composition and evolution of volcanic aerosol from eruptions of Kasatochi, Sarychev and Eyjafjallajökull in 2008–2010 based on CARIBIC observations. *Atmospheric Chemistry and Physics, 13*(4), 1781-1796.

Antos, J. A., & Zobel, D. B. (1985). Upward movement of underground plant parts into deposits of tephra from Mount St. Helens. *Canadian Journal of Botany, 63*(12), 2091-2096.

Antos, J. A., & Zobel, D. B. (1986). Recovery of forest understories buried by tephra from Mount St. Helens. *Vegetatio, 64*(2-3), 103-111.

Antos, J. A., & Zobel, D. B. (2005). Plant responses in forests of the tephra-fall zone *Ecological responses to the 1980 eruption of Mount St. Helens* (pp. 47-58): Springer.

Armbrust, D. (1984). Wind and sandblast injury to field crops: Effect of plant age. *Agronomy Journal, 76*(6), 991-993.

Armienta, M., De la Cruz-Reyna, S., Morton, O., Cruz, O., & Ceniceros, N. (2002). Chemical variations of tephra-fall deposit leachates for three eruptions from Popocatepetl volcano. *Journal of Volcanology and Geothermal Research, 113*(1), 61-80.

Ayris, P., Cimarelli, C., Delmelle, P., Wadsworth, F., Vasseur, J., Suzuki, Y., & Dingwell, D. (2015). A novel apparatus for the simulation of eruptive gas-rock interactions. *Bulletin of Volcanology, 77*(12), 104.

Ayris, P., & Delmelle, P. (2012a). Volcanic and atmospheric controls on ash iron solubility: A review. *Physics and Chemistry of the Earth, Parts A/B/C, 45*, 103-112.

Ayris, P., Lee, A., Wilson, K., Kueppers, U., Dingwell, D., & Delmelle, P. (2013). SO 2 sequestration in large volcanic eruptions: high-temperature scavenging by tephra. *Geochimica et Cosmochimica Acta, 110*, 58-69.

Ayris, P. M., & Delmelle, P. (2012b). The immediate environmental effects of tephra emission. *Bulletin of Volcanology, 74*(9), 1905-1936.

Ayris, P. M., Delmelle, P., Cimarelli, C., Maters, E. C., Suzuki, Y. J., & Dingwell, D. B. (2014). HCl uptake by volcanic ash in the high temperature eruption plume: mechanistic insights. *Geochimica et Cosmochimica Acta, 144*, 188-201.

Ayris, P. M., Delmelle, P., Pereira, B., Maters, E. C., Damby, D. E., Durant, A. J., & Dingwell, D. B. (2015). Spatial analysis of Mount St. Helens tephra leachate compositions: implications for future sampling strategies. *Bulletin of Volcanology, 77*(7), 1-17.

Bagnato, E., Aiuppa, A., Andronico, D., Cristaldi, A., Liotta, M., Brusca, L., & Miraglia, L. (2011). Leachate analyses of volcanic ashes from Stromboli volcano: A proxy for the volcanic gas plume composition? *Journal of Geophysical Research: Atmospheres, 116*(D17).

Bagnato, E., Aiuppa, A., Bertagnini, A., Bonadonna, C., Cioni, R., Pistolesi, M., . . . Hoskuldsson, A. (2013). Scavenging of sulphur, halogens and trace metals by volcanic ash: the 2010 Eyjafjallajökull eruption. *Geochimica et Cosmochimica Acta, 103*, 138-160.

Bank, W. (1993). *Argentina: from insolvency to growth. A World Bank country study*. Retrieved from Washington D. C. :

Belosi, F., Santachiara, G., & Prodi, F. (2011). Eyjafjallajökull volcanic eruption: Ice Nuclei and particle characterization. *Atmospheric and Climate Sciences, 1*(02), 48.

Bia, G., Borgnino, L., Gaiero, D., & García, M. (2015). Arsenic-bearing phases in South Andean volcanic ashes: Implications for As mobility in aquatic environments. *Chemical Geology, 393*, 26-35.

Black, R. A., & Mack, R. N. (1986). Mount St. Helens ash: recreating its effects on the steppe environment and ecophysiology. *Ecology*, 1289-1302.

Blake, D. M., Wilson, G., Stewart, C., Craig, H. M., Hayes, J. L., Jenkins, S. F., Wilson, T. M., Horwell, C. J., Andreastuti, S., Daniswara, R., Ferdiwijaya, D., Leonard, G. S., Hendrasto, M., Cronin, S. . (2015). *The 2014 eruption of Kelud volcano, Indonesia: impacts on infrastructure, utilities, agriculture and health* Retrieved from

Blott, S. J., & Pye, K. (2001). GRADISTAT: a grain size distribution and statistics package for the analysis of unconsolidated sediments. *Earth Surface Processes and Landforms, 26*(11), 1237-1248.

Borgnino, L., Garcia, M., Bia, G., Stupar, Y., Le Coustumer, P., & Depetris, P. (2013). Mechanisms of fluoride release in sediments of Argentina's central region. *Science of the total environment, 443*, 245-255.

Brantley, S. L., White, A. F., & Hodson, M. (1999). Surface area of primary silicate minerals *Growth, dissolution and pattern formation in geosystems* (pp. 291-326): Springer.

Brayshay, M., & Grattan, J. (1999). Environmental and social responses in Europe to the 1783 eruption of the Laki fissure volcano in Iceland: A consideration of contemporary documentary evidence. *Geological Society, London, Special Publications, 161*(1), 173-187.

Brown, R., Bonadonna, C., & Durant, A. (2012). A review of volcanic ash aggregation. *Physics and Chemistry of the Earth, Parts A/B/C, 45*, 65-78.

Brunauer, S., Emmett, P. H., & Teller, E. (1938). Adsorption of gases in multimolecular layers. *Journal of the American chemical society, 60*(2), 309-319.

Burket, S. D., Furlow, E. P., Grant, L. C., Lipovsky, Thomas G. Lopp, W. A. (1980). *The Economic effects of the eruptions of Mt. St. Helens* Retrieved from Washington, D.C. :

Burnell, J. N. (1988). The biochemistry of manganese in plants. *Developments in plant and soil sciences, 33*, 125-137.

Cas, R., & Wright, J. V. (1987). *Volcanic successions modern and ancient: A geological approach to processes, products and successions*: Springer Science & Business Media.

Christenson, B. (2000). Geochemistry of fluids associated with the 1995–1996 eruption of Mt. Ruapehu, New Zealand: signatures and processes in the magmatic-hydrothermal system. *Journal of Volcanology and Geothermal Research, 97*(1), 1-30.

Christenson, B., & Wood, C. (1993). Evolution of a vent-hosted hydrothermal system beneath Ruapehu Crater Lake, New Zealand. *Bulletin of Volcanology, 55*(8), 547-565.

Collins, B. D., & Dunne, T. (1986). Erosion of tephra from the 1980 eruption of Mount St. Helens. *Geological Society of America Bulletin, 97*(7), 896-905.

Cook, R. J., Barron, J., Papendick, R. I., & Williams, G. (1981). Impact on agriculture of the Mount St. Helens eruptions. *Science, 211*(4477), 16-22.

Coote, G. E., Cutress, T. W., & Suckling, G. W. (1997). Uptake of fluoride into developing sheep teeth, following the 1995 volcanic eruption of Mt Ruapehu, New Zealand. *Nuclear Instruments and Methods in Physics Research Section B: Beam Interactions with Materials and Atoms, 130*(1–4), 571-575. doi:http://dx.doi.org/10.1016/S0168-583X(97)00250-4

Craig, H., Wilson, T., Stewart, C., Outes, V., Villarosa, G., & Baxter, P. (2016). Impacts to agriculture and critical infrastructure in Argentina after ashfall from the 2011 eruption of the Cordón Caulle volcanic complex: an assessment of published damage and function thresholds. *Journal of Applied Volcanology, 5*(1), 1.

Craig, H., Wilson, T., Stewart, C., Villarosa, G., Outes, V., Cronin, S., & Jenkins, S. (2016). Agricultural impact assessment and management after three widespread tephra falls in Patagonia, South America. *Natural Hazards*, 1-63.

Craig, H. M. (2015). Agricultural vulnerability to tephra fall impacts.

Creed, J., Brockhoff, C., & Martin, T. (1994). Determination of Trace Elements in Waters and Wastes by ICPMS, Method 200.8 (Revision 5.4.). *US Environmental Protection Agency*.

Cronin, S., Hedley, M., Neall, V., & Smith, R. (1998). Agronomic impact of tephra fallout from the 1995 and 1996 Ruapehu Volcano eruptions, New Zealand. *Environmental geology, 34*(1), 21-30.

Cronin, S., Stewart, C., Zernack, A., Brenna, M., Procter, J., Pardo, N., . . . Irwin, M. (2014). Volcanic ash leachate compositions and assessment of health and agricultural hazards from 2012 hydrothermal eruptions, Tongariro, New Zealand. *Journal of Volcanology and Geothermal Research, 286*, 233-247.

Cronin, S. J., Hedley, M., Smith, R., & Neall, V. (1997). Impact of Ruapehu ash fall on soil and pasture nutrient status 1. October 1995 eruptions. *New Zealand Journal of Agricultural Research, 40*(3), 383-395.

Cronin, S. J., Lecointre, J., Palmer, A., & Neall, V. (2000). Transformation, internal stratification, and depositional processes within a channelised, multi-peaked lahar flow. *New Zealand Journal of Geology and Geophysics, 43*(1), 117-128.

Cronin, S. J., Manoharan, V., Hedley, M. J., & Loganathan, P. (2000). Fluoride: A review of its fate, bioavailability, and risks of fluorosis in grazed-pasture systems in New Zealand. *New Zealand Journal of Agricultural Research, 43*(3), 295.

Cronin, S. J., Neall, V., Lecointre, J., Hedley, M., & Loganathan, P. (2003). Environmental hazards of fluoride in volcanic ash: a case study from Ruapehu volcano, New Zealand. *Journal of Volcanology and Geothermal Research, 121*(3), 271-291.

Cronin, S. J., & Sharp, D. S. (2002). Environmental impacts on health from continuous volcanic activity at Yasur (Tanna) and Ambrym, Vanuatu. *International Journal of Environmental Health Research, 12*(2), 109-123.

D'Addabbo, M., Sulpizio, R., Guidi, M., Capitani, G., Mantecca, P., & Zanchetta, G. (2015). Ash leachates from some recent eruptions of Mount Etna (Italy) and Popocatépetl (Mexico) volcanoes and their impact on amphibian living freshwater organisms. *Biogeosciences, 12*(23), 7087-7106.

Dellino, P., Gudmundsson, M., Larsen, G., Mele, D., Stevenson, J., Thordarson, T., & Zimanowski, B. (2012). Ash from the Eyjafjallajökull eruption (Iceland): Fragmentation processes and aerodynamic behavior. *Journal of Geophysical Research: Solid Earth, 117*(B9).

Delmelle, P., Delfosse, T., & Delvaux, B. (2003). Sulfate, chloride and fluoride retention in Andosols exposed to volcanic acid emissions. *Environmental Pollution, 126*(3), 445-457.

Delmelle, P., Gerin, P., & Oskarsson, N. (2000). Surface and bulk studies of leached and unleached volcanic ashes. *EOS, Transactions, American Geophysical Union, 81*, F1311.

Delmelle, P., Lambert, M., Dufrêne, Y., Gerin, P., & Óskarsson, N. (2007). Gas/aerosol–ash interaction in volcanic plumes: New insights from surface analyses of fine ash particles. *Earth and Planetary Science Letters, 259*(1–2), 159-170. doi:http://dx.doi.org/10.1016/j.epsl.2007.04.052

Delmelle, P., Villiéras, F., & Pelletier, M. (2005). Surface area, porosity and water adsorption properties of fine volcanic ash particles. *Bulletin of Volcanology, 67*(2), 160-169.

Diaz, F., Jimenez, C. C., & Tejedor, M. (2005). Influence of the thickness and grain size of tephra mulch on soil water evaporation. *Agricultural water management, 74*(1), 47-55. doi:http://dx.doi.org/10.1016/j.agwat.2004.10.011

Durant, A., Rose, W., Sarna-Wojcicki, A., Carey, S., & Volentik, A. (2009). Hydrometeor-enhanced tephra sedimentation: Constraints from the 18 May 1980 eruption of Mount St. Helens. *Journal of Geophysical Research: Solid Earth, 114*(B3).

Edmeades, D., Thorrold, B., & Roberts, A. (2005). The diagnosis and correction of sulfur deficiency and the management of sulfur requirements in New Zealand pastures: a review. *Animal Production Science, 45*(10), 1205-1223.

Eggler, W. A. (1963). Plant life of Paricutín volcano, México, eight years after activity ceased. *American Midland Naturalist*, 38-68.

EPA. (2002). National Primary and Secondary Drinking Water Regulations. *EPA 816-F-02-013*.

Fisher, R. V., & Schmincke, H. U. (1984). *Pyroclastic rocks*: Springer Science & Business Media.

Floor, G. H., & Román-Ross, G. (2012). Selenium in volcanic environments: a review. *Applied Geochemistry, 27*(3), 517-531.

Flueck, W. T. (2016a). Brief communication: Extended chronology of the Cordón Caulle volcanic eruption beyond 2011 reveals toxic impacts. *Natural Hazards and Earth System Sciences, 16*(11), 2351.

Flueck, W. T. (2016b). The impact of recent volcanic ash depositions on herbivores in Patagonia: a review. *The Rangeland Journal, 38*(1), 27-34.

Flueck, W. T., & Smith-Flueck, J. A. M. (2013). Severe dental fluorosis in juvenile deer linked to a recent volcanic eruption in Patagonia. *Journal of wildlife diseases, 49*(2), 355-366.

Folch, A. (2012). A review of tephra transport and dispersal models: evolution, current status, and future perspectives. *Journal of Volcanology and Geothermal Research, 235*, 96-115.

Folk, R. L. (1954). The distinction between grain size and mineral composition in sedimentary-rock nomenclature. *The Journal of Geology, 62*(4), 344-359.

Folk, R. L., & Ward, W. C. (1957). Brazos River bar: a study in the significance of grain size parameters. *Journal of Sedimentary Research, 27*(1).

Fordyce, F. M. (2013). *Selenium deficiency and toxicity in the environment*: Springer.

Fowler, W., & Lopushinsky, W. (1986). Wind-blown volcanic ash in forest and agricultural locations as related to meteorological conditions. *Atmospheric Environment (1967), 20*(3), 421-425.

Frogner, P., Gíslason, S. R., & Óskarsson, N. (2001). Fertilizing potential of volcanic ash in ocean surface water. *Geology, 29*(6), 487-490.

Georgsson, G., & Pétursson, G. (1972). Fluorosis of sheep caused by the Hekla eruption in 1970. *Fluoride;(United States), 5*(CONF-7110101-).

Gilbert, J. S., & Lane, S. (1994). The origin of accretionary lapilli. *Bulletin of Volcanology, 56*(5), 398-411.

Grattan, J., & Pyatt, F. (1994). Acid damage to vegetation following the Laki fissure eruption in 1783—an historical review. *Science of the total environment, 151*(3), 241-247.

Hewitt, A. E. (2010). New Zealand soil classification. *Landcare research science series*(1).

Hinkley, T. K. (1987). *Chemistry of ash and leachates from the May 18, 1980 eruption of Mount St. Helens, Washington* (2330-7102). Retrieved from

Hodgson, K. A., Lecointre, J. A., & Neall, V. E. (2007). Onetapu formation: the last 2000 yr of laharic activity at Ruapehu volcano, New Zealand. *New Zealand Journal of Geology and Geophysics, 50*(2), 81-99.

Horiba, L. (2017). LA-950 Laser Particle Size Analyzer. Retrieved from http://www.horiba.com/pl/scientific/products/particle-characterization/particle-size-analysis/details/la-950-laser-particle-size-analyzer-108/

Humez, N. (1996). *Contribution à l'étude du comportement à long terme de résidus ultimes solidifiés/stabilisés.* Available from http://www.theses.fr/1996PA066811

Humez, N., Humez, A.-L., Juste, C., & Prost, R. (1997). A new assessment of mobility of elements in sediments and wastes. *Chemical Speciation & Bioavailability, 9*(2), 57-65.

Humez, N., & Prost, R. (1999). A new experimental approach to study the longterm behaviour of solidified/stabilized wastes. *Chemical Speciation & Bioavailability, 11*(1), 1-24.

Jones, M. T., & Gislason, S. R. (2008). Rapid releases of metal salts and nutrients following the deposition of volcanic ash into aqueous environments. *Geochimica et Cosmochimica Acta, 72*(15), 3661-3680.

Kabata-Pendias, A. (2010). *Trace elements in soils and plants*: CRC press.

Kilgour, G., Blundy, J., Cashman, K., & Mader, H. M. (2013). Small volume andesite magmas and melt–mush interactions at Ruapehu, New Zealand: evidence from melt inclusions. *Contributions to Mineralogy and Petrology, 166*(2), 371-392.

Kim, N. D., Taylor, M. D., & Drewry, J. J. (2016). Anthropogenic fluorine accumulation in the Waikato and Bay of Plenty regions of New Zealand: comparison of field data with projections. *Environmental Earth Sciences, 75*(2), 1-15.

Kirkby, E., & Pilbeam, D. (1984). Calcium as a plant nutrient. *Plant, Cell & Environment, 7*(6), 397-405.

Lacroix, A. (1907). Les mineraux des fumerolles de l'eruption du Vesuve en avril 1906. *Bulletin de la Societe Francaise de Mineralogie, 28*, 219-266.

Lathem, T., Kumar, P., Nenes, A., Dufek, J., Sokolik, I., Trail, M., & Russell, A. (2011). Hygroscopic properties of volcanic ash. *Geophysical Research Letters, 38*(11).

Le Guern, F., Bernard, A., & Chevrier, R. (1980). Soufriere of Guadeloupe 1976–1977 eruption—Mass and energy transfer and volcanic health hazards. *Bulletin of Volcanology, 43*(3), 577-593.

Loganathan, P., Hedley, M., Grace, N., Lee, J., Cronin, S., Bolan, N., & Zanders, J. (2003). Fertiliser contaminants in New Zealand grazed pasture with special reference to cadmium and fluorine—a review. *Soil Research, 41*(3), 501-532.

Loneragan, J., & Snowball, K. (1969). Calcium requirements of plants. *Australian Journal of Agricultural Research, 20*(3), 465-478.

Lowe, D. J. (1986). Controls on the rates of weathering and clay mineral genesis in airfall tephras: a review and New Zealand case study. *Rates of chemical weathering of rocks and minerals*, 265-330.

Mack, R. N. (1981). Initial effects of ashfall from Mount St. Helens on vegetation in eastern Washington and adjacent Idaho. *Science, 213*(4507), 537-539.

Mahler, R. (1984). The influence of mount St. Helens volcanic ash on alfalfa growth and nutrient uptake. *Communications in Soil Science & Plant Analysis, 15*(4), 449-460.

Mahler, R., & Fosberg, M. (1983). THE INFLUENCE OF MOUNT ST. HELENS VOLCANIC ASH ON PLANT GROWTH AND NUTRIENT UPTAKE 1. *Soil Science, 135*(3), 197.

Mahler, R., Mc Dole, R., & Fredrickson, M. (1984). The Influence of Mount St. Helens Ash on Wheat Growth and Phosphorus, Sulfur, Calcium, and Magnesium Uptake. *Journal of environmental quality, 13*(1), 91-96.

Martin, R., Watt, S., Pyle, D., Mather, T., Matthews, N., Georg, R., . . . Quayle, B. (2009). Environmental effects of ashfall in Argentina from the 2008 Chaitén volcanic eruption. *Journal of Volcanology and Geothermal Research, 184*(3), 462-472.

Martin, T., Creed, J., & Brockhoff, C. (1994). Method 200.2 (Revision 2.8): Sample preparation procedure for spectrochemical determination of total recoverable elements. *Methods for the Determination of Metals in Environmental Samples'.(USEPA: Cincinnati, OH.)*.

Mather, T., Pyle, D., & Oppenheimer, C. (2003). Tropospheric volcanic aerosol. *Volcanism and the Earth's Atmosphere*, 189-212.

McLaughlin, M. J., Simpson, P., Smart, M., Fleming, N., Stevens, D., & Cozens, G. (1997). Effect of fertiliser type on cadmium and fluorine concentrations in clover herbage. *Animal Production Science, 37*(8), 1019-1026.

Mereu, L., Marzano, F. S., Montopoli, M., & Bonadonna, C. (2015). Retrieval of Tephra Size Spectra and Mass Flow Rate From C-Band Radar During the 2010 Eyjafjallajökull

Eruption, Iceland. *IEEE Transactions on Geoscience and Remote Sensing, 53*(10), 5644-5660.

Metson, A. (1979). Sulphur in New Zealand soils: I. A review of sulphur in soils with particular reference to adsorbed sulphate-sulphur. *New Zealand Journal of Agricultural Research, 22*(1), 95-114.

Moebis, A. (2011). *Understanding the Holocene explosive eruption record of the Tongariro Volcanic Centre, New Zealand: a thesis presented in partial fulfilment of the requirements for the degree of Doctor of Philosophy in Earth Science at Massey University, Palmerston North, New Zealand.*

Moebis, A., Cronin, S. J., Neall, V. E., & Smith, I. E. (2011). Unravelling a complex volcanic history from fine-grained, intricate Holocene ash sequences at the Tongariro Volcanic Centre, New Zealand. *Quaternary International, 246*(1), 352-363.

MoH. (2008). *Drinking-water Standards for New Zealand 2005 (Revised 2008)*. Retrieved from

Molloy, L. (1988). Soils in the New Zealand landscape: the living mantle. *Soils in the New Zealand landscape: the living mantle.*

Moune, S., Gauthier, P.-J., Gislason, S. R., & Sigmarsson, O. (2006). Trace element degassing and enrichment in the eruptive plume of the 2000 eruption of Hekla volcano, Iceland. *Geochimica et Cosmochimica Acta, 70*(2), 461-479.

Mueller, S. B., Ayris, P. M., Wadsworth, F. B., Kueppers, U., Casas, A. S., Delmelle, P., Taddeucci, J., Jacob, M., Dingwell, D. B. . (2017). Ash aggregation enhanced by deposition and redistribution of salt on the surface of volcanic ash in eruption plumes. *Scientific Reports, 7*(45762), 9.

Mueller, S. B., Kueppers, U., Ayris, P. M., Jacob, M., & Dingwell, D. B. (2016). Experimental volcanic ash aggregation: Internal structuring of accretionary lapilli and the role of liquid bonding. *Earth and Planetary Science Letters, 433*, 232-240.

Naughton, J. J., Lewis, V. A., Hammond, D., & Nishimoto, D. (1974). The chemistry of sublimates collected directly from lava fountains at Kilauea Volcano, Hawaii. *Geochimica et Cosmochimica Acta, 38*(11), 1679-1690.

Neufeld, H., Jernstedt, J., & Haines, B. (1985). Direct foliar effects of simulated acid rain. *New Phytologist, 99*(3), 389-405.

Norvell, W. (1988). Inorganic reactions of manganese in soils *Manganese in soils and plants* (pp. 37-58): Springer.

Nye, P. (1977). THE RATE-LIMITING STEP IN PLANT NUTRIENT ABSORPTION FROM SOIL. *Soil Science, 123*(5), 292-297.

Oelkers, E. H., Schott, J., & Devidal, J.-L. (1994). The effect of aluminum, pH, and chemical affinity on the rates of aluminosilicate dissolution reactions. *Geochimica et Cosmochimica Acta, 58*(9), 2011-2024.

Olsson, J., Stipp, S. L. S., Dalby, K. N., & Gislason, S. R. (2013). Rapid release of metal salts and nutrients from the 2011 Grímsvötn, Iceland volcanic ash. *Geochimica et Cosmochimica Acta, 123*, 134-149. doi:http://dx.doi.org/10.1016/j.gca.2013.09.009

Óskarsson, N. (1980). The interaction between volcanic gases and tephra: fluorine adhering to tephra of the 1970 Hekla eruption. *Journal of Volcanology and Geothermal Research, 8*(2-4), 251-266.

Ozsvath, D. L. (2009). Fluoride and environmental health: a review. *Reviews in Environmental Science & Biotechnology, 8*(1), 59.

Pardo, N., Cronin, S. J., Palmer, A. S., & Németh, K. (2012). Reconstructing the largest explosive eruptions of Mt. Ruapehu, New Zealand: lithostratigraphic tools to understand subplinian–plinian eruptions at andesitic volcanoes. *Bulletin of Volcanology, 74*(3), 617-640.

Parfitt, R. (2009). Allophane and imogolite: role in soil biogeochemical processes. *Clay minerals, 44*(1), 135-155.

Pedro, G. (1961). An experimental study on the geochemical weathering of crystalline rocks by water. *Clay Miner. Bull, 4*(26), 266-281.

Peri, P. L., & Bloomberg, M. (2002). Windbreaks in southern Patagonia, Argentina: A review of research on growth models, windspeed reduction, and effects oncrops. *Agroforestry Systems, 56*(2), 129-144.

Rodriguez-Espinosa, P. F., Jonathan, M. P., Morales-García, S. S., Villegas, L. E. C., Martínez-Tavera, E., Muñoz-Sevilla, N. P., & Cardona, M. A. (2015). Metal enrichment of soils following the April 2012–2013 eruptive activity of the Popocatépetl volcano, Puebla, Mexico. *Environmental Monitoring and Assessment, 187*(11), 1-7. doi:10.1007/s10661-015-4938-z

Rose, W. I. (1977). Scavenging of volcanic aerosol by ash: atmospheric and volcanologic implications. *Geology, 5*(10), 621-624.

Rubin, C. H., Noji, E. K., Seligman, P. J., Holtz, J. L., Grande, J., & Vittani, F. (1994). Evaluating a fluorosis hazard after a volcanic eruption. *Archives of Environmental Health: An International Journal, 49*(5), 395-401.

Ruggieri, F., Fernández-Turiel, J.-L., Saavedra, J., Gimeno, D., Polanco, E., & Naranjo, J. A. (2011). Environmental geochemistry of recent volcanic ashes from the Southern Andes. *Environmental Chemistry, 8*(3), 236-247.

Ruggieri, F., Fernandez-Turiel, J., Saavedra, J., Gimeno, D., Polanco, E., Amigo, A., . . . Caselli, A. (2012). Contribution of volcanic ashes to the regional geochemical balance: The 2008 eruption of Chaitén volcano, Southern Chile. *Science of the total environment, 425*, 75-88.

Sabti, H., Hossain, M. M., Brooks, R. R., & Stewart, R. B. (2000). The current environmental impact of base-metal mining at the Tui Mine, Te Aroha, New Zealand. *Journal of the Royal Society of New Zealand, 30*(2), 197-207.

Sandrini, S., Giulianelli, L., Decesari, S., Fuzzi, S., Cristofanelli, P., Marinoni, A., . . . Canepari, S. (2014). In situ physical and chemical characterisation of the Eyjafjallajökull aerosol plume in the free troposphere over Italy. *Atmospheric Chemistry and Physics, 14*(2), 1075-1092.

Sarna-Wojcicki, A. M., Shipley, S., Waitt Jr, R. B., Dzurisin, D., & Wood, S. H. (1981). Areal distribution, thickness, mass, volume, and grain size of air-fall ash from the six major eruptions of 1980.

Scarpa, R., Tilling, R. I. (Ed.) (1996). *Monitoring and mitigation of volcano hazards*: Springer Science & Business Media.

Scasso, R. A., Corbella, H., & Tiberi, P. (1994). Sedimentological analysis of the tephra from the 12–15 August 1991 eruption of Hudson volcano. *Bulletin of Volcanology, 56*(2), 121-132.

Seymour, V., Hinckley, T., Morikawa, Y., & Franklin, J. (1983). Foliage damage in coniferous trees following volcanic ashfall from Mt. St. Helens. *Oecologia, 59*(2-3), 339-343.

Sheets, P. D., & Grayson, D. K. (1979). *Volcanic activity and human ecology*: Elsevier.

Shoji, S., Nanzyo, M., & Dahlgren, R. (1994). *Volcanic ash soils: genesis, properties and utilization* (Vol. 21): Elsevier.

Sigurdsson, H., Houghton, B., McNutt, S. Rymer, H., Stix, J. (Ed.) (2015). *The encyclopedia of volcanoes*: Elsevier.

Skidmore, E., Hagen, L., Armbrust, D., Durar, A., Fryrear, D., Potter, K., . . . Zobeck, T. (1994). Methods for investigating basic processes and conditions affecting wind erosion. *Soil erosion Research methods*, 295-330.

Smith, D. B., Zielinski, R. A., Taylor, H. E., & Sawyer, M. (1983). Leaching characteristics of ash from the May 18, 1980, eruption of Mount St. Helens volcano, Washington. *Bulletin volcanologique, 46*(2), 103-124.

Smith, W. H., & Staskawicz, B. J. (1977). Removal of atmospheric particles by leaves and twigs of urban trees: some preliminary observations and assessment of research needs. *Environmental management, 1*(4), 317-330.

Sneva, F. A., Britton, C., Mayland, H., Buckhouse, J., Evans, R., Young, J., & Vavra, M. (1982). Mt. St. Helens Ash: Considerations of its fallout on rangelands.

Soxhlet, F. (1879). Die gewichtsaiialytische Bestimmung des Milchfettes; von.

Sparks, R. S. J., & Walker, G. P. L. (1977). The significance of vitric-enriched air-fall ashes associated with crystal-enriched ignimbrites. *Journal of Volcanology and Geothermal Research, 2*(4), 329-341. doi:http://dx.doi.org/10.1016/0377-0273(77)90019-1

Stewart, C., Craig, H. M., Gaw, S., Wilson, T., Villarosa, G., Outes, V., . . . Oze, C. (2016). Fate and agricultural consequences of leachable elements added to the environment from the 2011 Cordón Caulle tephra fall. *Journal of Volcanology and Geothermal Research*. doi:http://dx.doi.org/10.1016/j.jvolgeores.2016.09.017

Stewart, C., Horwell, C., Plumlee, G., Cronin, S., Delmelle, P., Baxter, P., . . . Oppenheimer, C. (2015). Protocol for analysis of volcanic ash samples for assessment of hazards from leachable elements.

Taylor, M., & Kim, N. (2010). Dealumination as a mechanism for increased acid recoverable aluminium in Waikato mineral soils. *Soil Research, 47*(8), 828-838.

Taylor, M. D., Kim, N. D., Briggs, R. M., Taylor, A., & Guinto, D. F. (2012). An investigation into the process of dealumination in soils of the Auckland, Bay of Plenty and Waikato regions of New Zealand. *Applied Clay Science, 64*, 18-24.

Taylor, M. D., Lowe, D. J., Hardi, P., Smidt, G. A., & Schnug, E. (2016). Comparing volcanic glass shards in unfertilised and fertilised Andisols derived from rhyolitic tephras, New Zealand: Evidence for accelerated weathering and implications for land management. *Geoderma, 271*, 91-98. doi:http://dx.doi.org/10.1016/j.geoderma.2016.01.035

Taylor, P. S., & Stoiber, R. E. (1973). Soluble material on ash from active Central American volcanoes. *Geological Society of America Bulletin, 84*(3), 1031-1042.

Tejedor, M., Jiménez, C., & Dıaz, F. (2003). Volcanic materials as mulches for water conservation. *Geoderma, 117*(3), 283-295.

Textor, C., Graf, H.-F., Herzog, M., Oberhuber, J. M., Rose, W. I., & Ernst, G. G. (2006). Volcanic particle aggregation in explosive eruption columns. Part I: Parameterization of the microphysics of hydrometeors and ash. *Journal of Volcanology and Geothermal Research, 150*(4), 359-377.

Textor, C., Graf, H. F., Herzog, M., & Oberhuber, J. (2003). Injection of gases into the stratosphere by explosive volcanic eruptions. *Journal of Geophysical Research: Atmospheres, 108*(D19).

Thordarson, T., & Self, S. (2003). Atmospheric and environmental effects of the 1783–1784 Laki eruption: A review and reassessment. *Journal of Geophysical Research: Atmospheres, 108*(D1).

Ugolini, F. C., & Dahlgren, R. A. (2002). Soil development in volcanic ash. *GLOBAL ENVIRONMENTAL RESEARCH-ENGLISH EDITION-, 6*(2), 69-82.

Walter, P. B., Knutson, M. D., Paler-Martinez, A., Lee, S., Xu, Y., Viteri, F. E., & Ames, B. N. (2002). Iron deficiency and iron excess damage mitochondria and mitochondrial DNA in rats. *Proceedings of the National Academy of Sciences, 99*(4), 2264-2269.

White, J. (2015). *Magmatic versus phreatomagmatic fragmentation: absence of evidence is not evidence of absence.* Paper presented at the 2015 AGU Fall Meeting.

Wilson, L., & Huang, T. (1979). The influence of shape on the atmospheric settling velocity of volcanic ash particles. *Earth and Planetary Science Letters, 44*(2), 311-324.

Wilson, T., Cole, J., Cronin, S., Stewart, C., & Johnston, D. (2011). Impacts on agriculture following the 1991 eruption of Vulcan Hudson, Patagonia: lessons for recovery. *Natural Hazards, 57*(2), 185-212.

Wilson, T., Cole, J., Stewart, C., Cronin, S., & Johnston, D. (2011). Ash storms: impacts of wind-remobilised volcanic ash on rural communities and agriculture following the 1991 Hudson eruption, southern Patagonia, Chile. *Bulletin of Volcanology, 73*(3), 223-239.

Wilson, T. M., Jenkins, S., Stewart, C.,. (2014). Impacts from Volcanic Ash Fall. In P. Papale (Ed.), *Volcanic Hazards, Risks, and Disasters* (pp. 47).

Wilson, T. M., & Kaye, G. D. (2007). *Agricultural fragility estimates for volcanic ash fall hazards* (Vol. 2007): GNS Science.

Wilson, T. M., Stewart, C., Sword-Daniels, V., Leonard, G. S., Johnston, D. M., Cole, J. W., . . . Barnard, S. T. (2012). Volcanic ash impacts on critical infrastructure. *Physics and Chemistry of the Earth, Parts A/B/C, 45–46*, 5-23. doi:http://dx.doi.org/10.1016/j.pce.2011.06.006

Witham, C. S., Oppenheimer, C., & Horwell, C. J. (2005). Volcanic ash-leachates: a review and recommendations for sampling methods. *Journal of Volcanology and Geothermal Research, 141*(3–4), 299-326. doi:http://dx.doi.org/10.1016/j.jvolgeores.2004.11.010

Wohletz, K., Sheridan, M., & Brown, W. (1989). Particle size distributions and the sequential fragmentation/transport theory applied to volcanic ash. *J. Geophys. Res, 94*(B11), 15,703-715,721.

Wohletz, K. H. (1986). Explosive magma-water interactions: Thermodynamics, explosion mechanisms, and field studies. *Bulletin of Volcanology, 48*(5), 245-264.

Wolff-Boenisch, D., Gislason, S. R., & Oelkers, E. H. (2004). The effect of fluoride on the dissolution rates of natural glasses at pH 4 and 25 C. *Geochimica et Cosmochimica Acta, 68*(22), 4571-4582.

Wolff-Boenisch, D., Gislason, S. R., Oelkers, E. H., & Putnis, C. V. (2004). The dissolution rates of natural glasses as a function of their composition at pH 4 and 10.6, and temperatures from 25 to 74 C. *Geochimica et Cosmochimica Acta, 68*(23), 4843-4858.

Yao, F., Arbestain, M. C., Virgel, S., Blanco, F., Arostegui, J., Maciá-Agulló, J., & Macías, F. (2010). Simulated geochemical weathering of a mineral ash-rich biochar in a modified Soxhlet reactor. *Chemosphere, 80*(7), 724-732.

Zheng, S. J. (2010). Crop production on acidic soils: overcoming aluminium toxicity and phosphorus deficiency. *Annals of botany, 106*(1), 183-184.

Zimanowski, B., Wohletz, K., Dellino, P., & Büttner, R. (2003). The volcanic ash problem. *Journal of Volcanology and Geothermal Research, 122*(1), 1-5.

Appendix One:

Absolute concentrations of the seventeen elements analysed (mg/kg)

Experiment time	Cd	Ni	Co	Pb	Cr	Zn	Cu	Fe	Mn	Al	Ca	K	Mg	Na	F	Cl	SO_4^{2-}
	0.000	0.000	0.000	0.000	0.000	0.000	0.000	0.000	0.000	0.000	0.000	0.000	0.000	0.000	**0.000**	**0.000**	**0.000**
95/5 - L - 0.00	0.000	4.144	1.381	0.888	0.197	3.059	9.965	10.754	8.485	1388.867	532.381	0.000	114.744	3.157	0.123	5.104	105.899
95/5 L 1 1 .1	0.000	0.691	0.000	0.691	0.099	1.381	3.059	5.920	1.973	275.366	1108.765	0.000	28.217	0.000	0.000	0.051	3.495
95/5 L 1 1.2	0.000	0.000	0.000	0.789	0.000	0.691	0.493	1.677	0.099	14.997	956.924	0.000	2.565	0.000	0.062	0.218	49.259
95/5 L 1 1.3	0.000	0.000	0.000	0.789	0.000	0.493	0.296	1.085	0.099	4.736	809.128	0.000	1.677	0.000	0.000	0.021	6.338
95/5 L 1 1.4	0.000	0.000	0.000	0.592	0.000	0.395	0.197	0.493	0.000	0.888	425.826	0.000	1.381	0.000	0.034	0.210	20.399
95/5 L 1 1.5	0.000	0.000	0.000	0.592	0.000	0.395	0.099	0.691	0.000	0.789	494.889	0.000	1.480	0.000	0.020	0.321	25.391
95/5 L 1 1.6	0.000	0.000	0.000	0.592	0.000	0.493	0.099	0.691	0.000	0.395	435.297	0.000	1.381	0.000	0.097	0.007	0.848
95/5 L 1 1.7	0.000	0.000	0.000	0.888	0.000	0.888	0.691	12.925	0.592	5.426	3269.663	0.987	3.946	33.150	0.007	0.010	8.682
95/5 L 1 1.8	0.000	0.000	0.000	0.789	0.000	0.592	1.184	38.774	0.395	13.714	917.558	5.920	2.664	44.398	0.011	0.008	2.640
95/5 L 1 1.9	0.000	0.000	0.000	0.493	0.000	0.493	0.592	30.585	0.099	8.485	122.341	3.552	1.677	26.540	0.172	0.169	14.732
95/5 L 1 1.10	0.000	0.000	0.000	0.592	0.000	0.592	1.085	38.774	0.099	16.575	55.744	10.557	1.776	36.505	0.009	0.008	0.745
95/5 L 1 1.11	0.000	0.000	0.000	0.592	0.000	0.395	0.592	31.967	0.099	9.077	47.259	1.677	0.888	1.381	0.000	0.009	0.509
95/5 L 1 1.12	0.000	0.000	0.000	0.493	0.000	0.395	0.493	31.473	0.099	9.077	41.537	10.162	1.381	25.356	0.101	0.113	12.260
95/5 L 1 1.13	0.000	0.000	0.000	0.493	0.000	0.296	0.592	32.657	0.099	7.992	40.550	10.458	1.283	23.876	0.000	0.000	0.463

Experiment time	Cd	Ni	Co	Pb	Cr	Zn	Cu	Fe	Mn	Al	Ca	K	Mg	Na	F	Cl	SO_4^{2-}
	0.000	0.000	0.000	0.000	0.000	0.000	0.000	0.000	0.000	0.000	0.000	0.000	0.000	0.000	**0.000**	**0.000**	**0.000**
95/5 - U - 0.0	0.000	2.592	0.576	0.768	0.096	2.016	6.529	2.784	6.337	603.152	467.198	0.000	92.556	0.672	0.188	7.222	78.208
95/5 U 1 1.1	0.000	0.384	0.000	0.768	0.000	0.672	1.536	2.112	1.152	100.525	958.112	0.000	17.474	1.056	0.109	9.397	47.254
95/5 U 1 1.2	0.000	0.000	0.000	0.672	0.000	0.384	0.096	0.480	0.000	1.824	169.943	0.000	1.152	0.000	0.027	8.369	18.776
95/5 U 1 1.3	0.000	0.000	0.000	0.768	0.000	0.384	0.192	0.480	0.096	0.960	393.364	0.000	1.632	0.000	0.020	0.117	12.129
95/5 U 1 1.4	0.000	0.000	0.000	0.672	0.000	0.288	0.000	0.288	0.000	0.192	213.628	0.000	1.536	0.000	0.044	0.175	10.604
95/5 U 1 1.5	0.000	0.000	0.000	0.672	0.000	0.384	0.096	0.096	0.000	0.096	158.325	0.000	1.152	0.000	0.022	0.135	7.734
95/5 U 1 1.6	0.000	0.000	0.000	0.768	0.000	0.288	0.096	0.192	0.000	0.096	119.728	0.000	1.152	0.000	0.020	0.080	5.670
95/5 U 1 1.7	0.000	0.000	0.000	0.864	0.000	0.576	0.960	5.569	0.288	9.601	431.097	0.288	3.552	22.083	0.265	0.181	31.131
95/5 U 1 1.8	0.000	0.000	0.000	0.672	0.000	0.384	1.152	12.290	0.192	24.579	49.447	4.609	2.400	34.277	0.390	0.231	16.662
95/5 U 1 1.9	0.000	0.000	0.000	0.672	0.000	0.672	0.768	8.353	0.096	10.849	41.958	4.417	1.536	22.275	0.238	0.178	11.971
95/5 U 1 1.10	0.000	0.000	0.000	0.768	0.000	0.384	0.672	7.297	0.096	6.721	40.517	5.089	1.344	18.915	0.148	0.156	9.667
95/5 U 1 1.11	0.000	0.000	0.000	0.672	0.000	0.480	0.576	9.025	0.096	12.578	40.709	9.121	1.344	21.123	0.149	0.128	12.035
95/5 U 1 1.12	0.000	0.000	0.000	0.672	0.000	0.480	0.480	9.121	0.000	6.433	39.845	6.529	1.248	13.442	0.100	0.265	9.172
95/5 U 1 1.13	0.000	0.000	0.000	0.672	0.000	0.384	0.576	12.098	0.096	9.217	40.517	15.074	1.632	27.460	0.125	0.174	13.263

Experiment time	Cd	Ni	Co	Pb	Cr	Zn	Cu	Fe	Mn	Al	Ca	K	Mg	Na	F	Cl	SO_4^{2-}
	0.000	0.000	0.000	0.000	0.000	0.000	0.000	0.000	0.000	0.000	0.000	0.000	0.000	0.000	0.000	0.000	0.000
95/8 - 0.0	0.000	0.000	0.000	0.686	0.000	0.294	0.098	0.392	0.098	0.000	99.620	0.000	3.236	9.707	0.000	0.017	0.197
95/8 1 1.1	0.000	0.000	0.000	0.686	0.000	0.686	0.294	0.392	0.686	0.294	290.917	5.393	14.315	36.377	0.000	0.056	0.857
95/8 1 1.2	0.000	0.000	0.000	0.686	0.000	0.686	0.294	0.490	0.490	0.196	187.669	1.667	9.413	15.198	0.000	0.025	0.466
95/8 1 1.3	0.000	0.000	0.000	0.686	0.000	0.588	0.196	0.882	0.392	2.255	168.353	0.392	6.275	5.589	0.000	0.014	0.422
95/8 1 1.4	0.000	0.000	0.000	0.784	0.000	0.392	0.196	0.490	0.196	0.098	167.667	0.000	5.001	0.981	0.000	0.012	0.465
95/8 1 1.5	0.000	0.000	0.000	0.686	0.000	0.392	0.098	0.392	0.098	0.000	135.800	0.000	2.942	0.000	0.000	0.014	0.813
95/8 1 1.6	0.000	0.000	0.000	0.686	0.000	0.196	0.098	0.294	0.098	0.000	138.840	0.000	2.353	0.000	0.000	0.007	0.338
95/8 1 1.7	0.000	0.000	0.000	0.784	0.000	0.784	0.981	0.490	0.294	0.294	1418.304	5.981	5.687	9.119	0.008	0.008	4.804
95/8 1 1.8	0.000	0.000	0.000	0.882	0.000	0.490	0.490	0.490	0.196	0.000	1038.652	3.922	2.549	5.099	0.009	0.008	4.174
95/8 1 1.9	0.000	0.000	0.000	0.784	0.000	0.392	0.392	0.392	0.098	0.098	436.816	2.451	1.961	1.961	0.007	0.000	1.312
95/8 1 1.10	0.000	0.000	0.000	0.686	0.000	0.294	0.098	0.490	0.098	0.000	147.174	0.882	1.667	0.000	0.000	0.009	0.321
95/8 1 1.11	0.000	0.000	0.000	0.686	0.000	0.294	0.098	0.392	0.098	0.000	53.928	0.294	1.177	0.000	0.000	0.000	0.087
95/8 1 1.12	0.000	0.000	0.000	0.686	0.000	0.294	0.098	0.294	0.098	0.098	43.338	0.784	1.079	0.000	0.000	0.000	0.047
95/8 1 1.13	0.000	0.000	0.000	0.588	0.000	0.294	0.098	0.294	0.000	0.098	40.691	0.294	0.882	0.000	0.000	0.000	0.039

Experiment time	Cd	Ni	Co	Pb	Cr	Zn	Cu	Fe	Mn	Al	Ca	K	Mg	Na	F	Cl	SO_4^{2-}
	0.000	0.000	0.000	0.000	0.000	0.000	0.000	0.000	0.000	0.000	0.000	0.000	0.000	0.000	**0.000**	**0.000**	**0.000**
96/7 - 0.0	0.000	2.135	0.388	0.777	0.000	3.106	4.465	3.106	10.192	43.000	329.244	0.000	392.433	15.336	0.596	19.862	55.489
96/7 1 1.1	0.000	1.068	0.000	0.679	0.000	2.135	3.009	2.621	6.795	21.937	506.193	0.000	232.761	17.278	0.425	11.218	48.667
96/7 1 1.2	0.000	0.291	0.000	0.582	0.000	1.165	1.262	1.456	2.621	6.795	344.095	0.000	91.241	6.018	0.217	3.731	27.531
96/7 1 1.3	0.000	0.097	0.000	0.582	0.000	0.777	0.874	1.359	1.844	4.368	331.767	0.000	65.616	5.339	0.179	2.134	24.633
96/7 1 1.4	0.000	0.000	0.000	0.582	0.000	0.582	0.485	0.874	0.971	2.135	253.048	0.000	36.885	2.330	0.122	1.324	16.558
96/7 1 1.5	0.000	0.000	0.000	0.582	0.000	0.485	0.388	0.679	0.679	1.456	224.414	0.000	24.169	1.747	0.102	0.783	14.092
96/7 1 1.6	0.000	0.000	0.000	0.485	0.000	0.485	0.291	0.777	0.582	1.262	235.479	0.000	18.539	0.971	0.091	0.565	13.567
96/7 1 1.7	0.000	0.000	0.000	0.874	0.000	1.068	2.038	16.210	3.494	13.298	2650.353	0.000	61.733	43.291	0.741	1.398	119.747
96/7 1 1.8	0.000	0.000	0.000	0.874	0.000	0.485	1.068	24.849	1.068	12.910	1871.312	1.844	7.571	35.817	0.810	0.515	90.269
96/7 1 1.9	0.000	0.000	0.000	0.874	0.000	0.291	0.971	23.781	0.485	10.386	1265.433	3.106	4.174	25.819	0.650	0.334	68.923
96/7 1 1.10	0.000	0.000	0.000	0.679	0.000	0.388	0.679	18.345	0.291	7.183	806.802	4.077	2.815	16.598	0.460	0.361	50.540
96/7 1 1.11	0.000	0.000	0.000	0.777	0.000	0.388	0.582	20.578	0.194	7.086	719.250	6.018	2.524	18.151	0.431	0.249	42.627
96/7 1 1.12	0.000	0.000	0.000	0.777	0.000	0.291	0.582	22.519	0.194	7.086	513.861	5.824	2.330	16.113	0.016	0.010	1.445
96/7 1 1.13	0.000	0.000	0.000	0.679	0.000	0.194	0.485	20.869	0.194	6.503	391.074	4.271	2.038	11.842	0.015	0.009	1.230

Experiment time	Cd	Ni	Co	Pb	Cr	Zn	Cu	Fe	Mn	Al	Ca	K	Mg	Na	F	Cl	SO_4^{2-}
	0.000	0.000	0.000	0.000	0.000	0.000	0.000	0.000	0.000	0.000	0.000	0.000	0.000	0.000	0.000	0.000	0.000
96/46 - 0.0	0.000	0.503	0.805	0.000	0.101	0.402	0.201	0.000	0.704	0.000	74.553	0.000	20.525	16.400	0.000	0.051	0.180
96/46 1 1.1	0.000	0.402	0.906	0.000	0.101	0.302	0.201	0.000	0.201	0.101	67.510	0.000	8.954	2.415	0.000	0.019	0.094

96/46 1 1.2	0.000	0.402	0.906	0.000	0.101	0.101	0.201	0.101	0.201	0.101	59.965	0.000	5.835	0.000	0.033	0.403	2.059
96/46 1 1.3	0.201	0.402	0.906	0.000	0.101	0.201	0.201	0.101	0.101	0.101	57.550	0.000	4.628	0.000	0.031	0.279	1.780
96/46 1 1.4	0.402	0.302	1.006	0.000	0.101	0.000	0.201	0.000	0.101	0.000	51.413	0.000	3.421	0.000	0.030	0.577	1.457
96/46 1 1.5	0.604	0.402	0.906	0.000	0.101	0.101	0.201	0.101	0.101	0.000	50.507	0.000	2.918	0.000	0.022	0.188	1.296
96/46 1 1.6	0.805	0.402	0.906	0.000	0.101	0.302	0.201	0.101	0.000	0.000	48.595	0.000	2.616	0.000	0.051	0.142	1.129
96/46 1 1.7	1.006	0.503	1.006	0.000	0.101	0.805	0.704	0.503	0.704	0.805	208.065	0.000	18.814	6.640	0.158	0.473	11.431
96/46 1 1.8	0.906	0.402	1.006	0.000	0.101	0.906	0.704	0.302	0.201	0.805	145.786	0.000	6.137	2.616	0.142	0.167	7.184
96/46 1 1.9	1.207	0.402	1.107	0.000	0.101	0.503	0.302	0.201	0.101	0.402	70.328	0.000	2.012	0.000	0.113	0.186	2.880
96/46 1 1.10	1.107	0.402	1.107	0.000	0.101	0.302	0.201	0.101	0.000	0.201	49.602	0.302	1.308	0.000	0.083	0.195	1.517
96/46 1 1.11	1.409	0.402	1.107	0.000	0.101	0.402	0.402	0.201	0.000	0.402	45.678	0.101	1.207	0.000	0.115	0.154	1.375
96/46 1 1.12	1.207	0.402	1.308	0.000	0.101	0.201	0.302	0.201	0.000	0.604	43.665	0.000	1.107	0.000	0.123	0.129	1.367
96/46 1 1.13	1.207	0.302	1.107	0.000	0.101	0.201	0.503	0.402	0.000	0.704	42.861	0.000	1.006	0.000	0.130	0.104	1.380

Experiment time	Cd	Ni	Co	Pb	Cr	Zn	Cu	Fe	Mn	Al	Ca	K	Mg	Na	F	Cl	SO_4^{2-}
	0.000	0.000	0.000	0.000	0.000	0.000	0.000	0.000	0.000	0.000	0.000	0.000	0.000	0.000	0.000	0.000	0.000
Ruw - 0.0	0.000	0.000	0.000	0.500	0.000	0.000	0.000	0.000	0.000	0.000	39.397	0.000	0.800	8.199	0.000	0.313	0.737
Ruw 1 1.1	0.000	0.000	0.000	0.500	0.000	0.000	0.000	0.000	0.000	0.000	38.297	0.000	0.500	5.400	0.000	0.269	0.567
Ruw 1 1.2	0.000	0.000	0.000	0.500	0.000	0.100	0.000	0.000	0.000	0.000	37.797	0.000	0.400	1.000	0.000	23.864	0.232
Ruw 1 1.3	0.000	0.000	0.000	0.500	0.000	0.000	0.000	0.000	0.000	0.000	37.797	0.000	0.500	0.000	0.000	0.239	0.151
Ruw 1 1.4	0.000	0.000	0.000	0.500	0.000	0.100	0.000	0.000	0.000	0.000	37.497	0.000	0.500	0.000	0.000	5.737	0.078
Ruw 1 1.5	0.000	0.000	0.000	0.500	0.000	0.000	0.100	0.000	0.000	0.000	37.797	0.000	0.500	0.000	0.000	0.355	0.095
Ruw 1 1.6	0.000	0.000	0.000	0.400	0.000	0.000	0.000	0.000	0.000	0.000	38.297	0.000	0.500	0.000	0.000	0.240	0.087
Ruw 1 1.7	0.000	0.000	0.000	0.500	0.000	0.200	0.100	0.000	0.000	0.000	40.797	0.000	0.800	1.000	0.000	0.109	0.748
Ruw 1 1.8	0.000	0.000	0.000	0.500	0.000	0.200	0.000	0.000	0.000	0.000	40.097	0.000	0.700	0.800	0.000	0.116	0.581
Ruw 1 1.9	0.000	0.000	0.000	0.600	0.000	0.100	0.000	0.000	0.000	0.000	38.297	0.000	0.600	0.000	0.000	0.100	0.363
Ruw 1 1.10	0.000	0.000	0.000	0.300	0.000	0.000	0.000	0.000	0.000	0.000	38.097	0.000	0.500	0.000	0.000	0.077	0.191
Ruw 1 1.11	0.000	0.000	0.000	0.500	0.000	0.000	0.000	0.000	0.000	0.000	37.797	0.000	0.500	0.000	0.000	0.119	0.261
Ruw 1 1.12	0.000	0.000	0.000	0.500	0.000	0.100	0.000	0.000	0.000	0.000	38.197	0.000	0.500	0.000	0.000	0.106	0.161
Ruw 1 1.13	0.000	0.000	0.000	0.500	0.000	0.000	0.000	0.000	0.000	0.000	38.497	0.000	0.500	0.000	0.000	0.107	0.185

Experiment time	Cd	Ni	Co	Pb	Cr	Zn	Cu	Fe	Mn	Al	Ca	K	Mg	Na	F	Cl	SO_4^{2-}
	0.000	0.000	0.000	0.000	0.000	0.000	0.000	0.000	0.000	0.000	0.000	0.000	0.000	0.000	0.000	0.000	0.000
SK1 - 0.0	0.900	0.000	0.000	0.600	0.000	1.300	0.200	0.000	0.000	0.100	41.398	0.100	0.700	8.300	0.019	0.372	3.976
SK1 1.1	1.100	0.000	0.000	0.600	0.000	0.700	0.100	0.000	0.100	0.100	97.796	3.000	3.800	16.399	0.136	2.196	4.604
SK1 1.2	0.900	0.000	0.000	0.500	0.000	0.400	0.000	0.000	0.000	0.200	45.998	0.000	1.000	7.700	0.064	0.318	1.189
SK1 1.3	1.000	0.000	0.000	0.500	0.000	0.100	0.000	0.000	0.000	0.000	39.898	0.000	0.700	5.700	0.046	0.140	0.582
SK1 1.4	0.900	0.000	0.000	0.500	0.000	0.000	0.000	0.000	0.000	0.000	43.798	0.000	0.900	6.000	0.104	0.294	0.923
SK1 1.5	0.700	0.000	0.000	0.500	0.000	0.200	0.000	0.000	0.000	0.000	38.998	0.000	0.500	5.000	0.060	0.126	0.441
SK1 1.6	0.900	0.000	0.000	0.500	0.000	0.200	0.000	0.000	0.000	0.000	38.998	0.000	0.600	4.900	0.091	0.107	0.367
SK1 1.7	0.800	0.000	0.000	0.500	0.000	0.100	0.000	0.000	0.000	0.100	40.598	0.000	0.800	5.800	0.118	0.146	0.445
SK1 1.8	0.600	0.000	0.000	0.400	0.000	0.000	0.000	0.000	0.000	0.700	45.798	0.000	1.000	7.500	0.522	0.183	0.586

SK1 1.9	0.500	0.000	0.000	0.500	0.000	0.100	0.000	0.000	0.000	0.100	40.898	0.000	0.700	8.200	0.395	0.261	0.340
SK1 1.10	0.200	0.000	0.000	0.500	0.000	0.100	0.000	0.000	0.000	0.400	39.298	0.000	0.700	6.900	0.307	1.008	0.505
SK1 1.11	0.100	0.000	0.000	0.400	0.000	0.000	0.000	0.000	0.000	0.200	40.198	0.000	0.600	6.100	0.213	0.192	0.308
SK1 1.12	0.000	0.000	0.000	0.400	0.000	0.200	0.000	0.000	0.000	0.100	38.398	0.000	0.600	6.400	0.206	0.189	0.225
SK1 1.13	0.000	0.000	0.000	0.400	0.000	0.100	0.000	0.000	0.000	0.000	38.198	0.000	0.600	6.100	0.172	0.116	0.167
SK1 1.14	0.000	0.000	0.000	0.500	0.000	0.100	0.000	0.000	0.000	0.000	38.598	0.000	0.500	4.500	0.119	0.169	0.166

Experiment time	Cd	Ni	Co	Pb	Cr	Zn	Cu	Fe	Mn	Al	Ca	K	Mg	Na	F	Cl	SO_4^{2-}
	0.000	0.000	0.000	0.000	0.000	0.000	0.000	0.000	0.000	0.000	0.000	0.000	0.000	0.000	0.000	0.000	0.000
KL1 - 0.0	1.396	0.299	1.097	0.000	0.100	0.000	0.100	0.000	0.000	0.000	49.162	0.000	1.396	6.382	0.021	0.979	1.107
KL1 1.1	1.097	0.299	1.097	0.000	0.100	0.100	0.100	0.000	0.000	0.000	73.793	0.199	1.596	5.285	0.057	3.804	1.837
KL1 1.2	1.197	0.299	1.097	0.000	0.100	0.199	0.100	0.000	0.000	0.000	63.223	0.000	1.097	0.897	0.092	0.000	1.336
KL1 1.3	1.197	0.299	1.097	0.000	0.100	0.000	0.100	0.000	0.000	0.000	51.755	0.000	0.798	0.000	0.000	0.000	0.841
KL1 1.4	0.997	0.299	1.097	0.000	0.100	0.000	0.100	0.000	0.000	0.000	60.231	0.000	0.997	1.097	0.000	0.000	1.178
KL1 1.5	0.897	0.299	1.197	0.000	0.100	0.000	0.100	0.000	0.000	0.000	55.544	0.000	0.897	0.000	0.000	0.000	0.965
KL1 1.6	0.499	0.399	1.296	0.000	0.100	0.199	0.100	0.000	0.000	0.000	54.547	0.000	0.997	0.000	0.000	0.000	0.872
KL1 1.7	0.897	0.299	1.197	0.000	0.100	0.000	0.100	0.299	0.000	10.471	416.733	16.853	2.194	68.907	0.000	0.000	11.034
KL1 1.8	1.795	1.396	3.091	0.000	0.499	11.667	1.596	0.100	0.000	10.570	323.394	10.570	1.895	28.221	0.000	0.000	5.413
KL1 1.9	0.000	1.097	3.889	0.000	0.499	3.490	0.000	0.100	0.000	11.069	244.715	6.681	1.795	17.551	0.000	0.000	1.688
KL1 1.10	0.000	1.396	5.485	0.000	0.499	1.795	0.000	0.100	0.000	11.767	247.008	6.681	1.895	15.656	0.000	0.000	1.300
KL1 1.11	0.698	1.596	6.482	0.000	0.499	1.596	0.000	0.199	0.000	11.069	189.469	4.587	1.795	12.266	0.000	0.000	0.842
KL1 1.12	0.399	1.596	6.083	0.000	0.499	2.892	0.000	0.100	0.000	11.169	189.569	4.288	1.994	12.266	0.000	0.000	0.813
KL1 1.13	0.399	2.892	4.787	0.000	0.499	1.695	0.000	0.199	0.000	10.770	199.741	5.385	2.094	14.061	0.000	0.000	0.946

Experiment time	Cd	Ni	Co	Pb	Cr	Zn	Cu	Fe	Mn	Al	Ca	K	Mg	Na	F	Cl	SO_4^{2-}
	0.000	0.000	0.000	0.000	0.000	0.000	0.000	0.000	0.000	0.000	0.000	0.000	0.000	0.000	0.000	0.000	0.000
W. I. - 0.0	0.000	0.000	0.000	0.674	0.096	0.481	0.385	4.235	1.348	24.640	193.848	4.813	33.784	92.111	0.034	0.920	0.299
W. I. 1 1.1	0.000	0.000	0.000	2.214	1.925	4.043	6.834	108.859	29.068	664.222	1122.276	21.175	413.875	746.901	0.263	15.577	2.153
W. I. 1 1.2	0.000	0.000	0.096	2.695	2.503	4.813	8.663	134.943	36.864	795.988	955.763	17.325	520.713	875.876	0.332	17.449	1.904
W. I. 1 1.3	0.000	0.000	0.096	2.599	2.503	4.716	8.470	122.815	35.901	825.922	872.026	24.063	532.263	859.513	0.289	15.830	1.743
W. I. 1 1.4	0.000	0.000	0.000	2.214	1.925	4.139	7.796	105.298	30.896	684.338	866.251	14.438	464.888	1848.002	0.256	11.732	1.525
W. I. 1 1.5	0.000	0.193	0.000	0.963	0.481	1.444	2.214	33.495	8.855	181.624	408.678	16.074	166.416	319.743	0.189	4.574	1.134
W. I. 1 1.6	0.000	0.000	0.000	0.674	0.193	0.578	1.059	14.245	2.406	43.698	397.898	9.240	59.001	98.560	1.842	38.822	21.752
W. I. 1 1.7	0.000	0.000	0.000	2.214	0.096	1.155	0.000	0.000	0.000	0.000	7005.852	65.258	42.254	75.749	0.208	1.137	22.539
W. I. 1 1.8	0.000	0.000	0.000	0.866	0.096	0.866	0.096	91.438	0.385	48.318	7736.198	53.034	5.679	17.614	0.183	0.084	18.023
W. I. 1 1.9	0.000	0.000	0.481	0.963	0.193	0.866	0.385	67.375	0.193	30.608	7136.560	31.955	3.273	5.871	0.178	0.054	23.392
W. I. 1 1.10	0.000	0.096	1.348	0.000	0.096	0.578	0.963	64.295	0.193	24.448	7168.803	31.570	2.599	4.043	0.110	0.029	14.799
W. I. 1 1.11	0.000	0.000	0.193	0.000	0.193	0.578	0.481	48.991	0.096	15.496	6090.514	26.373	2.214	3.176	0.617	0.162	74.476

Appendix Two:

Cumulative concentrations of the seventeen elements analysed (mg/kg)

Experiment time	Cd	Ni	Co	Pb	Cr	Zn	Cu	Fe	Mn	Al	Ca	K	Mg	Na	F	Cl	SO_4^{2-}
	0.000	0.000	0.000	0.000	0.000	0.000	0.000	0.000	0.000	0.000	0.000	0.000	0.000	0.000	0.000	0.000	0.000
95/5 - L - 0.00	0.000	4.144	1.381	0.888	0.197	3.059	9.965	10.754	8.485	1388.867	532.381	0.000	114.744	3.157	0.123	5.104	105.899
95/5 L 1 1 .1	0.000	4.834	1.381	1.579	0.296	4.440	13.023	16.674	10.458	1664.233	1641.146	0.000	142.961	3.157	0.123	5.155	109.394
95/5 L 1 1.2	0.000	4.834	1.381	2.368	0.296	5.130	13.517	18.351	10.557	1679.230	2598.070	0.000	145.527	3.157	0.185	5.374	158.653
95/5 L 1 1.3	0.000	4.834	1.381	3.157	0.296	5.624	13.813	19.436	10.656	1683.965	3407.198	0.000	147.204	3.157	0.185	5.395	164.991
95/5 L 1 1.4	0.000	4.834	1.381	3.749	0.296	6.018	14.010	19.930	10.656	1684.853	3833.024	0.000	148.585	3.157	0.219	5.605	185.390
95/5 L 1 1.5	0.000	4.834	1.381	4.341	0.296	6.413	14.109	20.620	10.656	1685.643	4327.913	0.000	150.065	3.157	0.239	5.926	210.781
95/5 L 1 1.6	0.000	4.834	1.381	4.933	0.296	6.906	14.207	21.311	10.656	1686.037	4763.211	0.000	151.446	3.157	0.336	5.933	211.629
95/5 L 1 1.7	0.000	4.834	1.381	5.821	0.296	7.794	14.898	34.236	11.247	1691.464	8032.874	0.987	155.393	36.308	0.343	5.943	220.312
95/5 L 1 1.8	0.000	4.834	1.381	6.610	0.296	8.386	16.082	73.010	11.642	1705.178	8950.432	6.906	158.057	80.706	0.354	5.951	222.951
95/5 L 1 1.9	0.000	4.834	1.381	7.104	0.296	8.880	16.674	103.595	11.741	1713.663	9072.773	10.458	159.734	107.246	0.526	6.120	237.684
95/5 L 1 1.10	0.000	4.834	1.381	7.696	0.296	9.472	17.759	142.369	11.839	1730.238	9128.517	21.015	161.510	143.751	0.534	6.127	238.428
95/5 L 1 1.11	0.000	4.834	1.381	8.288	0.296	9.866	18.351	174.336	11.938	1739.315	9175.776	22.692	162.398	145.132	0.534	6.136	238.937
95/5 L 1 1.12	0.000	4.834	1.381	8.781	0.296	10.261	18.844	205.809	12.037	1748.392	9217.313	32.854	163.779	170.488	0.635	6.249	251.197
95/5 L 1 1.13	0.000	4.834	1.381	9.274	0.296	10.557	19.436	238.466	12.135	1756.383	9257.863	43.313	165.062	194.364	0.635	6.249	251.660

Experiment time	Cd	Ni	Co	Pb	Cr	Zn	Cu	Fe	Mn	Al	Ca	K	Mg	Na	F	Cl	SO_4^{2-}
	0.000	0.000	0.000	0.000	0.000	0.000	0.000	0.000	0.000	0.000	0.000	0.000	0.000	0.000	0.000	0.000	0.000
95/5 - U - 0.0	0.000	2.592	0.576	0.768	0.096	2.016	6.529	2.784	6.337	603.152	467.198	0.000	92.556	0.672	0.188	7.222	78.208
95/5 U 1 1.1	0.000	2.976	0.576	1.536	0.096	2.688	8.065	4.897	7.489	703.678	1425.310	0.000	110.031	1.728	0.296	16.619	125.462
95/5 U 1 1.2	0.000	2.976	0.576	2.208	0.096	3.072	8.161	5.377	7.489	705.502	1595.252	0.000	111.183	1.728	0.323	24.988	144.238
95/5 U 1 1.3	0.000	2.976	0.576	2.976	0.096	3.456	8.353	5.857	7.585	706.462	1988.617	0.000	112.815	1.728	0.343	25.104	156.367
95/5 U 1 1.4	0.000	2.976	0.576	3.648	0.096	3.744	8.353	6.145	7.585	706.654	2202.245	0.000	114.351	1.728	0.388	25.279	166.970
95/5 U 1 1.5	0.000	2.976	0.576	4.321	0.096	4.129	8.449	6.241	7.585	706.750	2360.570	0.000	115.503	1.728	0.410	25.414	174.704
95/5 U 1 1.6	0.000	2.976	0.576	5.089	0.096	4.417	8.545	6.433	7.585	706.846	2480.298	0.000	116.656	1.728	0.430	25.494	180.374
95/5 U 1 1.7	0.000	2.976	0.576	5.953	0.096	4.993	9.505	12.002	7.873	716.447	2911.396	0.288	120.208	23.811	0.695	25.675	211.505
95/5 U 1 1.8	0.000	2.976	0.576	6.625	0.096	5.377	10.657	24.291	8.065	741.027	2960.842	4.897	122.608	58.088	1.085	25.906	228.167
95/5 U 1 1.9	0.000	2.976	0.576	7.297	0.096	6.049	11.426	32.644	8.161	751.876	3002.800	9.313	124.145	80.363	1.323	26.084	240.138
95/5 U 1 1.10	0.000	2.976	0.576	8.065	0.096	6.433	12.098	39.941	8.257	758.597	3043.317	14.402	125.489	99.277	1.471	26.240	249.805
95/5 U 1 1.11	0.000	2.976	0.576	8.737	0.096	6.913	12.674	48.967	8.353	771.175	3084.027	23.523	126.833	120.400	1.621	26.368	261.840
95/5 U 1 1.12	0.000	2.976	0.576	9.409	0.096	7.393	13.154	58.088	8.353	777.608	3123.872	30.052	128.081	133.842	1.721	26.633	271.011
95/5 U 1 1.13	0.000	2.976	0.576	10.081	0.096	7.777	13.730	70.185	8.449	786.825	3164.389	45.126	129.713	161.301	1.846	26.807	284.275

Experiment time	Cd	Ni	Co	Pb	Cr	Zn	Cu	Fe	Mn	Al	Ca	K	Mg	Na	F	Cl	SO_4^{2-}
	0.000	0.000	0.000	0.000	0.000	0.000	0.000	0.000	0.000	0.000	0.000	0.000	0.000	0.000	0.000	0.000	0.000
95/8 - 0.0	0.000	0.000	0.000	0.686	0.000	0.294	0.098	0.392	0.098	0.000	99.620	0.000	3.236	9.707	0.000	0.017	0.197
95/8 1 1.1	0.000	0.000	0.000	1.373	0.000	0.981	0.392	0.784	0.784	0.294	390.536	5.393	17.551	46.084	0.000	0.073	1.054
95/8 1 1.2	0.000	0.000	0.000	2.059	0.000	1.667	0.686	1.275	1.275	0.490	578.205	7.060	26.964	61.282	0.000	0.099	1.520
95/8 1 1.3	0.000	0.000	0.000	2.745	0.000	2.255	0.882	2.157	1.667	2.745	746.558	7.452	33.239	66.871	0.000	0.113	1.942
95/8 1 1.4	0.000	0.000	0.000	3.530	0.000	2.647	1.079	2.647	1.863	2.843	914.225	7.452	38.240	67.851	0.000	0.124	2.407
95/8 1 1.5	0.000	0.000	0.000	4.216	0.000	3.040	1.177	3.040	1.961	2.843	1050.025	7.452	41.181	67.851	0.000	0.139	3.220
95/8 1 1.6	0.000	0.000	0.000	4.903	0.000	3.236	1.275	3.334	2.059	2.843	1188.865	7.452	43.535	67.851	0.000	0.146	3.559
95/8 1 1.7	0.000	0.000	0.000	5.687	0.000	4.020	2.255	3.824	2.353	3.138	2607.169	13.433	49.221	76.970	0.008	0.154	8.363
95/8 1 1.8	0.000	0.000	0.000	6.569	0.000	4.510	2.745	4.314	2.549	3.138	3645.821	17.355	51.771	82.068	0.017	0.162	12.537
95/8 1 1.9	0.000	0.000	0.000	7.354	0.000	4.903	3.138	4.706	2.647	3.236	4082.637	19.806	53.732	84.029	0.024	0.162	13.848
95/8 1 1.10	0.000	0.000	0.000	8.040	0.000	5.197	3.236	5.197	2.745	3.236	4229.811	20.689	55.399	84.029	0.024	0.171	14.170
95/8 1 1.11	0.000	0.000	0.000	8.727	0.000	5.491	3.334	5.589	2.843	3.236	4283.739	20.983	56.575	84.029	0.024	0.171	14.257
95/8 1 1.12	0.000	0.000	0.000	9.413	0.000	5.785	3.432	5.883	2.942	3.334	4327.078	21.767	57.654	84.029	0.024	0.171	14.304
95/8 1 1.13	0.000	0.000	0.000	10.001	0.000	6.079	3.530	6.177	2.942	3.432	4367.769	22.061	58.536	84.029	0.024	0.171	14.343

Experiment time	Cd	Ni	Co	Pb	Cr	Zn	Cu	Fe	Mn	Al	Ca	K	Mg	Na	F	Cl	SO_4^{2-}
	0.000	0.000	0.000	0.000	0.000	0.000	0.000	0.000	0.000	0.000	0.000	0.000	0.000	0.000	**0.000**	**0.000**	**0.000**
96/7 - 0.0	0.000	2.135	0.388	0.777	0.000	3.106	4.465	3.106	10.192	43.000	329.244	0.000	392.433	15.336	0.596	19.862	55.489
96/7 1 1.1	0.000	3.203	0.388	1.456	0.000	5.241	7.474	5.727	16.986	64.936	835.436	0.000	625.194	32.614	1.021	31.080	104.156
96/7 1 1.2	0.000	3.494	0.388	2.038	0.000	6.406	8.736	7.183	19.607	71.731	1179.531	0.000	716.435	38.632	1.239	34.811	131.687
96/7 1 1.3	0.000	3.591	0.388	2.621	0.000	7.183	9.609	8.542	21.451	76.099	1511.298	0.000	782.051	43.970	1.418	36.945	156.320
96/7 1 1.4	0.000	3.591	0.388	3.203	0.000	7.765	10.095	9.415	22.422	78.234	1764.346	0.000	818.935	46.300	1.540	38.269	172.877
96/7 1 1.5	0.000	3.591	0.388	3.786	0.000	8.251	10.483	10.095	23.101	79.690	1988.760	0.000	843.105	48.047	1.642	39.052	186.970
96/7 1 1.6	0.000	3.591	0.388	4.271	0.000	8.736	10.774	10.871	23.684	80.952	2224.239	0.000	861.644	49.018	1.733	39.617	200.536
96/7 1 1.7	0.000	3.591	0.388	5.144	0.000	9.804	12.813	27.081	27.178	94.250	4874.592	0.000	923.377	92.309	2.474	41.015	320.284
96/7 1 1.8	0.000	3.591	0.388	6.018	0.000	10.289	13.880	51.930	28.246	107.159	6745.904	1.844	930.948	128.125	3.285	41.530	410.552
96/7 1 1.9	0.000	3.591	0.388	6.892	0.000	10.580	14.851	75.711	28.731	117.545	8011.337	4.950	935.122	153.945	3.934	41.863	479.475
96/7 1 1.10	0.000	3.591	0.388	7.571	0.000	10.968	15.530	94.056	29.022	124.728	8818.139	9.027	937.937	170.543	4.394	42.225	530.015
96/7 1 1.11	0.000	3.591	0.388	8.348	0.000	11.357	16.113	114.633	29.216	131.814	9537.389	15.045	940.460	188.694	4.825	42.474	572.643
96/7 1 1.12	0.000	3.591	0.388	9.124	0.000	11.648	16.695	137.153	29.411	138.900	10051.250	20.869	942.790	204.807	4.841	42.484	574.088
96/7 1 1.13	0.000	3.591	0.388	9.804	0.000	11.842	17.180	158.021	29.605	145.403	10442.324	25.140	944.828	216.649	4.856	42.493	575.317

Experiment time	Cd	Ni	Co	Pb	Cr	Zn	Cu	Fe	Mn	Al	Ca	K	Mg	Na	F	Cl	SO_4^{2-}
	0.000	0.000	0.000	0.000	0.000	0.000	0.000	0.000	0.000	0.000	0.000	0.000	0.000	0.000	0.000	0.000	0.000
96/46 - 0.0	0.000	0.503	0.805	0.000	0.101	0.402	0.201	0.000	0.704	0.000	74.553	0.000	20.525	16.400	0.000	0.051	0.180
96/46 1 1.1	0.000	0.906	1.710	0.000	0.201	0.704	0.402	0.000	0.906	0.101	142.064	0.000	29.479	18.814	0.000	0.070	0.274

96/46 1 1.2	0.000	1.308	2.616	0.000	0.302	0.805	0.604	0.101	1.107	0.201	202.028	0.000	35.315	18.814	0.033	0.473	2.333
96/46 1 1.3	0.201	1.710	3.521	0.000	0.402	1.006	0.805	0.201	1.207	0.302	259.578	0.000	39.943	18.814	0.064	0.752	4.113
96/46 1 1.4	0.604	2.012	4.528	0.000	0.503	1.006	1.006	0.201	1.308	0.302	310.991	0.000	43.364	18.814	0.093	1.329	5.569
96/46 1 1.5	1.207	2.415	5.433	0.000	0.604	1.107	1.207	0.302	1.409	0.302	361.498	0.000	46.281	18.814	0.115	1.517	6.866
96/46 1 1.6	2.012	2.817	6.339	0.000	0.704	1.409	1.409	0.402	1.409	0.302	410.093	0.000	48.897	18.814	0.166	1.660	7.995
96/46 1 1.7	3.018	3.320	7.345	0.000	0.805	2.213	2.113	0.906	2.113	1.107	618.158	0.000	67.712	25.455	0.324	2.132	19.426
96/46 1 1.8	3.924	3.723	8.351	0.000	0.906	3.119	2.817	1.207	2.314	1.912	763.945	0.000	73.849	28.071	0.466	2.299	26.610
96/46 1 1.9	5.131	4.125	9.458	0.000	1.006	3.622	3.119	1.409	2.415	2.314	834.272	0.000	75.861	28.071	0.579	2.486	29.491
96/46 1 1.10	6.238	4.528	10.564	0.000	1.107	3.924	3.320	1.509	2.415	2.515	883.874	0.302	77.169	28.071	0.663	2.681	31.008
96/46 1 1.11	7.646	4.930	11.671	0.000	1.207	4.326	3.723	1.710	2.415	2.918	929.552	0.402	78.377	28.071	0.777	2.835	32.383
96/46 1 1.12	8.854	5.332	12.979	0.000	1.308	4.528	4.024	1.912	2.415	3.521	973.217	0.402	79.483	28.071	0.901	2.964	33.750
96/46 1 1.13	10.061	5.634	14.086	0.000	1.409	4.729	4.528	2.314	2.415	4.226	1016.08	0.402	80.489	28.071	1.031	3.069	35.131

Experiment time	Cd	Ni	Co	Pb	Cr	Zn	Cu	Fe	Mn	Al	Ca	K	Mg	Na	F	Cl	SO_4^{2-}
	0.000	0.000	0.000	0.000	0.000	0.000	0.000	0.000	0.000	0.000	0.000	0.000	0.000	0.000	0.000	0.000	0.000
Ruw - 0.0	0.000	0.000	0.000	0.500	0.000	0.000	0.000	0.000	0.000	0.000	39.397	0.000	0.800	8.199	0.000	0.313	0.737
Ruw 1 1.1	0.000	0.000	0.000	1.000	0.000	0.000	0.000	0.000	0.000	0.000	77.694	0.000	1.300	13.599	0.000	0.582	1.303
Ruw 1 1.2	0.000	0.000	0.000	1.500	0.000	0.100	0.000	0.000	0.000	0.000	115.491	0.000	1.700	14.599	0.000	24.446	1.536
Ruw 1 1.3	0.000	0.000	0.000	2.000	0.000	0.100	0.000	0.000	0.000	0.000	153.288	0.000	2.200	14.599	0.000	24.684	1.687
Ruw 1 1.4	0.000	0.000	0.000	2.500	0.000	0.200	0.000	0.000	0.000	0.000	190.785	0.000	2.700	14.599	0.000	30.421	1.765
Ruw 1 1.5	0.000	0.000	0.000	3.000	0.000	0.200	0.100	0.000	0.000	0.000	228.582	0.000	3.200	14.599	0.000	30.776	1.860
Ruw 1 1.6	0.000	0.000	0.000	3.400	0.000	0.200	0.100	0.000	0.000	0.000	266.879	0.000	3.700	14.599	0.000	31.016	1.947
Ruw 1 1.7	0.000	0.000	0.000	3.900	0.000	0.400	0.200	0.000	0.000	0.000	307.675	0.000	4.500	15.599	0.000	31.125	2.695
Ruw 1 1.8	0.000	0.000	0.000	4.400	0.000	0.600	0.200	0.000	0.000	0.000	347.772	0.000	5.200	16.399	0.000	31.240	3.276
Ruw 1 1.9	0.000	0.000	0.000	5.000	0.000	0.700	0.200	0.000	0.000	0.000	386.069	0.000	5.800	16.399	0.000	31.340	3.639
Ruw 1 1.10	0.000	0.000	0.000	5.300	0.000	0.700	0.200	0.000	0.000	0.000	424.166	0.000	6.299	16.399	0.000	31.417	3.830
Ruw 1 1.11	0.000	0.000	0.000	5.800	0.000	0.700	0.200	0.000	0.000	0.000	461.963	0.000	6.799	16.399	0.000	31.536	4.091
Ruw 1 1.12	0.000	0.000	0.000	6.299	0.000	0.800	0.200	0.000	0.000	0.000	500.160	0.000	7.299	16.399	0.000	31.643	4.251
Ruw 1 1.13	0.000	0.000	0.000	6.799	0.000	0.800	0.200	0.000	0.000	0.000	538.657	0.000	7.799	16.399	0.000	31.749	4.437

Experiment time	Cd	Ni	Co	Pb	Cr	Zn	Cu	Fe	Mn	Al	Ca	K	Mg	Na	F	Cl	SO_4^{2-}
	0.000	0.000	0.000	0.000	0.000	0.000	0.000	0.000	0.000	0.000	0.000	0.000	0.000	0.000	0.000	0.000	0.000
SK1 - 0.0	0.900	0.000	0.000	0.600	0.000	1.300	0.200	0.000	0.000	0.100	41.398	0.100	0.700	8.300	0.019	0.372	3.976
SK1 1.1	2.000	0.000	0.000	1.200	0.000	2.000	0.300	0.000	0.100	0.200	139.194	3.100	4.500	24.699	0.155	2.568	8.580
SK1 1.2	2.900	0.000	0.000	1.700	0.000	2.400	0.300	0.000	0.100	0.400	185.193	3.100	5.500	32.399	0.219	2.886	9.769
SK1 1.3	3.900	0.000	0.000	2.200	0.000	2.500	0.300	0.000	0.100	0.400	225.091	3.100	6.200	38.098	0.265	3.026	10.351
SK1 1.4	4.800	0.000	0.000	2.700	0.000	2.500	0.300	0.000	0.100	0.400	268.889	3.100	7.100	44.098	0.369	3.320	11.275
SK1 1.5	5.500	0.000	0.000	3.200	0.000	2.700	0.300	0.000	0.100	0.400	307.888	3.100	7.600	49.098	0.429	3.446	11.715
SK1 1.6	6.400	0.000	0.000	3.700	0.000	2.900	0.300	0.000	0.100	0.400	346.886	3.100	8.200	53.998	0.520	3.553	12.082
SK1 1.7	7.200	0.000	0.000	4.200	0.000	3.000	0.300	0.000	0.100	0.500	387.485	3.100	9.000	59.798	0.638	3.698	12.526
SK1 1.8	7.800	0.000	0.000	4.600	0.000	3.000	0.300	0.000	0.100	1.200	433.283	3.100	10.000	67.297	1.160	3.881	13.112

SK1 1.9	8.300	0.000	0.000	5.100	0.000	3.100	0.300	0.000	0.100	1.300	474.181	3.100	10.700	75.497	1.555	4.142	13.452
SK1 1.10	8.500	0.000	0.000	5.600	0.000	3.200	0.300	0.000	0.100	1.700	513.479	3.100	11.400	82.397	1.861	5.151	13.957
SK1 1.11	8.600	0.000	0.000	6.000	0.000	3.200	0.300	0.000	0.100	1.900	553.678	3.100	12.000	88.496	2.075	5.343	14.265
SK1 1.12	8.600	0.000	0.000	6.400	0.000	3.400	0.300	0.000	0.100	2.000	592.076	3.100	12.599	94.896	2.280	5.532	14.490
SK1 1.13	8.600	0.000	0.000	6.800	0.000	3.500	0.300	0.000	0.100	2.000	630.275	3.100	13.199	100.996	2.453	5.648	14.656
SK1 1.14	8.600	0.000	0.000	7.300	0.000	3.600	0.300	0.000	0.100	2.000	668.873	3.100	13.699	105.496	2.572	5.817	14.822

Experiment time	Cd	Ni	Co	Pb	Cr	Zn	Cu	Fe	Mn	Al	Ca	K	Mg	Na	F	Cl	SO_4^{2-}
	0.000	0.000	0.000	0.000	0.000	0.000	0.000	0.000	0.000	0.000	0.000	0.000	0.000	0.000	0.000	0.000	0.000
KL1 - 0.0	1.396	0.299	1.097	0.000	0.100	0.000	0.100	0.000	0.000	0.000	49.162	0.000	1.396	6.382	0.021	0.979	1.107
KL1 1.1	2.493	0.598	2.194	0.000	0.199	0.100	0.199	0.000	0.000	0.000	122.956	0.199	2.992	11.667	0.078	4.783	2.944
KL1 1.2	3.690	0.897	3.291	0.000	0.299	0.299	0.299	0.000	0.000	0.000	186.179	0.199	4.089	12.565	0.170	4.783	4.280
KL1 1.3	4.886	1.197	4.388	0.000	0.399	0.299	0.399	0.000	0.000	0.000	237.934	0.199	4.886	12.565	0.170	4.783	5.121
KL1 1.4	5.884	1.496	5.485	0.000	0.499	0.299	0.499	0.000	0.000	0.000	298.165	0.199	5.884	13.662	0.170	4.783	6.299
KL1 1.5	6.781	1.795	6.681	0.000	0.598	0.299	0.598	0.000	0.000	0.000	353.710	0.199	6.781	13.662	0.170	4.783	7.264
KL1 1.6	7.280	2.194	7.978	0.000	0.698	0.499	0.698	0.000	0.000	0.000	408.257	0.199	7.778	13.662	0.170	4.783	8.137
KL1 1.7	8.177	2.493	9.174	0.000	0.798	0.499	0.798	0.299	0.000	10.471	824.990	17.052	9.972	82.569	0.170	4.783	19.170
KL1 1.8	9.972	3.889	12.266	0.000	1.296	12.166	2.393	0.399	0.000	21.041	1148.385	27.623	11.867	110.790	0.170	4.783	24.584
KL1 1.9	9.972	4.986	16.155	0.000	1.795	15.656	2.393	0.499	0.000	32.110	1393.099	34.304	13.662	128.341	0.170	4.783	26.272
KL1 1.10	9.972	6.382	21.639	0.000	2.294	17.451	2.393	0.598	0.000	43.877	1640.108	40.985	15.556	143.997	0.170	4.783	27.572
KL1 1.11	10.670	7.978	28.121	0.000	2.792	19.047	2.393	0.798	0.000	54.946	1829.577	45.572	17.351	156.262	0.170	4.783	28.414
KL1 1.12	11.069	9.573	34.204	0.000	3.291	21.939	2.393	0.897	0.000	66.115	2019.146	49.860	19.346	168.528	0.170	4.783	29.227
KL1 1.13	11.468	12.47	38.991	0.000	3.789	23.634	2.393	1.097	0.000	76.885	2218.887	55.245	21.440	182.589	0.170	4.783	30.173

Experiment time	Cd	Ni	Co	Pb	Cr	Zn	Cu	Fe	Mn	Al	Ca	K	Mg	Na	F	Cl	SO_4^{2-}
	0.000	0.000	0.000	0.000	0.000	0.000	0.000	0.000	0.000	0.000	0.000	0.000	0.000	0.000	0.000	0.000	0.000
W. I. - 0.0	0.000	0.000	0.000	0.674	0.096	0.481	0.385	4.235	1.348	24.640	193.848	4.813	33.784	92.111	0.034	0.920	0.299
W. I. 1 1.1	0.000	0.000	0.000	2.888	2.021	4.524	7.219	113.094	30.415	688.862	1316.124	25.988	447.659	839.012	0.298	16.497	2.452
W. I. 1 1.2	0.000	0.000	0.096	5.583	4.524	9.336	15.881	248.036	67.279	1484.850	2271.887	43.313	968.372	1714.888	0.630	33.946	4.356
W. I. 1 1.3	0.000	0.000	0.193	8.181	7.026	14.053	24.351	370.852	103.180	2310.772	3143.913	67.375	1500.635	2574.401	0.919	49.775	6.099
W. I. 1 1.4	0.000	0.000	0.193	10.395	8.951	18.191	32.148	476.149	134.076	2995.110	4010.164	81.813	1965.523	4422.403	1.175	61.507	7.624
W. I. 1 1.5	0.000	0.193	0.193	11.358	9.433	19.635	34.361	509.644	142.931	3176.734	4418.842	97.886	2131.940	4742.146	1.364	66.081	8.759
W. I. 1 1.6	0.000	0.193	0.193	12.031	9.625	20.213	35.420	523.889	145.338	3220.432	4816.740	107.126	2190.941	4840.706	3.206	104.903	30.511
W. I. 1 1.7	0.000	0.193	0.193	14.245	9.721	21.368	35.420	523.889	145.338	3220.432	11822.592	172.384	2233.195	4916.455	3.414	106.040	53.050
W. I. 1 1.8	0.000	0.193	0.193	15.111	9.818	22.234	35.516	615.327	145.723	3268.750	19558.790	225.418	2238.873	4934.069	3.597	106.124	71.072
W. I. 1 1.9	0.000	0.193	0.674	16.074	10.010	23.100	35.901	682.702	145.915	3299.357	26695.349	257.373	2242.146	4939.940	3.775	106.178	94.465
W.I. 1 1.10	0.000	0.289	2.021	16.074	10.106	23.678	36.864	746.997	146.108	3323.805	33864.153	288.943	2244.745	4943.982	3.886	106.207	109.263
W.I. 11.11	0.000	0.289	2.214	16.074	10.299	24.255	37.345	795.988	146.204	3339.301	39954.666	315.315	2246.958	4947.159	4.502	106.369	183.739

Appendix Three:

Cumulative concentrations of elements normalised to the total recoverable metal concentrations.

Experiment time	Cd	Ni	Co	Pb	Cr	Zn	Cu	Fe	Mn	Al	Ca	K	Mg	Na
	0.0000	0.000	0.0000	0.0000	0.0000	0.0000	0.0000	0.0000	0.0000	0.0000	0.0000	0.0000	0.0000	0.0000
95/5 - L - 0.00	69.06%	4.144	49.33%	74.00%	6.58%	61.17%	41.52%	0.22%	73.78%	34.72%	7.72%	0.00%	44.13%	0.51%
95/5 L 1 1 .1	80.57%	4.834	49.33%	131.55%	9.87%	88.80%	54.26%	0.34%	90.94%	41.61%	23.78%	0.00%	54.99%	0.51%
95/5 L 1 1.2	80.57%	4.834	49.33%	197.32%	9.87%	102.61%	56.32%	0.37%	91.80%	41.98%	37.65%	0.00%	55.97%	0.51%
95/5 L 1 1.3	80.57%	4.834	49.33%	263.10%	9.87%	112.47%	57.55%	0.40%	92.66%	42.10%	49.38%	0.00%	56.62%	0.51%
95/5 L 1 1.4	80.57%	4.834	49.33%	312.43%	9.87%	120.37%	58.38%	0.41%	92.66%	42.12%	55.55%	0.00%	57.15%	0.51%
95/5 L 1 1.5	80.57%	4.834	49.33%	361.76%	9.87%	128.26%	58.79%	0.42%	92.66%	42.14%	62.72%	0.00%	57.72%	0.51%
95/5 L 1 1.6	80.57%	4.834	49.33%	411.09%	9.87%	138.13%	59.20%	0.43%	92.66%	42.15%	69.03%	0.00%	58.25%	0.51%
95/5 L 1 1.7	80.57%	4.834	49.33%	485.09%	9.87%	155.89%	62.07%	0.70%	97.80%	42.29%	116.42%	0.50%	59.77%	5.86%
95/5 L 1 1.8	80.57%	4.834	49.33%	550.86%	9.87%	167.73%	67.01%	1.49%	101.24%	42.63%	129.72%	3.52%	60.79%	13.02%
95/5 L 1 1.9	80.57%	4.834	49.33%	591.97%	9.87%	177.59%	69.47%	2.11%	102.09%	42.84%	131.49%	5.34%	61.44%	17.30%
95/5 L 1 1.10	80.57%	4.834	49.33%	641.30%	9.87%	189.43%	74.00%	2.91%	102.95%	43.26%	132.30%	10.72%	62.12%	23.19%
95/5 L 1 1.11	80.57%	4.834	49.33%	690.63%	9.87%	197.32%	76.46%	3.56%	103.81%	43.48%	132.98%	11.58%	62.46%	23.41%
95/5 L 1 1.12	80.57%	4.834	49.33%	731.74%	9.87%	205.22%	78.52%	4.20%	104.67%	43.71%	133.58%	16.76%	62.99%	27.50%
95/5 L 1 1.13	80.57%	4.834	49.33%	772.85%	9.87%	211.14%	80.99%	4.87%	105.53%	43.91%	134.17%	22.10%	63.49%	31.35%

Experiment time	Cd	Ni	Co	Pb	Cr	Zn	Cu	Fe	Mn	Al	Ca	K	Mg	Na
	0.000	0.0000	0.0000	0.0000	0.0000	0.0000	0.0000	0.0000	0.0000	0.0000	0.0000	0.0000	0.0000	0.0000
95/5 - U - 0.0	0.000	64.81%	28.80%	69.83%	3.20%	50.41%	32.64%	0.08%	56.58%	12.06%	10.62%	0.00%	38.57%	0.10%
95/5 U 1 1.1	0.000	74.41%	28.80%	139.65%	3.20%	67.21%	40.33%	0.13%	66.87%	14.07%	32.39%	0.00%	45.85%	0.25%
95/5 U 1 1.2	0.000	74.41%	28.80%	200.75%	3.20%	76.81%	40.81%	0.15%	66.87%	14.11%	36.26%	0.00%	46.33%	0.25%
95/5 U 1 1.3	0.000	74.41%	28.80%	270.58%	3.20%	86.41%	41.77%	0.16%	67.72%	14.13%	45.20%	0.00%	47.01%	0.25%
95/5 U 1 1.4	0.000	74.41%	28.80%	331.68%	3.20%	93.61%	41.77%	0.17%	67.72%	14.13%	50.05%	0.00%	47.65%	0.25%
95/5 U 1 1.5	0.000	74.41%	28.80%	392.78%	3.20%	103.21%	42.25%	0.17%	67.72%	14.14%	53.65%	0.00%	48.13%	0.25%
95/5 U 1 1.6	0.000	74.41%	28.80%	462.61%	3.20%	110.41%	42.73%	0.17%	67.72%	14.14%	56.37%	0.00%	48.61%	0.25%
95/5 U 1 1.7	0.000	74.41%	28.80%	541.16%	3.20%	124.82%	47.53%	0.32%	70.30%	14.33%	66.17%	0.16%	50.09%	3.50%
95/5 U 1 1.8	0.000	74.41%	28.80%	602.26%	3.20%	134.42%	53.29%	0.66%	72.01%	14.82%	67.29%	2.74%	51.09%	8.54%
95/5 U 1 1.9	0.000	74.41%	28.80%	663.36%	3.20%	151.22%	57.13%	0.88%	72.87%	15.04%	68.25%	5.20%	51.73%	11.82%
95/5 U 1 1.10	0.000	74.41%	28.80%	733.19%	3.20%	160.82%	60.49%	1.08%	73.72%	15.17%	69.17%	8.05%	52.29%	14.60%
95/5 U 1 1.11	0.000	74.41%	28.80%	794.29%	3.20%	172.82%	63.37%	1.32%	74.58%	15.42%	70.09%	13.14%	52.85%	17.71%
95/5 U 1 1.12	0.000	74.41%	28.80%	855.39%	3.20%	184.82%	65.77%	1.57%	74.58%	15.55%	71.00%	16.79%	53.37%	19.68%
95/5 U 1 1.13	0.000	74.41%	28.80%	916.49%	3.20%	194.43%	68.65%	1.90%	75.44%	15.74%	71.92%	25.21%	54.05%	23.72%

Experiment time	Cd	Ni	Co	Pb	Cr	Zn	Cu	Fe	Mn	Al	Ca	K	Mg	Na
	0.000	0.000	0.000	0.0000	0.000	0.0000	0.0000	0.0000	0.0000	0.0000	0.0000	0.0000	0.0000	0.0000
95/8 - 0.0	0.000	0.000	0.000	31.20%	0.000	4.90%	0.25%	0.01%	0.77%	0.00%	2.08%	0.00%	1.04%	1.33%
95/8 1 1.1	0.000	0.000	0.000	62.40%	0.000	16.34%	0.98%	0.02%	6.13%	0.01%	8.14%	2.07%	5.66%	6.31%
95/8 1 1.2	0.000	0.000	0.000	93.59%	0.000	27.78%	1.72%	0.03%	9.96%	0.01%	12.05%	2.72%	8.70%	8.39%
95/8 1 1.3	0.000	0.000	0.000	124.79%	0.000	37.59%	2.21%	0.06%	13.02%	0.05%	15.55%	2.87%	10.72%	9.16%
95/8 1 1.4	0.000	0.000	0.000	160.45%	0.000	44.12%	2.70%	0.07%	14.55%	0.05%	19.05%	2.87%	12.34%	9.29%
95/8 1 1.5	0.000	0.000	0.000	191.64%	0.000	50.66%	2.94%	0.08%	15.32%	0.05%	21.88%	2.87%	13.28%	9.29%
95/8 1 1.6	0.000	0.000	0.000	222.84%	0.000	53.93%	3.19%	0.09%	16.09%	0.05%	24.77%	2.87%	14.04%	9.29%
95/8 1 1.7	0.000	0.000	0.000	258.50%	0.000	67.00%	5.64%	0.10%	18.38%	0.06%	54.32%	5.17%	15.88%	10.54%
95/8 1 1.8	0.000	0.000	0.000	298.61%	0.000	75.17%	6.86%	0.12%	19.92%	0.06%	75.95%	6.67%	16.70%	11.24%
95/8 1 1.9	0.000	0.000	0.000	334.26%	0.000	81.71%	7.84%	0.13%	20.68%	0.06%	85.05%	7.62%	17.33%	11.51%
95/8 1 1.10	0.000	0.000	0.000	365.46%	0.000	86.61%	8.09%	0.14%	21.45%	0.06%	88.12%	7.96%	17.87%	11.51%
95/8 1 1.11	0.000	0.000	0.000	396.66%	0.000	91.51%	8.33%	0.15%	22.21%	0.06%	89.24%	8.07%	18.25%	11.51%
95/8 1 1.12	0.000	0.000	0.000	427.86%	0.000	96.42%	8.58%	0.16%	22.98%	0.06%	90.15%	8.37%	18.60%	11.51%
95/8 1 1.13	0.000	0.000	0.000	454.60%	0.000	101.32%	8.82%	0.17%	22.98%	0.06%	91.00%	8.49%	18.88%	11.51%

Experiment time	Cd	Ni	Co	Pb	Cr	Zn	Cu	Fe	Mn	Al	Ca	K	Mg	Na
	0.000	0.0000	0.0000	0.0000	0.000	0.0000	0.0000	0.0000	0.0000	0.0000	0.0000	0.0000	0.0000	0.0000
96/7 - 0.0	0.000	21.35%	8.82%	32.35%	0.000	38.83%	12.40%	0.04%	28.31%	0.81%	3.47%	0.00%	30.66%	1.32%
96/7 1 1.1	0.000	32.03%	8.82%	60.67%	0.000	65.52%	20.76%	0.07%	47.18%	1.23%	8.79%	0.00%	48.84%	2.81%
96/7 1 1.2	0.000	34.94%	8.82%	84.93%	0.000	80.08%	24.27%	0.09%	54.46%	1.35%	12.42%	0.00%	55.97%	3.33%
96/7 1 1.3	0.000	35.91%	8.82%	109.20%	0.000	89.78%	26.69%	0.11%	59.59%	1.44%	15.91%	0.00%	61.10%	3.79%
96/7 1 1.4	0.000	35.91%	8.82%	133.46%	0.000	97.06%	28.04%	0.12%	62.28%	1.48%	18.57%	0.00%	63.98%	3.99%
96/7 1 1.5	0.000	35.91%	8.82%	157.73%	0.000	103.13%	29.12%	0.13%	64.17%	1.50%	20.93%	0.00%	65.87%	4.14%
96/7 1 1.6	0.000	35.91%	8.82%	177.95%	0.000	109.20%	29.93%	0.14%	65.79%	1.53%	23.41%	0.00%	67.32%	4.23%
96/7 1 1.7	0.000	35.91%	8.82%	214.35%	0.000	122.54%	35.59%	0.34%	75.49%	1.78%	51.31%	0.00%	72.14%	7.96%
96/7 1 1.8	0.000	35.91%	8.82%	250.75%	0.000	128.61%	38.56%	0.65%	78.46%	2.02%	71.01%	0.38%	72.73%	11.05%
96/7 1 1.9	0.000	35.91%	8.82%	287.15%	0.000	132.25%	41.25%	0.95%	79.81%	2.22%	84.33%	1.01%	73.06%	13.27%
96/7 1 1.10	0.000	35.91%	8.82%	315.46%	0.000	137.10%	43.14%	1.18%	80.62%	2.35%	92.82%	1.84%	73.28%	14.70%
96/7 1 1.11	0.000	35.91%	8.82%	347.82%	0.000	141.96%	44.76%	1.43%	81.16%	2.49%	100.39%	3.07%	73.47%	16.27%
96/7 1 1.12	0.000	35.91%	8.82%	380.17%	0.000	145.60%	46.38%	1.71%	81.70%	2.62%	105.80%	4.26%	73.66%	17.66%
96/7 1 1.13	0.000	35.91%	8.82%	408.48%	0.000	148.02%	47.72%	1.98%	82.24%	2.74%	109.92%	5.13%	73.81%	18.68%

Experiment time	Cd	Ni	Co	Pb	Cr	Zn	Cu	Fe	Mn	Al	Ca	K	Mg	Na
	0.0000	0.0000	0.0000	0.000	0.0000	0.0000	0.0000	0.0000	0.0000	0.0000	0.0000	0.0000	0.0000	0.0000
96/46 - 0.0	0.00%	12.58%	57.49%	0.000	5.03%	10.06%	0.69%	0.00%	4.79%	0.00%	1.66%	0.00%	5.86%	1.55%
96/46 1 1.1	0.00%	22.64%	122.17%	0.000	10.06%	17.61%	1.39%	0.00%	6.16%	0.00%	3.16%	0.00%	8.42%	1.77%
96/46 1 1.2	0.00%	32.70%	186.85%	0.000	15.09%	20.12%	2.08%	0.00%	7.53%	0.00%	4.49%	0.00%	10.09%	1.77%
96/46 1 1.3	201.22%	42.76%	251.53%	0.000	20.12%	25.15%	2.78%	0.01%	8.21%	0.00%	5.77%	0.00%	11.41%	1.77%
96/46 1 1.4	603.67%	50.31%	323.39%	0.000	25.15%	25.15%	3.47%	0.01%	8.90%	0.00%	6.91%	0.00%	12.39%	1.77%

96/46 1 1.5	1207.34%	60.37%	388.07%	0.000	30.18%	27.67%	4.16%	0.01%	9.58%	0.00%	8.03%	0.00%	13.22%	1.77%
96/46 1 1.6	2012.23%	70.43%	452.75%	0.000	35.21%	35.21%	4.86%	0.01%	9.58%	0.00%	9.11%	0.00%	13.97%	1.77%
96/46 1 1.7	3018.35%	83.00%	524.62%	0.000	40.24%	55.34%	7.29%	0.03%	14.37%	0.02%	13.74%	0.00%	19.35%	2.40%
96/46 1 1.8	3923.86%	93.07%	596.48%	0.000	45.28%	77.97%	9.71%	0.04%	15.74%	0.03%	16.98%	0.00%	21.10%	2.65%
96/46 1 1.9	5131.20%	103.13%	675.54%	0.000	50.31%	90.55%	10.76%	0.05%	16.43%	0.03%	18.54%	0.00%	21.67%	2.65%
96/46 1 1.10	6237.93%	113.19%	754.59%	0.000	55.34%	98.10%	11.45%	0.05%	16.43%	0.04%	19.64%	0.16%	22.05%	2.65%
96/46 1 1.11	7646.49%	123.25%	833.64%	0.000	60.37%	108.16%	12.84%	0.06%	16.43%	0.04%	20.66%	0.22%	22.39%	2.65%
96/46 1 1.12	8853.83%	133.31%	927.07%	0.000	65.40%	113.19%	13.88%	0.06%	16.43%	0.05%	21.63%	0.22%	22.71%	2.65%
96/46 1 1.13	10061.17%	140.86%	1006.12%	0.000	70.43%	118.22%	15.61%	0.07%	16.43%	0.06%	22.58%	0.22%	23.00%	2.65%

Experiment time	Cd	Ni	Co	Pb	Cr	Zn	Cu	Fe	Mn	Al	Ca	K	Mg	Na
	0.000	0.000	0.000	0.0000	0.000	0.0000	0.0000	0.000	0.000	0.000	0.0000	0.000	0.0000	0.0000
Ruw - 0.0	0.000	0.000	0.000	55.55%	0.000	0.00%	0.00%	0.000	0.000	0.000	0.98%	0.000	0.20%	1.28%
Ruw 1 1.1	0.000	0.000	0.000	111.10%	0.000	0.00%	0.00%	0.000	0.000	0.000	1.94%	0.000	0.32%	2.12%
Ruw 1 1.2	0.000	0.000	0.000	166.65%	0.000	2.00%	0.00%	0.000	0.000	0.000	2.89%	0.000	0.41%	2.28%
Ruw 1 1.3	0.000	0.000	0.000	222.20%	0.000	2.00%	0.00%	0.000	0.000	0.000	3.83%	0.000	0.54%	2.28%
Ruw 1 1.4	0.000	0.000	0.000	277.76%	0.000	4.00%	0.00%	0.000	0.000	0.000	4.77%	0.000	0.66%	2.28%
Ruw 1 1.5	0.000	0.000	0.000	333.31%	0.000	4.00%	1.25%	0.000	0.000	0.000	5.71%	0.000	0.78%	2.28%
Ruw 1 1.6	0.000	0.000	0.000	377.75%	0.000	4.00%	1.25%	0.000	0.000	0.000	6.67%	0.000	0.90%	2.28%
Ruw 1 1.7	0.000	0.000	0.000	433.30%	0.000	8.00%	2.50%	0.000	0.000	0.000	7.69%	0.000	1.10%	2.44%
Ruw 1 1.8	0.000	0.000	0.000	488.85%	0.000	12.00%	2.50%	0.000	0.000	0.000	8.69%	0.000	1.27%	2.56%
Ruw 1 1.9	0.000	0.000	0.000	555.51%	0.000	14.00%	2.50%	0.000	0.000	0.000	9.65%	0.000	1.41%	2.56%
Ruw 1 1.10	0.000	0.000	0.000	588.84%	0.000	14.00%	2.50%	0.000	0.000	0.000	10.60%	0.000	1.54%	2.56%
Ruw 1 1.11	0.000	0.000	0.000	644.39%	0.000	14.00%	2.50%	0.000	0.000	0.000	11.55%	0.000	1.66%	2.56%
Ruw 1 1.12	0.000	0.000	0.000	699.94%	0.000	16.00%	2.50%	0.000	0.000	0.000	12.50%	0.000	1.78%	2.56%
Ruw 1 1.13	0.000	0.000	0.000	755.50%	0.000	16.00%	2.50%	0.000	0.000	0.000	13.47%	0.000	1.90%	2.56%

Experiment time	Cd	Ni	Co	Pb	Cr	Zn	Cu	Fe	Mn	Al	Ca	K	Mg	Na
	0.0000	0.000	0.000	0.0000	0.000	0.0000	0.0000	0.000	0.0000	0.0000	0.0000	0.0000	0.0000	0.0000
SK1 - 0.0	899.96%	0.000	0.000	50.00%	0.000	11.82%	1.67%	0.000	0.00%	0.001%	0.37%	0.09%	0.16%	0.58%
SK1 1.1	1999.92%	0.000	0.000	100.00%	0.000	18.18%	2.50%	0.000	0.19%	0.001%	1.23%	2.65%	1.00%	1.74%
SK1 1.2	2899.88%	0.000	0.000	141.66%	0.000	21.82%	2.50%	0.000	0.19%	0.003%	1.64%	2.65%	1.22%	2.28%
SK1 1.3	3899.84%	0.000	0.000	183.33%	0.000	22.73%	2.50%	0.000	0.19%	0.003%	1.99%	2.65%	1.38%	2.68%
SK1 1.4	4799.81%	0.000	0.000	224.99%	0.000	22.73%	2.50%	0.000	0.19%	0.003%	2.38%	2.65%	1.58%	3.11%
SK1 1.5	5499.78%	0.000	0.000	266.66%	0.000	24.54%	2.50%	0.000	0.19%	0.003%	2.72%	2.65%	1.69%	3.46%
SK1 1.6	6399.74%	0.000	0.000	308.32%	0.000	26.36%	2.50%	0.000	0.19%	0.003%	3.07%	2.65%	1.82%	3.80%
SK1 1.7	7199.71%	0.000	0.000	349.99%	0.000	27.27%	2.50%	0.000	0.19%	0.003%	3.43%	2.65%	2.00%	4.21%
SK1 1.8	7799.69%	0.000	0.000	383.32%	0.000	27.27%	2.50%	0.000	0.19%	0.008%	3.83%	2.65%	2.22%	4.74%
SK1 1.9	8299.67%	0.000	0.000	424.98%	0.000	28.18%	2.50%	0.000	0.19%	0.008%	4.20%	2.65%	2.38%	5.32%
SK1 1.10	8499.66%	0.000	0.000	466.65%	0.000	29.09%	2.50%	0.000	0.19%	0.011%	4.54%	2.65%	2.53%	5.80%
SK1 1.11	8599.66%	0.000	0.000	499.98%	0.000	29.09%	2.50%	0.000	0.19%	0.012%	4.90%	2.65%	2.67%	6.23%

SK1 1.12	8599.66%	0.000	0.000	533.31%	0.000	30.91%	2.50%	0.000	0.19%	0.013%	5.24%	2.65%	2.80%	6.68%
SK1 1.13	8599.66%	0.000	0.000	566.64%	0.000	31.82%	2.50%	0.000	0.19%	0.013%	5.58%	2.65%	2.93%	7.11%
SK1 1.14	8599.66%	0.000	0.000	608.31%	0.000	32.73%	2.50%	0.000	0.19%	0.013%	5.92%	2.65%	3.04%	7.43%

Experiment time	Cd	Ni	Co	Pb	Cr	Zn	Cu	Fe	Mn	Al	Ca	K	Mg	Na
	0.0000	0.0000	0.0000	0.000	0.0000	0.0000	0.0000	0.0000	0.000	0.0000	0.0000	0.0000	0.0000	0.0000
KL1 - 0.0	1396.09%	9.97%	39.18%	0.000	3.32%	0.00%	0.33%	0.000%	0.000	0.000%	0.18%	0.00%	0.13%	0.21%
KL1 1.1	2493.02%	19.94%	78.35%	0.000	6.65%	1.11%	0.66%	0.000%	0.000	0.000%	0.44%	0.06%	0.27%	0.38%
KL1 1.2	3689.67%	29.92%	117.53%	0.000	9.97%	3.32%	1.00%	0.000%	0.000	0.000%	0.66%	0.06%	0.37%	0.41%
KL1 1.3	4886.32%	39.89%	156.70%	0.000	13.30%	3.32%	1.33%	0.000%	0.000	0.000%	0.85%	0.06%	0.44%	0.41%
KL1 1.4	5883.53%	49.86%	195.88%	0.000	16.62%	3.32%	1.66%	0.000%	0.000	0.000%	1.06%	0.06%	0.53%	0.44%
KL1 1.5	6781.01%	59.83%	238.62%	0.000	19.94%	3.32%	1.99%	0.000%	0.000	0.000%	1.26%	0.06%	0.61%	0.44%
KL1 1.6	7279.62%	73.13%	284.92%	0.000	23.27%	5.54%	2.33%	0.000%	0.000	0.000%	1.46%	0.06%	0.70%	0.44%
KL1 1.7	8177.10%	83.10%	327.65%	0.000	26.59%	5.54%	2.66%	0.003%	0.000	0.039%	2.95%	4.87%	0.90%	2.66%
KL1 1.8	9972.08%	129.64%	438.06%	0.000	43.21%	135.18%	7.98%	0.004%	0.000	0.078%	4.10%	7.89%	1.07%	3.57%
KL1 1.9	9972.08%	166.20%	576.96%	0.000	59.83%	173.96%	7.98%	0.005%	0.000	0.119%	4.98%	9.80%	1.23%	4.14%
KL1 1.10	9972.08%	212.74%	772.84%	0.000	76.45%	193.90%	7.98%	0.006%	0.000	0.163%	5.86%	11.71%	1.40%	4.65%
KL1 1.11	10670.12%	265.92%	1004.33%	0.000	93.07%	211.63%	7.98%	0.008%	0.000	0.204%	6.53%	13.02%	1.56%	5.04%
KL1 1.12	11069.01%	319.11%	1221.58%	0.000	109.69%	243.76%	7.98%	0.009%	0.000	0.245%	7.21%	14.25%	1.74%	5.44%
KL1 1.13	11467.89%	415.50%	1392.53%	0.000	126.31%	262.60%	7.98%	0.012%	0.000	0.285%	7.92%	15.78%	1.93%	5.89%

Experiment time	Cd	Ni	Co	Pb	Cr	Zn	Cu	Fe	Mn	Al	Ca	K	Mg	Na
	0.000	0.0000	0.0000	0.0000	0.0000	0.0000	0.0000	0.0000	0.0000	0.0000	0.0000	0.0000	0.0000	0.0000
W. I. - 0.0	0.000	0.00%	0.00%	15.31%	0.44%	1.93%	0.41%	0.02%	1.35%	0.50%	0.48%	0.31%	1.09%	1.30%
W. I. 1 1.1	0.000	0.00%	0.00%	65.63%	9.19%	18.10%	7.68%	0.62%	30.42%	14.06%	3.29%	1.66%	14.44%	11.82%
W. I. 1 1.2	0.000	0.00%	0.46%	126.88%	20.56%	37.35%	16.89%	1.36%	67.28%	30.30%	5.68%	2.76%	31.24%	24.15%
W. I. 1 1.3	0.000	0.00%	0.92%	185.94%	31.94%	56.21%	25.91%	2.03%	103.18%	47.16%	7.86%	4.29%	48.41%	36.26%
W. I. 1 1.4	0.000	0.00%	0.92%	236.25%	40.69%	72.77%	34.20%	2.60%	134.08%	61.12%	10.03%	5.21%	63.40%	62.29%
W. I. 1 1.5	0.000	0.42%	0.92%	258.13%	42.88%	78.54%	36.55%	2.78%	142.93%	64.83%	11.05%	6.23%	68.77%	66.79%
W. I. 1 1.6	0.000	0.42%	0.92%	273.44%	43.75%	80.85%	37.68%	2.86%	145.34%	65.72%	12.04%	6.82%	70.68%	68.18%
W. I. 1 1.7	0.000	0.42%	0.92%	323.75%	44.19%	85.47%	37.68%	2.86%	145.34%	65.72%	29.56%	10.98%	72.04%	69.25%
W. I. 1 1.8	0.000	0.42%	0.92%	343.44%	44.63%	88.94%	37.78%	3.36%	145.72%	66.71%	48.90%	14.36%	72.22%	69.49%
W. I. 1 1.9	0.000	0.42%	3.21%	365.31%	45.50%	92.40%	38.19%	3.73%	145.92%	67.33%	66.74%	16.39%	72.33%	69.58%
W. I. 1 1.10	0.000	0.63%	9.63%	365.31%	45.94%	94.71%	39.22%	4.08%	146.11%	67.83%	84.66%	18.40%	72.41%	69.63%
W. I. 1 1.11	0.000	0.63%	10.54%	365.31%	46.81%	97.02%	39.73%	4.35%	146.20%	68.15%	99.89%	20.08%	72.48%	69.68%

Appendix Four:

Cumulative concentrations flux (q) normalised to the geometric surface area. (mg/m$^{2/}$minute)

Experiment time	Cd	Ni	Co	Pb	Cr	Zn	Cu	Fe	Mn	Al	Ca	K	Mg	Na	F	Cl	SO_4^{2-}
	0.000	0.000	0.000	0.000	0.000	0.000	0.000	0.000	0.000	0.000	0.000	0.000	0.000	0.000	0.000	0.000	0.000
95/5 - L - 0.00	0.000	0.072	0.024	0.015	0.003	0.053	0.172	0.186	0.147	24.013	9.205	0.000	1.984	0.055	0.00003613	0.0882	0.0310
95/5 L 1 1 .1	0.000	0.011	0.000	0.011	0.002	0.022	0.049	0.094	0.031	4.389	17.673	0.000	0.450	0.000	0.00000000	0.0008	0.0005
95/5 L 1 1.2	0.000	0.005	0.000	0.011	0.001	0.016	0.027	0.059	0.016	2.244	15.964	0.000	0.238	0.000	0.00000252	0.0021	0.0021
95/5 L 1 1.3	0.000	0.004	0.000	0.012	0.001	0.013	0.020	0.045	0.011	1.544	15.039	0.000	0.170	0.000	0.00000128	0.0015	0.0012
95/5 L 1 1.4	0.000	0.003	0.000	0.012	0.000	0.012	0.017	0.037	0.009	1.208	13.468	0.000	0.138	0.000	0.00000126	0.0020	0.0010
95/5 L 1 1.5	0.000	0.002	0.000	0.011	0.000	0.011	0.013	0.032	0.007	0.949	12.137	0.000	0.113	0.000	0.00000098	0.0026	0.0009
95/5 L 1 1.6	0.000	0.002	0.000	0.011	0.000	0.011	0.012	0.029	0.006	0.813	11.571	0.000	0.100	0.000	0.00000135	0.0023	0.0007
95/5 L 1 1.7	0.000	0.000	0.000	0.003	0.000	0.003	0.003	0.017	0.002	0.214	5.310	0.001	0.029	0.023	0.00000010	0.0006	0.0001
95/5 L 1 1.8	0.000	0.000	0.000	0.002	0.000	0.002	0.002	0.022	0.001	0.112	2.971	0.002	0.015	0.027	0.00000003	0.0003	0.0000
95/5 L 1 1.9	0.000	0.000	0.000	0.001	0.000	0.001	0.002	0.022	0.001	0.076	2.002	0.002	0.011	0.024	0.00000002	0.0002	0.0000
95/5 L 1 1.10	0.000	0.000	0.000	0.001	0.000	0.001	0.001	0.023	0.001	0.060	1.521	0.004	0.008	0.025	0.00000001	0.0002	0.0000
95/5 L 1 1.11	0.000	0.000	0.000	0.001	0.000	0.001	0.001	0.023	0.000	0.049	1.218	0.003	0.007	0.020	0.00000001	0.0001	0.0000
95/5 L 1 1.12	0.000	0.000	0.000	0.001	0.000	0.001	0.001	0.023	0.000	0.042	1.024	0.004	0.006	0.020	0.00000001	0.0001	0.0000
95/5 L 1 1.13	0.000	0.000	0.000	0.001	0.000	0.001	0.001	0.023	0.000	0.037	0.883	0.004	0.005	0.019	0.00000001	0.0001	0.0000

Experiment time	Cd	Ni	Co	Pb	Cr	Zn	Cu	Fe	Mn	Al	Ca	K	Mg	Na	F	Cl	SO_4^{2-}
	0.000	0.000	0.000	0.000	0.000	0.000	0.000	0.000	0.000	0.000	0.000	0.000	0.000	0.000	0.000	0.000	0.000
95/5 - U - 0.0	0.000	0.049	0.011	0.014	0.002	0.038	0.123	0.052	0.119	11.332	8.778	0.000	1.739	0.013	0.004	0.136	1.4694
95/5 U 1 1.1	0.000	0.005	0.000	0.011	0.000	0.010	0.022	0.030	0.016	1.438	13.709	0.000	0.250	0.015	0.002	0.134	0.6761
95/5 U 1 1.2	0.000	0.003	0.000	0.012	0.000	0.009	0.014	0.022	0.010	0.859	9.469	0.000	0.156	0.009	0.001	0.149	0.5542
95/5 U 1 1.3	0.000	0.002	0.000	0.012	0.000	0.008	0.010	0.016	0.007	0.544	8.005	0.000	0.107	0.006	0.001	0.094	0.4113
95/5 U 1 1.4	0.000	0.002	0.000	0.011	0.000	0.007	0.007	0.013	0.005	0.409	6.856	0.000	0.086	0.004	0.001	0.071	0.3507
95/5 U 1 1.5	0.000	0.001	0.000	0.012	0.000	0.007	0.006	0.011	0.004	0.338	6.182	0.000	0.075	0.003	0.001	0.059	0.3151
95/5 U 1 1.6	0.000	0.001	0.000	0.012	0.000	0.006	0.005	0.010	0.003	0.281	5.451	0.000	0.065	0.003	0.001	0.049	0.2766
95/5 U 1 1.7	0.000	0.000	0.000	0.004	0.000	0.002	0.002	0.006	0.001	0.078	1.692	0.000	0.019	0.016	0.000	0.013	0.0923
95/5 U 1 1.8	0.000	0.000	0.000	0.002	0.000	0.001	0.001	0.007	0.001	0.048	0.861	0.002	0.010	0.020	0.000	0.006	0.0518
95/5 U 1 1.9	0.000	0.000	0.000	0.002	0.000	0.001	0.001	0.007	0.000	0.035	0.589	0.002	0.007	0.019	0.000	0.004	0.0376
95/5 U 1 1.10	0.000	0.000	0.000	0.001	0.000	0.001	0.001	0.007	0.000	0.027	0.453	0.003	0.006	0.017	0.000	0.003	0.0302
95/5 U 1 1.11	0.000	0.000	0.000	0.001	0.000	0.001	0.001	0.007	0.000	0.024	0.369	0.003	0.005	0.017	0.000	0.003	0.0259
95/5 U 1 1.12	0.000	0.000	0.000	0.001	0.000	0.001	0.001	0.007	0.000	0.021	0.319	0.004	0.004	0.016	0.000	0.002	0.0231
95/5 U 1 1.13	0.000	0.000	0.000	0.001	0.000	0.001	0.001	0.007	0.000	0.018	0.267	0.004	0.004	0.016	0.000	0.002	0.0204

Experiment time	Cd	Ni	Co	Pb	Cr	Zn	Cu	Fe	Mn	Al	Ca	K	Mg	Na	F	Cl	SO_4^{2-}
	0.000	0.000	0.000	0.000	0.000	0.000	0.000	0.000	0.000	0.00000	0.000	0.000	0.000	0.000	0.000	0.000	0.000
95/8 - 0.0	0.000	0.000	0.000	0.004	0.000	0.002	0.001	0.002	0.001	0.00000	0.571	0.000	0.019	0.056	0.00000	0.000	0.0011
95/8 1 1.1	0.000	0.000	0.000	0.003	0.000	0.003	0.001	0.002	0.003	0.00125	1.233	0.023	0.061	0.154	0.00000	0.000	0.0036
95/8 1 1.2	0.000	0.000	0.000	0.003	0.000	0.003	0.001	0.002	0.003	0.00117	1.138	0.017	0.056	0.123	0.00000	0.000	0.0031
95/8 1 1.3	0.000	0.000	0.000	0.003	0.000	0.003	0.001	0.003	0.003	0.00439	1.034	0.012	0.048	0.091	0.00000	0.000	0.0028
95/8 1 1.4	0.000	0.000	0.000	0.003	0.000	0.003	0.001	0.003	0.002	0.00327	0.938	0.009	0.040	0.067	0.00000	0.000	0.0025
95/8 1 1.5	0.000	0.000	0.000	0.003	0.000	0.003	0.001	0.003	0.002	0.00270	0.903	0.007	0.036	0.055	0.00000	0.000	0.0029
95/8 1 1.6	0.000	0.000	0.000	0.003	0.000	0.002	0.001	0.002	0.002	0.00222	0.852	0.006	0.032	0.045	0.00000	0.000	0.0026
95/8 1 1.7	0.000	0.000	0.000	0.001	0.000	0.001	0.000	0.001	0.000	0.00064	0.511	0.003	0.009	0.014	0.00000	0.000	0.0017
95/8 1 1.8	0.000	0.000	0.000	0.001	0.000	0.000	0.000	0.000	0.000	0.00032	0.361	0.002	0.005	0.007	0.00000	0.000	0.0013
95/8 1 1.9	0.000	0.000	0.000	0.000	0.000	0.000	0.000	0.000	0.000	0.00022	0.270	0.001	0.003	0.005	0.00000	0.000	0.0009
95/8 1 1.10	0.000	0.000	0.000	0.000	0.000	0.000	0.000	0.000	0.000	0.00016	0.210	0.001	0.003	0.004	0.00000	0.000	0.0007
95/8 1 1.11	0.000	0.000	0.000	0.000	0.000	0.000	0.000	0.000	0.000	0.00013	0.170	0.001	0.002	0.003	0.00000	0.000	0.0006
95/8 1 1.12	0.000	0.000	0.000	0.000	0.000	0.000	0.000	0.000	0.000	0.00011	0.143	0.001	0.002	0.003	0.00000	0.000	0.0005
95/8 1 1.13	0.000	0.000	0.000	0.000	0.000	0.000	0.000	0.000	0.000	0.00010	0.124	0.001	0.002	0.002	0.00000	0.000	0.0004

Experiment time	Cd	Ni	Co	Pb	Cr	Zn	Cu	Fe	Mn	Al	Ca	K	Mg	Na	F	Cl	SO_4^{2-}
	0.000	0.000	0.000	0.000	0.000	0.000	0.000	0.000	0.000	0.000	0.000	0.000	0.000	0.000	0.000	0.000	0.000
96/7 - 0.0	0.000	0.014	0.003	0.005	0.000	0.021	0.030	0.021	0.068	0.286	2.190	0.000	2.610	0.102	0.004	0.132	0.369
96/7 1 1.1	0.000	0.006	0.000	0.004	0.000	0.012	0.016	0.014	0.037	0.119	2.735	0.000	1.258	0.093	0.002	0.061	0.263
96/7 1 1.2	0.000	0.004	0.000	0.003	0.000	0.009	0.012	0.011	0.026	0.079	2.353	0.000	0.896	0.064	0.002	0.041	0.211
96/7 1 1.3	0.000	0.003	0.000	0.003	0.000	0.008	0.010	0.010	0.021	0.061	2.186	0.000	0.721	0.053	0.002	0.032	0.186
96/7 1 1.4	0.000	0.002	0.000	0.004	0.000	0.007	0.008	0.009	0.018	0.052	2.103	0.000	0.625	0.045	0.001	0.027	0.172
96/7 1 1.5	0.000	0.002	0.000	0.003	0.000	0.006	0.007	0.008	0.015	0.042	1.882	0.000	0.511	0.037	0.001	0.022	0.149
96/7 1 1.6	0.000	0.001	0.000	0.003	0.000	0.005	0.006	0.007	0.013	0.036	1.801	0.000	0.446	0.032	0.001	0.019	0.138
96/7 1 1.7	0.000	0.000	0.000	0.001	0.000	0.002	0.002	0.005	0.004	0.012	1.036	0.000	0.121	0.018	0.000	0.005	0.060
96/7 1 1.8	0.000	0.000	0.000	0.001	0.000	0.001	0.001	0.006	0.002	0.008	0.768	0.000	0.064	0.013	0.000	0.003	0.042
96/7 1 1.9	0.000	0.000	0.000	0.000	0.000	0.001	0.001	0.006	0.001	0.006	0.607	0.001	0.043	0.011	0.000	0.002	0.034
96/7 1 1.10	0.000	0.000	0.000	0.000	0.000	0.000	0.001	0.005	0.001	0.005	0.509	0.002	0.033	0.009	0.000	0.001	0.028
96/7 1 1.11	0.000	0.000	0.000	0.000	0.000	0.000	0.001	0.005	0.001	0.004	0.440	0.004	0.026	0.008	0.000	0.001	0.025
96/7 1 1.12	0.000	0.000	0.000	0.000	0.000	0.000	0.000	0.005	0.001	0.004	0.389	0.005	0.022	0.008	0.000	0.001	0.021
96/7 1 1.13	0.000	0.000	0.000	0.000	0.000	0.000	0.000	0.005	0.001	0.003	0.346	0.006	0.019	0.007	0.000	0.001	0.018

Experiment time	Cd	Ni	Co	Pb	Cr	Zn	Cu	Fe	Mn	Al	Ca	K	Mg	Na	F	Cl	SO_4^{2-}
	0.000	0.000	0.000	0.000	0.000	0.000	0.000	0.000	0.000	0.000	0.000	0.000	0.000	0.000	0.000	0.000	0.000
96/46 - 0.0	0.000	0.002	0.004	0.000	0.000	0.002	0.001	0.000	0.003	0.000	0.370	0.000	0.102	0.081	0.000	0.000	0.00089
96/46 1 1.1	0.000	0.002	0.004	0.000	0.000	0.001	0.001	0.000	0.001	0.000	0.269	0.000	0.036	0.010	0.000	0.000	0.00037
96/46 1 1.2	0.000	0.002	0.004	0.000	0.000	0.001	0.001	0.000	0.001	0.000	0.260	0.000	0.030	0.005	0.000	0.001	0.00440
96/46 1 1.3	0.000	0.002	0.004	0.000	0.000	0.001	0.001	0.000	0.001	0.000	0.251	0.000	0.026	0.003	0.000	0.001	0.00534
96/46 1 1.4	0.001	0.002	0.004	0.000	0.000	0.001	0.001	0.000	0.001	0.000	0.237	0.000	0.023	0.002	0.000	0.001	0.00539

96/46 1 1.5	0.001	0.002	0.004	0.000	0.000	0.001	0.001	0.000	0.001	0.000	0.229	0.000	0.021	0.002	0.000	0.001	0.00533
96/46 1 1.6	0.001	0.002	0.004	0.000	0.000	0.001	0.001	0.000	0.000	0.000	0.219	0.000	0.019	0.002	0.000	0.001	0.00511
96/46 1 1.7	0.001	0.000	0.001	0.000	0.000	0.000	0.000	0.000	0.000	0.000	0.092	0.000	0.008	0.002	0.000	0.000	0.00327
96/46 1 1.8	0.000	0.000	0.001	0.000	0.000	0.000	0.000	0.000	0.000	0.000	0.058	0.000	0.005	0.001	0.000	0.000	0.00223
96/46 1 1.9	0.000	0.000	0.000	0.000	0.000	0.000	0.000	0.000	0.000	0.000	0.042	0.000	0.003	0.001	0.000	0.000	0.00162
96/46 1 1.10	0.000	0.000	0.000	0.000	0.000	0.000	0.000	0.000	0.000	0.000	0.034	0.000	0.002	0.000	0.000	0.000	0.00128
96/46 1 1.11	0.000	0.000	0.000	0.000	0.000	0.000	0.000	0.000	0.000	0.000	0.029	0.000	0.002	0.000	0.000	0.000	0.00109
96/46 1 1.12	0.000	0.000	0.000	0.000	0.000	0.000	0.000	0.000	0.000	0.000	0.025	0.000	0.002	0.000	0.000	0.000	0.00094
96/46 1 1.13	0.000	0.000	0.000	0.000	0.000	0.000	0.000	0.000	0.000	0.000	0.023	0.000	0.001	0.000	0.000	0.000	0.00084

Experiment time	Cd	Ni	Co	Pb	Cr	Zn	Cu	Fe	Mn	Al	Ca	K	Mg	Na	F	Cl	SO_4^{2-}
	0.000	0.000	0.000	0.000	0.000	0.000	0.000	0.000	0.000	0.000	0.000	0.000	0.000	0.000	0.000	0.000	0.000
Ruw - 0.0	0.000	0.000	0.000	0.008	0.000	0.000	0.000	0.000	0.000	0.000	0.595	0.000	0.012	0.124	0.000	0.0047	0.0111
Ruw 1 1.1	0.000	0.000	0.000	0.009	0.000	0.000	0.000	0.000	0.000	0.000	0.664	0.000	0.009	0.094	0.000	0.0047	0.0098
Ruw 1 1.2	0.000	0.000	0.000	0.008	0.000	0.001	0.000	0.000	0.000	0.000	0.605	0.000	0.007	0.051	0.000	0.1919	0.0064
Ruw 1 1.3	0.000	0.000	0.000	0.008	0.000	0.001	0.000	0.000	0.000	0.000	0.608	0.000	0.007	0.034	0.000	0.1302	0.0051
Ruw 1 1.4	0.000	0.000	0.000	0.009	0.000	0.001	0.000	0.000	0.000	0.000	0.659	0.000	0.008	0.028	0.000	0.1310	0.0045
Ruw 1 1.5	0.000	0.000	0.000	0.009	0.000	0.001	0.000	0.000	0.000	0.000	0.656	0.000	0.008	0.022	0.000	0.1056	0.0039
Ruw 1 1.6	0.000	0.000	0.000	0.008	0.000	0.001	0.000	0.000	0.000	0.000	0.641	0.000	0.008	0.018	0.000	0.0866	0.0034
Ruw 1 1.7	0.000	0.000	0.000	0.002	0.000	0.000	0.000	0.000	0.000	0.000	0.190	0.000	0.003	0.005	0.000	0.0218	0.0014
Ruw 1 1.8	0.000	0.000	0.000	0.001	0.000	0.000	0.000	0.000	0.000	0.000	0.113	0.000	0.002	0.003	0.000	0.0113	0.0009
Ruw 1 1.9	0.000	0.000	0.000	0.001	0.000	0.000	0.000	0.000	0.000	0.000	0.084	0.000	0.001	0.002	0.000	0.0075	0.0007
Ruw 1 1.10	0.000	0.000	0.000	0.001	0.000	0.000	0.000	0.000	0.000	0.000	0.071	0.000	0.001	0.002	0.000	0.0057	0.0006
Ruw 1 1.11	0.000	0.000	0.000	0.001	0.000	0.000	0.000	0.000	0.000	0.000	0.062	0.000	0.001	0.001	0.000	0.0046	0.0005
Ruw 1 1.12	0.000	0.000	0.000	0.001	0.000	0.000	0.000	0.000	0.000	0.000	0.056	0.000	0.001	0.001	0.000	0.0038	0.0004
Ruw 1 1.13	0.000	0.000	0.000	0.001	0.000	0.000	0.000	0.000	0.000	0.000	0.052	0.000	0.001	0.001	0.000	0.0033	0.0004

Experiment time	Cd	Ni	Co	Pb	Cr	Zn	Cu	Fe	Mn	Al	Ca	K	Mg	Na	F	Cl	SO_4^{2-}
	0.000	0.000	0.000	0.000	0.000	0.000	0.000	0.000	0.000	0.000	0.000	0.000	0.000	0.000	0.000	0.000	0.000
SK1 - 0.0	30.485	0.000	0.000	0.045	0.000	0.098	0.015	0.000	0.000	0.008	3.117	0.008	0.053	0.625	0.0014	0.028	0.299
SK1 1.1	26.588	0.000	0.000	0.042	0.000	0.049	0.007	0.000	0.007	0.007	6.906	0.212	0.268	1.158	0.0096	0.155	0.325
SK1 1.2	27.616	0.000	0.000	0.041	0.000	0.041	0.004	0.000	0.004	0.011	5.377	0.112	0.179	0.901	0.0075	0.094	0.217
SK1 1.3	28.710	0.000	0.000	0.038	0.000	0.029	0.002	0.000	0.002	0.007	4.405	0.072	0.132	0.715	0.0059	0.064	0.153
SK1 1.4	40.142	0.000	0.000	0.028	0.000	0.016	0.001	0.000	0.001	0.004	3.001	0.040	0.084	0.472	0.0046	0.039	0.096
SK1 1.5	48.718	0.000	0.000	0.024	0.000	0.013	0.001	0.000	0.001	0.003	2.456	0.028	0.064	0.376	0.0038	0.028	0.071
SK1 1.6	57.992	0.000	0.000	0.020	0.000	0.010	0.001	0.000	0.001	0.002	1.978	0.019	0.049	0.296	0.0032	0.021	0.052
SK1 1.7	80.280	0.000	0.000	0.015	0.000	0.007	0.000	0.000	0.000	0.002	1.413	0.012	0.034	0.210	0.0025	0.014	0.035
SK1 1.8	298.256	0.000	0.000	0.004	0.000	0.002	0.000	0.000	0.000	0.001	0.393	0.003	0.009	0.059	0.0011	0.004	0.009
SK1 1.9	557.386	0.000	0.000	0.002	0.000	0.001	0.000	0.000	0.000	0.001	0.217	0.002	0.005	0.034	0.0008	0.002	0.005
SK1 1.10	813.517	0.000	0.000	0.002	0.000	0.001	0.000	0.000	0.000	0.001	0.158	0.001	0.004	0.025	0.0006	0.002	0.003
SK1 1.11	1073.59	0.000	0.000	0.001	0.000	0.000	0.000	0.000	0.000	0.000	0.128	0.001	0.003	0.020	0.0005	0.001	0.003

SK1 1.12	1342.0	0.000	0.000	0.001	0.000	0.000	0.000	0.000	0.000	0.000	0.110	0.001	0.002	0.017	0.0005	0.001	0.002
SK1 1.13	1611.14	0.000	0.000	0.001	0.000	0.000	0.000	0.000	0.000	0.000	0.098	0.000	0.002	0.015	0.0004	0.001	0.002
SK1 1.14	1877.30	0.000	0.000	0.001	0.000	0.000	0.000	0.000	0.000	0.000	0.090	0.000	0.002	0.014	0.0004	0.001	0.002

Experiment time	Cd	Ni	Co	Pb	Cr	Zn	Cu	Fe	Mn	Al	Ca	K	Mg	Na	F	Cl	SO_4^{2-}
	0.000	0.000	0.000	0.000	0.000	0.000	0.000	0.000	0.000	0.000	0.000	0.000	0.000	0.000	0.000	0.000	0.000
KL1 - 0.0	0.0078	0.0017	0.0061	0.000	0.0006	0.0000	0.0006	0.0000	0.000	0.0000	0.2747	0.0000	0.0078	0.0357	0.000	0.005	0.006
KL1 1.1	0.0044	0.0012	0.0044	0.000	0.0004	0.0004	0.0004	0.0000	0.000	0.0000	0.2963	0.0008	0.0064	0.0212	0.000	0.015	0.007
KL1 1.2	0.0047	0.0012	0.0045	0.000	0.0004	0.0006	0.0004	0.0000	0.000	0.0000	0.2817	0.0004	0.0055	0.0127	0.000	0.008	0.007
KL1 1.3	0.0050	0.0013	0.0048	0.000	0.0004	0.0004	0.0004	0.0000	0.000	0.0000	0.2725	0.0003	0.0050	0.0089	0.000	0.005	0.006
KL1 1.4	0.0046	0.0012	0.0045	0.000	0.0004	0.0003	0.0004	0.0000	0.000	0.0000	0.2549	0.0002	0.0046	0.0075	0.000	0.004	0.005
KL1 1.5	0.0044	0.0012	0.0046	0.000	0.0004	0.0002	0.0004	0.0000	0.000	0.0000	0.2492	0.0002	0.0044	0.0060	0.000	0.003	0.005
KL1 1.6	0.0041	0.0013	0.0047	0.000	0.0004	0.0003	0.0004	0.0000	0.000	0.0000	0.2474	0.0001	0.0044	0.0050	0.000	0.003	0.005
KL1 1.7	0.0012	0.0004	0.0014	0.000	0.0001	0.0001	0.0001	0.0001	0.000	0.0019	0.1376	0.0030	0.0015	0.0135	0.000	0.001	0.003
KL1 1.8	0.0008	0.0003	0.0010	0.000	0.0001	0.0011	0.0002	0.0000	0.000	0.0019	0.0980	0.0025	0.0009	0.0093	0.000	0.000	0.002
KL1 1.9	0.0005	0.0003	0.0009	0.000	0.0001	0.0009	0.0001	0.0000	0.000	0.0019	0.0796	0.0020	0.0007	0.0072	0.000	0.000	0.001
KL1 1.10	0.0004	0.0003	0.0009	0.000	0.0001	0.0008	0.0001	0.0000	0.000	0.0020	0.0707	0.0018	0.0006	0.0061	0.000	0.000	0.001
KL1 1.11	0.0003	0.0003	0.0010	0.000	0.0001	0.0007	0.0001	0.0000	0.000	0.0020	0.0635	0.0016	0.0006	0.0053	0.000	0.000	0.001
KL1 1.12	0.0003	0.0003	0.0010	0.000	0.0001	0.0007	0.0001	0.0000	0.000	0.0020	0.0585	0.0015	0.0005	0.0048	0.000	0.000	0.001
KL1 1.13	0.0003	0.0003	0.0010	0.000	0.0001	0.0006	0.0001	0.0000	0.000	0.0020	0.0551	0.0014	0.0005	0.0045	0.000	0.000	0.001

Experiment time	Cd	Ni	Co	Pb	Cr	Zn	Cu	Fe	Mn	Al	Ca	K	Mg	Na	F	Cl	SO_4^{2-}
	0.0	0.000	0.000	0.000	0.000	0.000	0.000	0.000	0.000	0.000	0.000	0.000	0.000	0.000	0.000	0.000	0.000
W. I. - 0.0	0.0	0.0000	0.0000	0.0038	0.0005	0.0027	0.0022	0.0240	0.0076	0.1394	1.0970	0.0272	0.1912	0.5213	0.000	0.0052	0.0017
W. I. 1 1.1	0.0	0.0000	0.0000	0.0111	0.0096	0.0202	0.0341	0.5439	0.1452	3.3186	5.6071	0.1058	2.0678	3.7317	0.001	0.0778	0.0108
W. I. 1 1.2	0.0	0.0000	0.0003	0.0137	0.0124	0.0248	0.0434	0.6821	0.1845	4.0854	5.8139	0.1077	2.6148	4.5402	0.002	0.0924	0.0114
W. I. 1 1.3	0.0	0.0000	0.0004	0.0139	0.0129	0.0252	0.0445	0.6809	0.1891	4.2459	5.4790	0.1162	2.7243	4.6102	0.002	0.0907	0.0108
W. I. 1 1.4	0.0	0.0000	0.0003	0.0132	0.0121	0.0241	0.0433	0.6427	0.1808	4.0454	5.1973	0.1049	2.6308	5.8973	0.002	0.0825	0.0100
W. I. 1 1.5	0.0	0.0002	0.0002	0.0119	0.0104	0.0213	0.0379	0.5631	0.1578	3.5121	4.7076	0.1037	2.3378	5.1811	0.001	0.0726	0.0094
W. I. 1 1.6	0.0	0.0002	0.0002	0.0108	0.0091	0.0188	0.0333	0.4941	0.1369	3.0384	4.3952	0.0973	2.0509	4.5147	0.003	0.0989	0.0287
W. I. 1 1.7	0.0	0.0000	0.0000	0.0033	0.0023	0.0050	0.0084	0.1246	0.0345	0.7663	2.7883	0.0402	0.5274	1.1568	0.001	0.0252	0.0126
W. I. 1 1.8	0.0	0.0000	0.0000	0.0017	0.0011	0.0025	0.0041	0.0712	0.0168	0.3782	2.2577	0.0257	0.2571	0.5645	0.000	0.0123	0.0083
W. I. 1 1.9	0.000	0.0000	0.0001	0.0012	0.0008	0.0018	0.0028	0.0527	0.0112	0.2544	2.0585	0.0196	0.1715	0.3766	0.000	0.0082	0.0073
W. I. 1 1.10	0.0	0.0000	0.0001	0.0009	0.0006	0.0013	0.0021	0.0431	0.0084	0.1913	1.9525	0.0165	0.1282	0.2814	0.000	0.0061	0.0063
W. I. 1 1.11	0.0	0.0000	0.0001	0.0007	0.0005	0.0011	0.0017	0.0370	0.0068	0.1547	1.8562	0.0145	0.1033	0.2267	0.000	0.0049	0.0086

Appendix Five:

Cumulative flux (q) non-normalised.

Experiment time	Cd	Ni	Co	Pb	Cr	Zn	Cu	Fe	Mn	Al	Ca	K	Mg	Na	F	Cl	SO_4^{2-}
	0.00	0.000	0.000	0.000	0.000	0.000	0.000	0.000	0.000	0.000	0.000	0.000	0.000	0.000	0.000	0.000	0.000
95/5 - L - 0.00	0.00	0.070	0.023	0.015	0.003	0.052	0.169	0.182	0.144	23.540	9.023	0.054	1.945	0.054	3.54131E-05	0.086507918	0.030422106
95/5 L 1 1 .1	0.00	0.011	0.000	0.011	0.002	0.022	0.048	0.092	0.031	4.303	17.324	0.000	0.441	0.000	0.000000000	0.000800457	0.000443964
95/5 L 1 1.2	0.00	0.005	0.000	0.011	0.001	0.016	0.027	0.058	0.016	2.200	15.649	0.000	0.233	0.000	0.000002467	0.002041958	0.002092418
95/5 L 1 1.3	0.00	0.004	0.000	0.012	0.001	0.013	0.020	0.045	0.011	1.513	14.743	0.000	0.166	0.000	0.000001256	0.001491472	0.001193054
95/5 L 1 1.4	0.00	0.003	0.000	0.011	0.000	0.012	0.016	0.037	0.009	1.184	13.203	0.000	0.135	0.000	0.000001240	0.002004315	0.001029008
95/5 L 1 1.5	0.00	0.002	0.000	0.011	0.000	0.011	0.013	0.031	0.007	0.930	11.898	0.000	0.111	0.000	0.000000962	0.002576574	0.000869798
95/5 L 1 1.6	0.00	0.002	0.000	0.011	0.000	0.010	0.011	0.028	0.006	0.797	11.343	0.000	0.098	0.000	0.000001320	0.002222159	0.000656153
95/5 L 1 1.7	0.00	0.000	0.000	0.003	0.000	0.003	0.003	0.016	0.002	0.210	5.205	0.023	0.028	0.023	0.000000101	0.000582144	5.29319E-05
95/5 L 1 1.8	0.00	0.000	0.000	0.002	0.000	0.002	0.002	0.022	0.001	0.109	2.913	0.027	0.015	0.027	0.000000027	0.00029303	1.37343E-05
95/5 L 1 1.9	0.00	0.000	0.000	0.001	0.000	0.001	0.002	0.021	0.001	0.075	1.963	0.024	0.010	0.024	0.000000021	0.000233406	6.86809E-06
95/5 L 1 1.10	0.00	0.000	0.000	0.001	0.000	0.001	0.001	0.023	0.001	0.059	1.491	0.024	0.008	0.024	0.000000012	0.000177412	3.94448E-06
95/5 L 1 1.11	0.00	0.000	0.000	0.001	0.000	0.001	0.001	0.023	0.000	0.048	1.194	0.020	0.007	0.020	0.000000008	0.000142534	2.51683E-06
95/5 L 1 1.12	0.00	0.000	0.000	0.001	0.000	0.001	0.001	0.023	0.000	0.042	1.004	0.019	0.006	0.019	0.000000007	0.000132328	1.92741E-06
95/5 L 1 1.13	0.00	0.000	0.000	0.001	0.000	0.001	0.001	0.023	0.000	0.036	0.865	0.019	0.005	0.019	0.000000005	0.000113538	1.4248E-06

Experiment time	Cd	Ni	Co	Pb	Cr	Zn	Cu	Fe	Mn	Al	Ca	K	Mg	Na	F	Cl	SO_4^{2-}
	0.000	0.000	0.000	0.000	0.000	0.000	0.000	0.000	0.000	0.000	0.000	0.000	0.000	0.000	0.000000	0.00000	0.000
95/5 - U - 0.0	0.000	0.048	0.011	0.014	0.002	0.037	0.121	0.052	0.117	11.161	8.645	0.000	1.713	0.012	0.003470	0.13364	0.00000
95/5 U 1 1.1	0.000	0.005	0.000	0.011	0.000	0.009	0.022	0.030	0.016	1.417	13.502	0.000	0.246	0.015	0.001531	0.13243	1.44722
95/5 U 1 1.2	0.000	0.003	0.000	0.012	0.000	0.009	0.013	0.021	0.010	0.846	9.326	0.000	0.154	0.009	0.001123	0.14687	0.66593
95/5 U 1 1.3	0.000	0.002	0.000	0.011	0.000	0.007	0.009	0.016	0.006	0.535	7.885	0.000	0.105	0.005	0.000808	0.09267	0.54588
95/5 U 1 1.4	0.000	0.001	0.000	0.011	0.000	0.007	0.007	0.013	0.005	0.403	6.752	0.000	0.085	0.004	0.000778	0.07027	0.40505
95/5 U 1 1.5	0.000	0.001	0.000	0.011	0.000	0.007	0.006	0.011	0.004	0.333	6.089	0.000	0.074	0.003	0.000714	0.05850	0.34543
95/5 U 1 1.6	0.000	0.001	0.000	0.012	0.000	0.006	0.005	0.010	0.003	0.277	5.369	0.000	0.064	0.003	0.000646	0.04873	0.31032
95/5 U 1 1.7	0.000	0.000	0.000	0.004	0.000	0.002	0.002	0.006	0.001	0.077	1.666	0.000	0.019	0.016	0.000346	0.01258	0.27247
95/5 U 1 1.8	0.000	0.000	0.000	0.002	0.000	0.001	0.001	0.007	0.001	0.047	0.848	0.002	0.010	0.020	0.000305	0.00636	0.09087
95/5 U 1 1.9	0.000	0.000	0.000	0.001	0.000	0.001	0.001	0.007	0.000	0.034	0.580	0.002	0.007	0.018	0.000260	0.00431	0.05101
95/5 U 1 1.10	0.000	0.000	0.000	0.001	0.000	0.001	0.001	0.006	0.000	0.027	0.447	0.002	0.006	0.017	0.000223	0.00330	0.03703
95/5 U 1 1.11	0.000	0.000	0.000	0.001	0.000	0.001	0.001	0.006	0.000	0.023	0.363	0.003	0.005	0.017	0.000199	0.00266	0.02974
95/5 U 1 1.12	0.000	0.000	0.000	0.001	0.000	0.001	0.001	0.007	0.000	0.021	0.314	0.004	0.004	0.016	0.000181	0.00229	0.02548

95/5 U 1 1.13	0.000	0.000	0.000	0.001	0.000	0.001	0.001	0.007	0.000	0.018	0.263	0.004	0.004	0.016	0.000162	0.00191	0.02278

Experiment time	Cd	Ni	Co	Pb	Cr	Zn	Cu	Fe	Mn	Al	Ca	K	Mg	Na	F	Cl	SO_4^{2-}
	0.000	0.000	0.000	0.000	0.000	0.000	0.000	0.000	0.000	0.000	0.000	0.000	0.000	0.000	0.00000000	0.000	0.000
95/8 - 0.0	0.000	0.000	0.000	0.013	0.000	0.006	0.002	0.008	0.002	0.000	1.953	0.000	0.063	0.190	0.00000000	0.000332597	0.003867035
95/8 1 1.1	0.000	0.000	0.000	0.010	0.000	0.010	0.004	0.006	0.010	0.004	4.216	0.078	0.207	0.527	0.00000000	0.000816305	0.012421009
95/8 1 1.2	0.000	0.000	0.000	0.011	0.000	0.011	0.005	0.007	0.010	0.004	3.891	0.057	0.193	0.419	0.00000000	0.000663796	0.01075535
95/8 1 1.3	0.000	0.000	0.000	0.011	0.000	0.011	0.004	0.010	0.009	0.015	3.535	0.041	0.164	0.312	0.00000000	0.000522883	0.009535191
95/8 1 1.4	0.000	0.000	0.000	0.011	0.000	0.009	0.004	0.009	0.007	0.011	3.207	0.029	0.138	0.229	0.00000000	0.000423374	0.008700735
95/8 1 1.5	0.000	0.000	0.000	0.011	0.000	0.009	0.004	0.009	0.006	0.009	3.086	0.024	0.123	0.189	0.00000000	0.00039526	0.009815617
95/8 1 1.6	0.000	0.000	0.000	0.011	0.000	0.008	0.003	0.008	0.005	0.008	2.912	0.020	0.108	0.155	0.00000000	0.000343736	0.008988361
95/8 1 1.7	0.000	0.000	0.000	0.003	0.000	0.003	0.002	0.002	0.002	0.002	1.746	0.009	0.032	0.047	0.00000565	9.52895E-05	0.005686287
95/8 1 1.8	0.000	0.000	0.000	0.002	0.000	0.001	0.001	0.001	0.001	0.001	1.233	0.006	0.017	0.025	0.00000590	5.04958E-05	0.004289039
95/8 1 1.9	0.000	0.000	0.000	0.002	0.000	0.001	0.001	0.001	0.001	0.001	0.922	0.005	0.012	0.017	0.00000554	3.36444E-05	0.003161443
95/8 1 1.10	0.000	0.000	0.000	0.001	0.000	0.001	0.001	0.001	0.000	0.001	0.717	0.004	0.009	0.013	0.00000415	2.67717E-05	0.002424519
95/8 1 1.11	0.000	0.000	0.000	0.001	0.000	0.001	0.000	0.001	0.000	0.000	0.580	0.003	0.007	0.010	0.00000332	2.13988E-05	0.001949979
95/8 1 1.12	0.000	0.000	0.000	0.001	0.000	0.001	0.000	0.001	0.000	0.000	0.489	0.003	0.006	0.009	0.00000277	1.78406E-05	0.001631177
95/8 1 1.13	0.000	0.000	0.000	0.001	0.000	0.001	0.000	0.001	0.000	0.000	0.423	0.002	0.005	0.007	0.00000238	1.53076E-05	0.00140345

Experiment time	Cd	Ni	Co	Pb	Cr	Zn	Cu	Fe	Mn	Al	Ca	K	Mg	Na	F	Cl	SO_4^{2-}
	0.000	0.000	0.000	0.000	0.000	0.000	0.000	0.000	0.000	0.000	0.000	0.000	0.000	0.000	0.000000	0.000000	0.000
96/7 - 0.0	0.000	0.041	0.007	0.015	0.000	0.060	0.086	0.060	0.196	0.827	6.332	0.000	7.547	0.295	0.011469	0.381952	1.0670978
96/7 1 1.1	0.000	0.017	0.000	0.011	0.000	0.033	0.047	0.041	0.106	0.343	7.909	0.000	3.637	0.270	0.006638	0.175282	0.7604218
96/7 1 1.2	0.000	0.011	0.000	0.010	0.000	0.026	0.034	0.033	0.075	0.230	6.802	0.000	2.592	0.186	0.005138	0.119593	0.6095819
96/7 1 1.3	0.000	0.008	0.000	0.010	0.000	0.022	0.028	0.029	0.060	0.177	6.321	0.000	2.084	0.153	0.004393	0.091355	0.5392017
96/7 1 1.4	0.000	0.006	0.000	0.010	0.000	0.020	0.024	0.027	0.052	0.149	6.081	0.000	1.807	0.131	0.003997	0.077997	0.4974085
96/7 1 1.5	0.000	0.005	0.000	0.010	0.000	0.017	0.020	0.023	0.042	0.120	5.441	0.000	1.478	0.107	0.003428	0.062918	0.4310835
96/7 1 1.6	0.000	0.004	0.000	0.010	0.000	0.015	0.017	0.021	0.037	0.104	5.206	0.000	1.289	0.093	0.003123	0.054273	0.3984817
96/7 1 1.7	0.000	0.001	0.000	0.003	0.000	0.004	0.006	0.016	0.011	0.034	2.996	0.000	0.350	0.051	0.001238	0.013944	0.1745515
96/7 1 1.8	0.000	0.001	0.000	0.002	0.000	0.002	0.003	0.017	0.006	0.022	2.220	0.001	0.186	0.039	0.000930	0.007498	0.1228593
96/7 1 1.9	0.000	0.000	0.000	0.001	0.000	0.002	0.002	0.017	0.004	0.017	1.755	0.001	0.124	0.032	0.000763	0.005027	0.0968668
96/7 1 1.10	0.000	0.000	0.000	0.001	0.000	0.001	0.002	0.016	0.003	0.014	1.471	0.002	0.095	0.027	0.000658	0.003876	0.0822545
96/7 1 1.11	0.000	0.000	0.000	0.001	0.000	0.001	0.002	0.015	0.003	0.012	1.271	0.002	0.076	0.024	0.000584	0.003122	0.0714004
96/7 1 1.12	0.000	0.000	0.000	0.001	0.000	0.001	0.001	0.016	0.002	0.011	1.125	0.002	0.064	0.022	0.000491	0.002618	0.0600230
96/7 1 1.13	0.000	0.000	0.000	0.001	0.000	0.001	0.001	0.015	0.002	0.010	0.999	0.002	0.055	0.020	0.000421	0.002236	0.0513563

Experiment time	Cd	Ni	Co	Pb	Cr	Zn	Cu	Fe	Mn	Al	Ca	K	Mg	Na	F	Cl	SO_4^{2-}
	0.000	0.000	0.000	0.000	0.000	0.000	0.000	0.000	0.000	0.000	0.000	0.000	0.000	0.000	0.0000000	0.0000000	0.000
96/46 - 0.0	0.000	0.010	0.016	0.000	0.002	0.008	0.004	0.000	0.014	0.000	1.521	0.000	0.419	0.335	0.0000000	0.0010385	0.0036740

96/46 1 1.1	0.000	0.007	0.015	0.000	0.002	0.005	0.003	0.000	0.003	0.002	1.107	0.000	0.147	0.040	0.0000000	0.0003140	0.0015363
96/46 1 1.2	0.000	0.007	0.015	0.000	0.002	0.003	0.003	0.001	0.003	0.002	1.071	0.000	0.124	0.020	0.0002777	0.0035451	0.0180918
96/46 1 1.3	0.001	0.007	0.015	0.000	0.002	0.003	0.003	0.001	0.003	0.002	1.034	0.000	0.108	0.013	0.0003568	0.0039164	0.0219701
96/46 1 1.4	0.002	0.006	0.015	0.000	0.002	0.002	0.003	0.001	0.002	0.001	0.973	0.000	0.094	0.010	0.0003846	0.0052600	0.0221786
96/46 1 1.5	0.004	0.006	0.015	0.000	0.002	0.002	0.003	0.001	0.002	0.001	0.941	0.000	0.084	0.008	0.0003787	0.0048080	0.0219206
96/46 1 1.6	0.005	0.006	0.015	0.000	0.002	0.003	0.003	0.001	0.002	0.001	0.902	0.000	0.076	0.006	0.0004470	0.0043245	0.0210084
96/46 1 1.7	0.002	0.002	0.005	0.000	0.000	0.001	0.001	0.001	0.001	0.001	0.380	0.000	0.033	0.006	0.0002268	0.0014555	0.0134590
96/46 1 1.8	0.001	0.001	0.003	0.000	0.000	0.001	0.001	0.000	0.001	0.001	0.240	0.000	0.019	0.004	0.0001620	0.0007819	0.0091899
96/46 1 1.9	0.001	0.001	0.002	0.000	0.000	0.001	0.001	0.000	0.000	0.001	0.172	0.000	0.013	0.003	0.0001314	0.0005521	0.0066464
96/46 1 1.10	0.001	0.001	0.002	0.000	0.000	0.001	0.001	0.000	0.000	0.000	0.138	0.000	0.010	0.002	0.0001130	0.0004487	0.0052590
96/46 1 1.11	0.001	0.001	0.002	0.000	0.000	0.001	0.000	0.000	0.000	0.000	0.119	0.000	0.008	0.002	0.0001079	0.0003865	0.0044708
96/46 1 1.12	0.001	0.001	0.001	0.000	0.000	0.000	0.000	0.000	0.000	0.000	0.104	0.000	0.007	0.001	0.0001040	0.0003363	0.0038756
96/46 1 1.13	0.001	0.001	0.001	0.000	0.000	0.000	0.000	0.000	0.000	0.000	0.093	0.000	0.006	0.001	0.0001023	0.0002994	0.0034676

Experiment time	Cd	Ni	Co	Pb	Cr	Zn	Cu	Fe	Mn	Al	Ca	K	Mg	Na	F	Cl	SO_4^{2-}
	0.000	0.000	0.000	0.000	0.000	0.000	0.00	0.00	0.00	0.00	0.000	0.00	0.000	0.000	0.00	0.000000	0.000
Ruw - 0.0	0.000	0.000	0.000	0.007	0.000	0.000	0.00	0.00	0.00	0.00	0.563	0.00	0.011	0.117	0.00	0.004468	0.01052351
Ruw 1 1.1	0.000	0.000	0.000	0.008	0.000	0.000	0.00	0.00	0.00	0.00	0.628	0.00	0.008	0.089	0.00	0.004414	0.009289817
Ruw 1 1.2	0.000	0.000	0.000	0.007	0.000	0.001	0.00	0.00	0.00	0.00	0.572	0.00	0.007	0.048	0.00	0.181450	0.006007672
Ruw 1 1.3	0.000	0.000	0.000	0.008	0.000	0.001	0.00	0.00	0.00	0.00	0.575	0.00	0.007	0.032	0.00	0.123088	0.004797854
Ruw 1 1.4	0.000	0.000	0.000	0.011	0.000	0.002	0.00	0.00	0.00	0.00	0.623	0.00	0.008	0.026	0.00	0.123902	0.00423114
Ruw 1 1.5	0.000	0.000	0.000	0.008	0.000	0.001	0.00	0.00	0.00	0.00	0.620	0.00	0.008	0.021	0.00	0.099878	0.003682059
Ruw 1 1.6	0.000	0.000	0.000	0.006	0.000	0.000	0.00	0.00	0.00	0.00	0.607	0.00	0.008	0.017	0.00	0.081875	0.003227369
Ruw 1 1.7	0.000	0.000	0.000	0.002	0.000	0.000	0.00	0.00	0.00	0.00	0.180	0.00	0.002	0.005	0.00	0.020624	0.001310977
Ruw 1 1.8	0.000	0.000	0.000	0.000	0.000	0.000	0.00	0.00	0.00	0.00	0.107	0.00	0.002	0.003	0.00	0.010698	0.000878328
Ruw 1 1.9	0.000	0.000	0.000	0.001	0.000	0.000	0.00	0.00	0.00	0.00	0.079	0.00	0.001	0.002	0.00	0.007100	0.000664163
Ruw 1 1.10	0.000	0.000	0.000	0.000	0.000	0.000	0.00	0.00	0.00	0.00	0.067	0.00	0.001	0.001	0.00	0.005398	0.000536887
Ruw 1 1.11	0.000	0.000	0.000	0.001	0.000	0.000	0.00	0.00	0.00	0.00	0.058	0.00	0.001	0.001	0.00	0.004306	0.000462511
Ruw 1 1.12	0.000	0.000	0.000	0.000	0.000	0.000	0.00	0.00	0.00	0.00	0.053	0.00	0.001	0.001	0.00	0.003614	0.000405496
Ruw 1 1.13	0.000	0.000	0.000	0.001	0.000	0.000	0.00	0.00	0.00	0.00	0.049	0.00	0.001	0.001	0.00	0.003101	0.000364973

Experiment time	Cd	Ni	Co	Pb	Cr	Zn	Cu	Fe	Mn	Al	Ca	K	Mg	Na	F	Cl	SO_4^{2-}
	0.000	0.00	0.00	0.000	0.00	0.000	0.000	0.00	0.000	0.000	0.000	0.000	0.000	0.000	0.0000000	0.000	0.000000
SK1 - 0.0	21.212	0.00	0.00	0.031	0.00	0.068	0.010	0.00	0.000	0.005	2.169	0.005	0.037	0.435	0.0010048	0.019477948	0.208289
SK1 1.1	18.501	0.00	0.00	0.029	0.00	0.034	0.005	0.00	0.005	0.005	4.806	0.147	0.187	0.806	0.0066890	0.107921893	0.226230
SK1 1.2	19.216	0.00	0.00	0.029	0.00	0.029	0.003	0.00	0.003	0.008	3.742	0.078	0.125	0.627	0.0051982	0.065428415	0.150736
SK1 1.3	19.977	0.00	0.00	0.027	0.00	0.020	0.002	0.00	0.002	0.005	3.065	0.050	0.092	0.497	0.0040985	0.044292815	0.106377
SK1 1.4	27.932	0.00	0.00	0.019	0.00	0.011	0.001	0.00	0.001	0.003	2.088	0.028	0.059	0.329	0.0032115	0.027066658	0.067001
SK1 1.5	33.899	0.00	0.00	0.017	0.00	0.009	0.001	0.00	0.001	0.002	1.709	0.019	0.044	0.262	0.0026274	0.019714575	0.049631
SK1 1.6	40.353	0.00	0.00	0.014	0.00	0.007	0.000	0.00	0.000	0.001	1.377	0.014	0.034	0.206	0.0022570	0.014333061	0.036523
SK1 1.7	55.861	0.00	0.00	0.010	0.00	0.005	0.000	0.00	0.000	0.001	0.983	0.009	0.024	0.146	0.0017592	0.009452928	0.024297

SK1 1.8	207.534	0.00	0.00	0.003	0.00	0.001	0.000	0.00	0.000	0.001	0.274	0.002	0.006	0.041	0.0007966	0.002450628	0.006380
SK1 1.9	387.844	0.00	0.00	0.002	0.00	0.001	0.000	0.00	0.000	0.000	0.151	0.001	0.003	0.023	0.0005350	0.001313807	0.003302
SK1 1.10	566.066	0.00	0.00	0.001	0.00	0.000	0.000	0.00	0.000	0.000	0.110	0.001	0.002	0.017	0.0004282	0.001110896	0.002320
SK1 1.11	747.034	0.00	0.00	0.001	0.00	0.000	0.000	0.00	0.000	0.000	0.089	0.001	0.002	0.014	0.0003573	0.000864256	0.001789
SK1 1.12	933.794	0.00	0.00	0.001	0.00	0.000	0.000	0.00	0.000	0.000	0.077	0.000	0.002	0.012	0.0003145	0.000717663	0.001462
SK1 1.13	1121.08	0.00	0.00	0.001	0.00	0.000	0.000	0.00	0.000	0.000	0.068	0.000	0.001	0.011	0.0002819	0.000611215	0.001237
SK1 1.14	1306.28	0.00	0.00	0.001	0.00	0.000	0.000	0.00	0.000	0.000	0.062	0.000	0.001	0.010	0.0002538	0.00054135	0.001078

Experiment time	Cd	Ni	Co	Pb	Cr	Zn	Cu	Fe	Mn	Al	Ca	K	Mg	Na	F	Cl	SO_4^{2-}
	0.000	0.000	0.00000	0.00	0.0000	0.000	0.000	0.000	0.00	0.000	0.000	0.000	0.000	0.00000000	0.000	0.000	0.000
KL1 - 0.0	0.0303	0.006	0.02386	0.00	0.00217	0.0000	0.0022	0.00000	0.00	0.0000	1.0687	0.0000	0.0303	0.13874196	0.00046301	0.02129	0.02406
KL1 1.1	0.0171	0.006	0.01714	0.00	0.00156	0.0016	0.0016	0.00000	0.00	0.0000	1.1530	0.0031	0.0249	0.08258127	0.00088413	0.05944	0.02870
KL1 1.2	0.0183	0.004	0.01751	0.00	0.0016	0.0024	0.0016	0.00000	0.00	0.0000	1.0961	0.0016	0.0215	0.04946151	0.00118596	0.03043	0.02538
KL1 1.3	0.0196	0.005	0.01848	0.00	0.0017	0.0017	0.0017	0.00000	0.00	0.0000	1.0605	0.0011	0.0196	0.03473420	0.00083284	0.02137	0.02255
KL1 1.4	0.0179	0.004	0.01748	0.00	0.0016	0.0012	0.0016	0.00000	0.00	0.0000	0.9920	0.0008	0.0179	0.02900246	0.00059062	0.01516	0.02068
KL1 1.5	0.0171	0.004	0.01778	0.00	0.0016	0.0010	0.0016	0.00000	0.00	0.0000	0.9699	0.0006	0.0171	0.02318349	0.00047212	0.01211	0.01960
KL1 1.6	0.0158	0.005	0.01844	0.00	0.00160	0.0013	0.0016	0.00000	0.00	0.0000	0.9627	0.0005	0.0171	0.01951640	0.00039744	0.01019	0.01884
KL1 1.7	0.0047	0.001	0.00557	0.00	0.0005	0.0003	0.0005	0.00021	0.00	0.0072	0.5354	0.0118	0.0059	0.05257880	0.00010230	0.00262	0.01246
KL1 1.8	0.0030	0.001	0.00387	0.00	0.0005	0.0042	0.0008	0.00014	0.00	0.0073	0.3813	0.0096	0.0036	0.03621494	5.14207E-05	0.00131	0.00814
KL1 1.9	0.0020	0.001	0.00347	0.00	0.00039	0.0036	0.0005	0.00011	0.00	0.0074	0.3097	0.0079	0.0028	0.02810752	3.41659E-05	0.00087	0.00579
KL1 1.10	0.0015	0.000	0.00355	0.00	0.00037	0.0030	0.0004	0.00010	0.00	0.0076	0.2752	0.0071	0.0024	0.02380053	2.56392E-05	0.00065	0.00457
KL1 1.11	0.0013	0.001	0.00375	0.00	0.00037	0.0026	0.0003	0.00011	0.00	0.0076	0.2472	0.0063	0.0022	0.02081382	2.05869E-05	0.00052	0.00379
KL1 1.12	0.0011	0.001	0.00382	0.00	0.00036	0.0025	0.0003	0.00010	0.00	0.0076	0.2277	0.0058	0.0021	0.01874520	1.71383E-05	0.00043	0.00325
KL1 1.13	0.0010	0.001	0.00374	0.00	0.00036	0.0023	0.0002	0.00011	0.00	0.0076	0.2144	0.0055	0.0020	0.01741172	1.46488E-05	0.00037	0.00287

Experiment time	Cd	Ni	Co	Pb	Cr	Zn	Cu	Fe	Mn	Al	Ca	K	Mg	Na	F	Cl	SO_4^{2-}
	0.000	0.000	0.000	0.00000	0.000	0.000	0.000	0.000	0.00000	0.000	0.000	0.000	0.000	0.000	0.0000000	0.00000	0.00000
W. I. - 0.0	0.000	0.0000	0.0000	0.01131	0.0016	0.0081	0.007	0.0711	0.02263	0.4138	3.2552	0.0808	0.5673	1.54678996	0.0005786	0.01545	0.00501
W. I. 1 1.1	0.000	0.0000	0.0000	0.03282	0.0285	0.0599	0.101	1.6139	0.43095	9.8476	16.6386	0.3139	6.1360	11.07339877	0.0039045	0.23094	0.03192
W. I. 1 1.2	0.000	0.0000	0.0008	0.04075	0.0368	0.0735	0.129	2.0241	0.54737	12.1230	17.2523	0.3196	7.7591	13.47261621	0.0049416	0.27418	0.03368
W. I. 1 1.3	0.000	0.0000	0.0011	0.04138	0.0382	0.0748	0.132	2.0205	0.56122	12.5992	16.2583	0.3448	8.0841	13.68029751	0.0048742	0.26925	0.03197
W. I. 1 1.4	0.000	0.0000	0.0008	0.03929	0.0358	0.0716	0.128	1.9071	0.53639	12.0043	15.4226	0.3112	7.8066	17.49966389	0.0046086	0.24484	0.02961
W. I. 1 1.5	0.000	0.0006	0.0006	0.03532	0.0309	0.0633	0.112	1.6711	0.46812	10.4219	13.9692	0.3077	6.9372	15.37455662	0.0043958	0.21544	0.02797
W. I. 1 1.6	0.000	0.0005	0.0005	0.03204	0.0269	0.0557	0.099	1.4661	0.40624	9.0162	13.0424	0.2887	6.0859	13.39707927	0.0089472	0.29336	0.08524
W. I. 1 1.7	0.000	0.0001	0.0001	0.00966	0.0068	0.0149	0.025	0.3697	0.10245	2.2739	8.2740	0.1192	1.5649	3.432597086	0.0024044	0.07479	0.03753
W. I. 1 1.8	0.000	0.0001	0.0001	0.00499	0.0034	0.0075	0.012	0.2114	0.04995	1.1224	6.6996	0.0763	0.7629	1.675156928	0.0012324	0.03640	0.02449
W. I. 1 1.9	0.000	0.0000	0.0002	0.00355	0.0023	0.0052	0.008	0.1564	0.03332	0.7548	6.1085	0.0582	0.5090	1.117410273	0.0008622	0.02426	0.02171
W.I. 1 1.10	0.000	0.0000	0.0003	0.00265	0.0017	0.0040	0.006	0.1278	0.02491	0.5677	5.7938	0.0489	0.3804	0.834881329	0.0006627	0.01812	0.01875
W.I. 1 1.11	0.000	0.0000	0.0003	0.00213	0.0014	0.0033	0.005	0.1097	0.02007	0.4592	5.5082	0.0430	0.3066	0.672588624	0.0006189	0.01461	0.02541